The Regulatory Role of sRNAs in *Mycobacterium tuberculosis*

Joanna Houghton

A thesis submitted in partial fulfilment of the requirements of

University College London for the degree of Doctor of Philosophy

Division of Mycobacterial Research

MRC National Institute for Medical Research

Mill Hill

London

2015

Declaration

I Joanna Houghton confirm that the work presented in this thesis is my own. Where information has been derived from other sources, I confirm that this has been indicated in the thesis.

Acknowledgements

My first thank you goes to my supervisor Dr. Kristine Arnvig for giving me the opportunity to work with her in the exciting field of *M. tuberculosis* sRNAs. I very much enjoyed working on the project and feel extremely lucky to have benefited from her guidance. The PhD journey however would not have begun without Dr. Elaine Davis who encouraged me to apply and I will be eternally grateful for her belief in me.

I would like to thank my second supervisor Dr. Douglas Young for valuable advice and discussion in addition to critical reading of the thesis. Thanks to my thesis committee, Dr. Mark Wilson and Dr. Ian Taylor for advice on the project and in particular Dr. Ian Taylor's help with sucrose gradient ultracentrifugation.

The members of the mycobacterial research division past and present deserve a shout out for valuable input with thanks in particular to Debbie Hunt for listening to my endless moaning and being super supportive. Also I thank Dr. Graham Rose and Dr. Teresa Cortes for kindly doing the sequencing mapping and providing TSS data.

A huge thank you to Dr. Olga Schubert who performed the shotgun mass spectrometry analysis and MSstats, she went beyond the call of duty to get results back to me quickly. Thanks to Dr. Angela Rodgers for the mouse infection experiments and BμG@S for allowing the scanning of the microarrays and advice on analysis.

Finally, I would like to thank my family for all their support and motivation. Thanks to my partner Niall for his encouragement and unfaltering belief in me, and who without a word could produce a glass of Malbec just when I needed it most.

Last but not least I owe the biggest thanks to my mother in law Elizabeth Densley for supporting my return to work after having my son and providing childcare among a long list of other amazing things! I have no doubt that I would not have made it otherwise. This thesis is dedicated to you.

Abstract

The presence of small regulatory RNAs (sRNA) have now been identified in many bacteria. With the ability to regulate multiple targets at the post transcriptional level, sRNAs allow bacteria to adapt to changing environments through a regulatory step that is independent of any transcriptional signals of the target mRNAs. Previous reports show a role for sRNAs in the stress response [1]. Therefore *Mycobacterium tuberculosis* sRNAs could be critical for the adaptive response to the harsh environment encountered during infection.

Multiple potential sRNAs have been identified in *M. tuberculosis* within the last few years using cDNA cloning and high throughput RNA sequencing techniques [2, 3]. Four verified sRNAs found using these two approaches, were selected for detailed investigation. The aims of the study were to identify function and interactions for the sRNAs ncRv10243, ncRv11690, ncRv12659 and ncRv13661 of *Mycobacterium tuberculosis* and assess their role in virulence. Transcriptomic and proteomic approaches were used to investigate sRNA expression strains for regulatory targets.

Deletion and/or over expression were shown to result in changes of both mRNA and protein abundance, indicating that all candidates were functional in *M. tb*. Each sRNA had a varied pattern of expression, induced under a variety of stress conditions including infection. Deletion of 3 of the sRNAs however did not result in attenuation in the mouse model of infection.

The challenge of characterising sRNAs demonstrates that one single technique is inadequate to identify function and a multi-pronged approach is more likely to identify direct targets.

Table of Contents

List of Figures

List of Tables

List of Abbreviations

BMDMs	bone marrow derived macrophages
cDNA	Complementary Deoxyribonucleic acid
CFU	colony forming unit
DCO	Double Crossover
dH_2O	distilled water
DNA	Deoxyribonucleic acid
DNase	Deoxyribonuclease
dNTPs	2'Deoxynucleoside 5'Triphosphate
HIV	human immunodeficiency virus
IFNγ	Interferon gamma
Kan^R	Kanamycin Resistance
kb	Kilo Base
KDa	Kilo Dalton
MCC	Methyl Citrate Cycle
MMP	Methyl Malonyl Pathway
mRNA	Messenger Ribonucleic Acid

OD	Optical Density
PBS	Phosphate Buffered Saline
PCR	Polymerase Chain Reaction
qRT-PCR	Quantitative Reverse Transcription PCR
RACE	Rapid Amplification of cDNA ends
RNA	Ribonucleic Acid
rpm	Revolutions per minute
rRNA	Ribosomal Ribonucleic Acid
SCO	Single Crossover
SDM	Site Directed Mutagenesis
sRNA	Small Ribonucleic Acid
TBS	Tris-buffered Saline
TCA	Tricarboxylic Acid
X-Gal	5-Bromo-4-chloro-3-β-D-galactoside

1 Introduction

1.1 Tuberculosis

Tuberculosis (TB) is one of the world's biggest and oldest killers among the infectious diseases. It is an ancient disease, and evidence of tubercular decay has been found in the skulls and spines of Egyptian mummies showing direct evidence of TB colonising humans more than 5,000 years ago [4]. Recently, analysis of whole genome sequences from the *Mycobacterium tuberculosis* Complex (MBTC) alongside human mitochondrial genomes has led to the estimation that TB is actually more than 70,000 years old [5].

Tuberculosis can be caused by various species of mycobacteria but mainly by *Mycobacterium tuberculosis (M. tb).* The discovery of *M. tb* as the cause of TB infection was famously demonstrated by Robert Koch to the Berlin Physiological Society in 1882, which contributed greatly to him being awarded the Nobel Prize in 1905, [6, 7]. In 1993 the WHO declared TB to be a 'global emergency' due to the rapid spread of disease accelerated by HIV, drug resistance and the movement of people around the world.

The latest estimations by the World Health Organisation (WHO) show that TB is responsible for killing approximately 1.3 million people a year, and it is estimated that one third of the world's population is latently infected with TB [8]. The greatest incidence of disease by far is in Southern Africa where it has escalated due to its deadly synergy with HIV. TB is a leading cause of death among those infected with HIV; in 2012 it was estimated that 20% of deaths among people with HIV/AIDS are due to TB [8].

Although the burden of disease falls generally on the developing world, it is increasingly becoming a problem in lower incidence countries in the west mainly due to immigration, poverty and homelessness [9]. In the UK, almost three quarters of TB cases occurred amongst people born outside of the country, but only 15% of these were recent migrants. In 2013 70% of all TB cases in the UK, were found to be residents in deprived areas, with almost half of these people being unemployed. These are similar statistics to the 2003 study by Antoine et al indicating no change in trend [10].

1.1.1 Mycobacteria and the Mycobacterium tuberculosis Complex

M. tb is an actinomycete belonging to the family Mycobacteriaceae. This genus includes the *M. tuberculosis* Complex (MTBC), *Mycobacterium leprae*, and non-tuberculous mycobacteria [11]. The MTBC is made up of mycobacteria causing TB in human and animal hosts; comprising the well-known *M. tb, Mycobacterium bovis* and the vaccine strain *M. bovis Bacille Calmette-Guérin* (BCG) as well as *Mycobacterium africanum, Mycobacterium canettii and Mycobacterium microti* [12].The members of the complex differ in host specificity, pathogenicity and a small number of phenotypic and/or genotypic characteristics

Pathogenic mycobacteria are capable of causing a variety of diseases. In addition to the well-known human pathogen *M. tb,* is *M. leprae,* which causes leprosy and *M. ulcerans* which results in Buruli ulcers. Other mycobacteria can act as opportunistic pathogens of humans as is the case for *M. avium* and *M. marinum* are also common pathogens of birds,

and fish, causing granulomatous lesions of the organs or skin respectively.

Mycobacteria can be divided into two categories of slow and fast growers. The slow growers such as *M. tb* take a week or more to grow on solid agar while the fast growers such as *M. smegmatis* take 2-3 days [13]. This equates to a doubling time of approximately 17 hours for *M. tb* and 4 hours for *M. smegmatis*. Environmental mycobacteria are distinguished from the members of the MTBC and *M. leprae* by the fact that they are not obligate pathogens. In general it appears that slow growers such as *M. tb* and *M. marinum* are pathogens whereas fast growers such as *M. smegmatis* are environmental species [14]. Chemostat experiments have shown that the control of growth rate in mycobacteria is not due to acceleration or deceleration of cellular processes but through the control of particular gene sets [15]. These genes include transcriptional regulators e.g. *hspR* and some genes previously implicated in virulence and persistence (*pps*A and *pps*B) [15]. It is advantageous for the pathogenic species to be slow growers in order to establish an infection and transmit to another host. If the disease were to progress too quickly the host may die before transmission.

It is of note that rapidly growing mycobacteria still grow significantly more slowly than most bacteria. This could be in part due to differences in rRNA. The number of ribosomal (*rrn*) operons varies between species and a correlation has been observed between the bacterial maximum growth rate and the number of *rrn* operons in the genome [16]. The slow

growing *M. tb* contains but one *rrn* operon, whereas the faster growing *M. smegmatis* contains two, *rrnA* and *rrnB* [17]. However, if you remove all but one ribosomal operon from the fast growing species *Escherichia coli* (*E. coli*) a fast doubling time is still maintained [18]. This suggests that it is not the number of *rrn* operons that dictates the maximum doubling time, but in fact the contrary, with the growth rate dictating the number of *rrn* required.

M. tb is a gram positive bacterium that is distinct from other gram positive bacteria as it possesses an acid fast cell wall that contributes to its hydrophobic nature. This complex cell envelope is rich in lipids containing mycolic acids (Figure 1.1) and accounts for 60% of the dry weight of the bacteria [19]. It is this lipid rich layer that is believed to confer resistance to killing through acidic and alkaline compounds, antibiotics, and free radicals [20] and it has been shown that these lipids are critical for virulence [21].

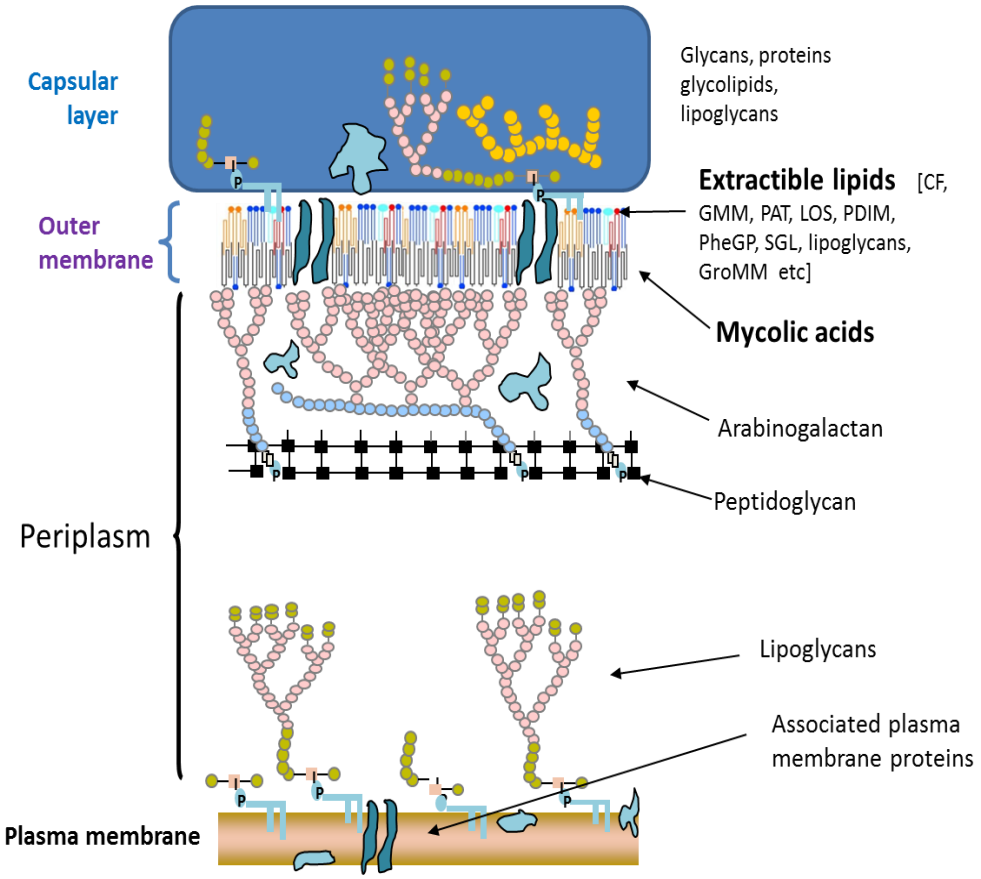

Figure 1.1 The structure of the *M. tuberculosis* cell envelope

CF = cord factor, GMM = glucose monomycolate, PAT =polyacyltrehalose, LOS = lipooligosaccharides, PDIM = phthiocerol dimycoserosates, PheGP = phenolic glycolipids, SGL = sulphoglycolipids, GroMM = glycerol monomycolate.

1.2 The pathogenesis of tuberculosis

M. tb predominantly presents as a pulmonary infection in humans, with the ability to lie dormant in the body for decades. It is transmitted through the inhalation of aerosolised droplets and once the bacteria are inside the lung, they are taken up by alveolar macrophages [22, 23]. Upon phagocytosis of the bacteria an induction of a localised proinflammatory response leads to the recruitment of mononuclear cells from neighbouring blood vessels. This is the initial step that leads to the granuloma formation that is a common feature of tuberculosis. The granuloma consists of centrally infected macrophages surrounded by foamy giant cells and macrophages with a mantle of lymphocytes [24]. The bacteria reside in the macrophages through an ability to block phagosome maturation and to resist damage by free radicals, thereby allowing them to replicate freely. This strategy is part of the success story of tuberculosis as it is these cells that are supposed to sustain an effective initial barrier to bacterial infection (Figure 1.2).

In an immuno-competent individual this aggregation of immune cells prevents the spread of infection. The granuloma serves both to prevent dissemination of the bacteria and to provide an environment for cross talk between immune cells. During this stage there are usually no symptoms and the host is not infectious. If immunity is weakened such as in the case of HIV infection, the granulomatous lesion fails to contain the mycobacteria. These lesions can contain large numbers of bacteria (>10^9 bacilli), and their rupture can result in the dissemination of *M. tb* to other organs through the circulatory system. Active

disease then develops and the patient becomes infectious, spreading the disease by aerosol [25].

It had long been accepted that *M. tb* resides exclusively within membrane-enclosed vacuoles within the macrophage. Some experiments in the 1980's and 1990's discovered *M. tb* free of the phagosomal membrane after a few days of infection. There is now a growing debate on the localisation of the bacterium within the phagosome, reviewed in [26]. Translocation of the bacilli into the cytosol has been observed by several groups [27-29]. In the study by Van der Wel et al. involving infections of human monocyte-derived dendritic cells and macrophages, it was observed that *M. tb* containing phagosomes fused with lysosomes and then gradually the bacteria translocate to the cytosol after 2 days infection [29]. The results were interpreted as evidence that the cytosol was more permissive to bacterial growth than the endosome. These findings are quite controversial as this phenomenon has not been observed by all groups.

The infectious life cycle of TB is complex, it must adopt various growth states in order to transmit, infect and also remain latent for years undetected in many hosts. For this reason, *M. tb* has been found to exist in many states on a spectrum ranging from an active, to persistent or dormant (latent) TB infection [30], Figure 1.3. The term dormant refers to bacteria, which are in a non-replicating drug-resistant state. These bacteria are viable but unable to form colonies directly or immediately on plating but which can be resuscitated to form colonies under appropriate conditions [31, 32]. Persistence refers to genetically drug-susceptible bacteria that can survive indefinitely within the host despite

continued exposure to the drug in question [33]. Separate granulomatous lesions within the lung of one individual can have different fates, with some lesions being active while others are sterile [34], and in fact the population within the granuloma itself could be phenotypically heterogeneous. A greater understanding of the mechanisms controlling the life cycle of *M. tb* will enhance future drug development and allow both dormant and actively replicating bacteria to be targeted in concert.

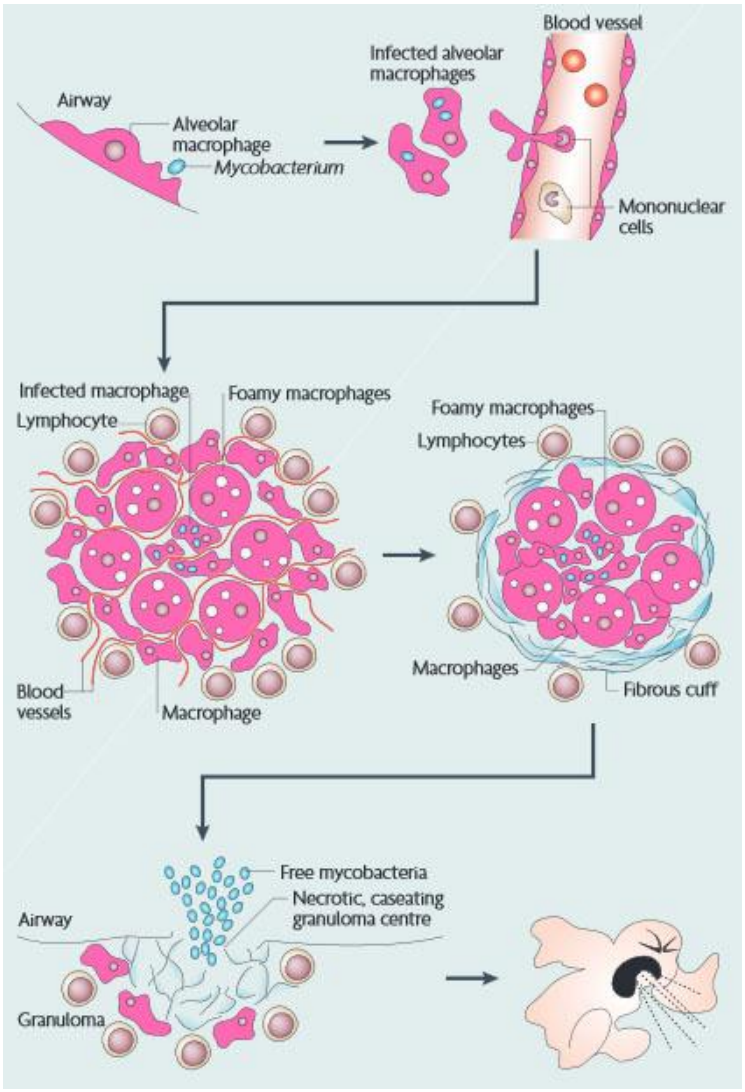

Figure 1.2 The pathology of the granuloma taken from (Russell 2007)

Aerosolised droplets are delivered to the lung where the first infected cells are the alveolar macrophages. The infected macrophage then invades the adjoining epithelium where a proinflammatory response then leads to the recruitment of monocytes from neighbouring blood vessels. A granuloma develops with macrophages, giant cells and foamy macrophages. In many of these lesions, the cells are separated by a fibrous layer of extracellular matrix.

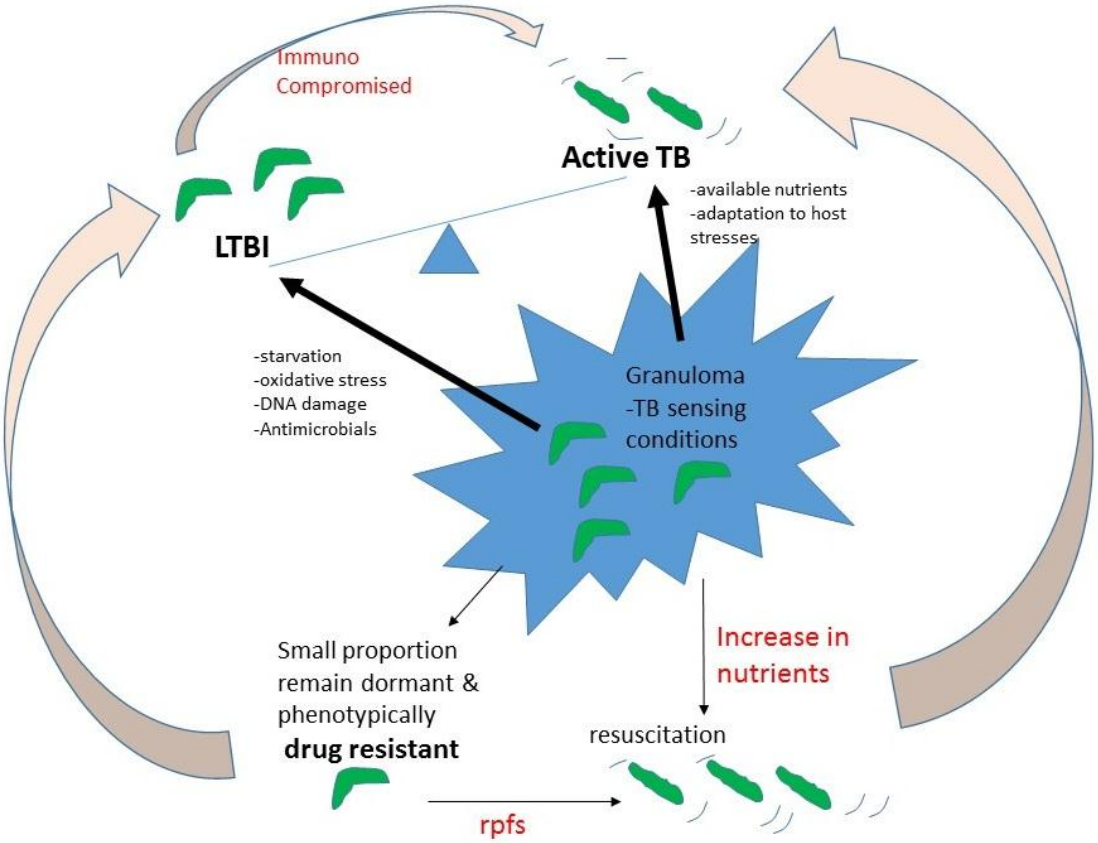

Figure 1.3 The Differing Physiological States of *M. tuberculosis*

LTBI = Latent tuberculosis infection, rpfs = resuscitation promoting factors.

1.3 Tuberculosis therapy

Most of the first line drugs still used today were discovered decades ago and drug resistance is increasing. Multidrug-resistant tuberculosis (MDR-TB) is a form of TB caused by bacteria that do not respond to at least isoniazid and rifampicin, which are the two most powerful front line drugs. 450,000 cases of MDR-TB were reported in 2012 [8]. Extensively drug-resistant TB (XDR-TB) cases also exist, in these cases the patient presents with resistance not only to the front line drugs rifampicin, isoniazid, ethambutol and pyrazinamide, but also to some of the most effective second-line anti-TB drugs. Second line drugs include, fluoroquinolones, and the injectables; capreomycin, kanamycin or amikacin. Totally drug resistant tuberculosis (TDR-TB) cases have also been characterised with *in vitro* resistance to all first and second line drugs tested, (isoniazid, rifampicin, streptomycin, ethambutol, pyrazinamide, ethionamide, para-aminosalicylic acid, cycloserine, ofloxacin, amikacin, ciprofloxacin, capreomycin, and kanamycin). These TDR-TB bacilli have been found to be morphologically different from other *M. tb* with variations in shape, cell division and thickness of cell wall [35]. Resistant strains exhibit different fitness profiles when grown in competition with different susceptible strains. Drug-resistant strains often demonstrate decreased competitive ability against susceptible strains in the absence of the drug [36] [37]. The problem of drug resistance hampering treatment has led to an urgent need for new therapies.

Part of the problem with drug resistance stems from the prolonged treatment period required to cure the patient. The long treatment period coupled with potential side effects of the drugs lead to non-compliance followed by the

emergence of drug resistance. The current regime for active pulmonary disease is a 6 month course of four antimicrobial drugs, consisting of isoniazid (an inhibitor of mycolic acid synthesis) and rifampicin (an inhibitor of RNA synthesis) [38] for 6 months. Pyrazinamide (an inhibitor of trans-translation [39]) and ethambutol (an inhibitor of cell wall synthesis) must be taken in addition to isoniazid and rifampicin for the first two months of treatment [38]. MDR-TB and XDR-TB patients require an even longer treatment period with a combination of first line and second line drugs.

1.4 Vaccination

The only vaccine currently in use for *M. tb* is BCG, which was developed at the Pasteur Institute by Albert Calmette and Camille Guérin, who attenuated a mycobacterium related to *M. tb* (*M. bovis),* by passaging it for 13 years and monitoring its decrease in virulence [40]. In 1921, the vaccine was administered to infants in France, where it reduced mortality by approximately 90%. Since this time BCG has become widely used due to its low cost and safety. Unfortunately the BCG vaccine has had limited efficacy in the developing world, especially against the pulmonary form. It is thought that this is due to prior sensitisation to environmental mycobacteria. In order for more effective vaccines to be designed we need to gain a better understanding of *M. tb* and its host response during infection [41].

1.5 Gene Regulation

The *M. tuberculosis* genome consists of ~4,000 protein encoding genes whose expression is controlled by 13 sigma factors, responsible for global regulation of gene transcription. During exponential growth, bacteria constitutively express

so-called ‘housekeeping’ genes, which possess promoters that are recognised by primary group 1 sigma factors such as σ70 [42]. This house keeping sigma factor homologue is termed SigA in *M. tb* [43].

When the bacteria sense stress, for example low oxygen (hypoxia) and low pH, which may be encountered in the different host environments, they must adapt to these stresses quickly. One common strategy adopted is to replace the primary sigma factor that is associated with the core RNA polymerase (RNAP) with an alternative sigma factor. This changes the promoter specificity of the RNAP and thereby allows expression of a different set of genes [44]. This conventional form of transcriptional regulation is complemented by approximately 200 transcription factors in *M. tb.* One such example is that of CarD which interacts directly with the β subunit of RNAP [45]. These transcription factors dictate the expression of subsets of genes through direct interaction with either the DNA or RNAP.

The central dogma of molecular biology is the concept that information flows from DNA to RNA to protein, and it is this, which determines the cellular phenotype. Gradually this simplified idea is becoming more and more out dated as the understanding of the role of RNA in the cell grows. It has long been understood that tRNA, mRNA, and rRNA are fundamental parts of all bacterial cells. They are necessary for translation, but in addition to these transcripts are also small RNAs (sRNAs). The complementary network of sRNAs, capable of acting at the transcriptional and post transcriptional level has challenged the central dogma. There is now a growing appreciation of the abundance of sRNAs and their importance in cell processes.

sRNAs are short RNA transcripts (typically consisting of ~50-250 nucleotides) which are not translated [46]. These sRNAs are capable of interacting with mRNA and proteins, either as RNA alone or in association with proteins as part of a ribonucleoprotein (RNP) complex. Many roles have been described for sRNAs including transcriptional regulation, RNA processing and modification, mRNA stability and translation as well as protein degradation and translocation [47].

1.6 Identification of sRNAs

Non-coding RNAs were initially identified by the detection of highly abundant sRNAs through direct labelling and sequencing. This led to the discoveries of housekeeping RNAs such as RNaseP, tmRNA and 4.5S RNA, which are involved in tRNA maturation, ribosome rescue and protein translocation respectively.

To date, *E. coli* and *Salmonella typhimurium (Salmonella*) have by far the most identified sRNAs, with over 80 having been described [48-50] for *E. coli* and approximately 280 identified for *Salmonella* [51, 52]. A mixture of techniques have been used to find sRNAs, from *in silico* prediction and bioinformatic based approaches [53] to cloning and sequence based methods.

Even when the complete genome sequence of an organism is known, new sRNAs can be overlooked because there are no specific classes of sRNAs that can be found based solely on sequence. In 2001 a combination of techniques were employed to look for new sRNAs in *E. coli* [54]. The sequences of intergenic regions longer than 180bp were compared to *Salmonella* and

Klebsiella pneumonia by NCBI Unfinished Microbial Genomes database using the BLAST program [55]. Sequences with greater than 80 nucleotides conservation were then filtered based on their orientation and distance in relation to the flanking ORFs. Finally the remaining potential sRNAs were examined for promoters, terminators and inverted repeat regions. These predictions were compared with microarray data and resulted in a possible 59 sRNAs of which 17 were confirmed by northern blot and considered to be new sRNAs [54].

An alternative approach using bioinformatics to identify sRNAs has been taken to conduct genome-wide annotations for putative sRNA genes in the intergenic regions of eleven pathogens using the sRNAPredict2 program [56]. In total, more than 2700 sRNAs were revealed as unannotated candidate sRNA loci in the diverse bacteria, although these remain to be experimentally confirmed.

One unbiased method to investigate the sRNA component of an organism is to clone and directly sequence short bacterial transcripts by parallel RNA sequencing. This approach was adopted with the pathogen *Vibrio cholerae,* in which they discovered 500 new putative intergenic sRNAs and 127 putative antisense sRNAs from the growth conditions examined [57].

Most recent work employs new technologies such as high-throughput RNA sequencing (RNA seq) and high-density tiling arrays to detect the expression of sRNAs in both pathogenic and non-pathogenic species [58, 59].

Many sRNAs were identified in *Salmonella* by the co-immunoprecipitation (coIP) with the epitope-tagged RNA chaperone Hfq. High throughput sequencing analysis from RNA co-immunoprecipitated with either the epitope-tagged Hfq or

the control coIP, identified new sRNAs doubling the number of sRNAs previously known to be expressed in *Salmonella* [60].

1.7 Hfq

Approximately half of all sequenced bacterial genomes encode an Hfq homologue. The Hfq protein is highly conserved in prokaryotes and belongs to the Sm protein family whose members are known to be involved in RNA interactions [61, 62]. Hfq is an RNA chaperone known to bind to both sRNA and mRNA, facilitating their pairing.

The protein forms a hexameric ring structure which contains at least two RNA binding faces [63, 64]. One face binds to single stranded A/U-rich regions (i.e. sRNA and mRNA) [65], the other to polyA (i.e. mRNA) [66]. Hfq has been shown to play a central role in sRNA–mRNA interactions facilitating the short and imperfect base pairing between the sRNAs and their mRNA targets. Förster resonance energy transfer studies (FRET) showed that Hfq promotes both RNA annealing and strand exchange by binding rapidly to both the sRNA DsrA and *rpoS* mRNA [67]. Strand exchange occurs as the internal structure of rpoS is disrupted and pairing occurs with DsrA resulting in the Shine-Dalgarno sequence of the mRNA *rpoS* becoming exposed.

In Gram-negative pathogens deletion of Hfq often leads to a loss of virulence, which is attributed in part to loss of proper sRNA function [58, 68]. However, Hfq is not always required for proper sRNA function. For instance, there is no homologue in the Actinomycetes-Deinococcus-Cyanobacteria [49, 69]**,** of which *M. tb* is a member. There is conflicting evidence as to whether Hfq is required for virulence in *Staphylococcus aureus*. One study found that deletion of Hfq

had no effect on the expression of virulence genes, nor was the protein highly expressed [70]. A later study however found 116 genes to be differentially expressed in an Hfq mutant, and 49 of these were shown to bind Hfq by immunoprecipitation [71]. It was concluded from the latter study that the differences in Hfq phenotype observed, could be due to strain variation as the initial study strain lacked Hfq expression [71].

The lack of a homologue for Hfq in *M. tb* could possibly be due to the existence of a functional analogue. Due to the lack of sequence homology this would be very difficult to identify. Alternatively, it could simply be that *M. tb* lacks the requirement for such a protein. It could be that there is more extended base pairing between the sRNA and the mRNA. Or a higher percentage of G or C bases present in the binding sequence would be expected to result in more stable conformations. The high GC content of *M. tb* (67%) could favour this theory as the low frequency of AU-rich stretches provide fewer potential binding sites that are known to mediate Hfq interactions [72].

It is possible that other proteins could contribute to base-pairing sRNA function thereby substituting for the lack of an Hfq homologue. In *B. subtilis* three proteins (FbpA-FbpC) have been identified as possible RNA chaperones needed for the FsrA sRNA to regulate *sdhC* expression [73]. However these are specific for one RNA and not global regulators as is the case for Hfq.

The YbeY protein found in most bacteria was suggested as a possible candidate as an Hfq analog. This protein in *M. tb* is Rv2367c and shares structural similarities with eukaryotic Argonaute proteins which are known to bind small non-coding RNAs [74]. The *E. coli* YbeY has been shown to be a

strand-specific endoribonuclease, playing key roles in 70S ribosome quality control and 16S ribosomal RNA maturation [75]. In addition, deletion of YbeY results in similar phenotypes to those of a Hfq mutant [76] demonstrating that YbeY plays a role in sRNA regulation in bacteria that is of equal importance to that of Hfq.

In addition to binding RNAs, Hfq is also thought to interact with components of the ribosome and degradosome [77].

1.8 The Degradosome and RNases.

The degradosome is an RNA degrading complex that consists of key RNA enzymes that are responsible for RNA degradation processes. In *E. coli* the complex is comprised of RNase E, RNA helicase B, enolase, and the exoribonuclease polynucleotide phosphorylase (PNPase) [78-82]. RNase E is present in many bacteria, including mycobacteria [83], however the components of the degradosome are not conserved between species. Very little is known about the degradosome and RNA metabolism in mycobacteria. *M. tb* possesses RNaseE but it was found to interact with only some of the degradosome components identified in enteric bacteria [83].

It is known from other bacteria that RNase E functions as a scaffold for the assembly of the RNA degrading complex and acts as an endoribonuclease being the primary instigator of transcript degradation. Once RNase E has initiated cleavage, degradation of the RNA quickly follows [84]. However, RNA maturation is also a function of RNase E, cleaving precursors of structured RNAs resulting in processed transcripts that are not marked for decay [85].

In *Salmonella* there exist two pathways for the degradation of sRNA MicA which controls the outer membrane porins (OMPs) OmpA and LamB. Turnover

of this sRNA is either through RNase E cleaving the unpaired MicA, or by the endoribonuclease RNase III, which cleaves MicA in complex with its target mRNA due to the enzyme specificity for double stranded RNA [86].

The mechanism for RNase III has similarity to the eukaryotic RNAi system where the double stranded enzymes Dicer and Drosha play an important role [86-88]. *M. tb* possesses an RNaseIII enzyme which has been shown in *S. aureus* to be important in antisense regulation [89] the maturation of rRNAs and tRNAs, and regulating the turnover of mRNAs and sRNAs [90].

In a co-IP study, RNase III was shown to have a positive effect on protein synthesis with RNase III–mediated cleavage in the 5′UTR enhancing the stability and translation of *cspA* mRNA, which encodes a major cold-shock protein. Moreover, RNase III cleaved overlapping 5′UTRs of divergently transcribed genes to generate leaderless mRNAs, resulting in a new mechanism for co-regulating neighbouring genes [90].

Another RNase of significant importance as a post-transcriptional regulator of sRNAs is the 3'-5' exoribonuclease PNPase. PNPase has been found to stabilize several sRNAs in *E. coli* including RhyB, SgrS, CyaR [91], and its action is growth phase dependent [92]. When a sRNA is not associated with Hfq, it is degraded in a target independent pathway. As the 3' ends to the sRNA are exposed when not bound by Hfq PNPase degradation can occur [92].

1.9 Regulation of Gene Expression by sRNAs in bacteria

sRNAs can be divided into two types, *trans*-encoded/intergenic and *cis*-encoded/antisense. *Cis*-encoded sRNAs are located on the opposite strand to a coding region and have extensive complementarity (>75 nucleotides) to their

targets [50]. *Trans*-encoded sRNAs are located in intergenic regions of the chromosome and can regulate multiple mRNAs across the genome (Figure 1.4). Due to their interaction with multiple targets they have limited complementarity (10-30 nucleotides) to the mRNA and form imperfect base-pairing interactions [50]. The sRNA pairing with the mRNA can result in the enhancement or repression of translation. In addition to effects on translation, several *trans*-encoded sRNAs have also been shown to bind proteins to modulate their activity [69, 93].

The first sRNAs were observed in *E. coli* in the 1970's with the discovery of 4.5S and 10S, although no function was ascertained at the time [94, 95]. The next sRNA discovery was in the 1980's when the plasmid-encoded antisense RNA, termed RNA I, was discovered and found to control plasmid copy number in *E. coli* [96, 97]. Studies by the Tomizawa and Stougard groups led to the understanding of the importance of secondary structure that allows RNA/RNA duplex formation [98-100]. At the same time the idea that an RNA transcript could interact with an mRNA from a distal gene was also proposed [101, 102].

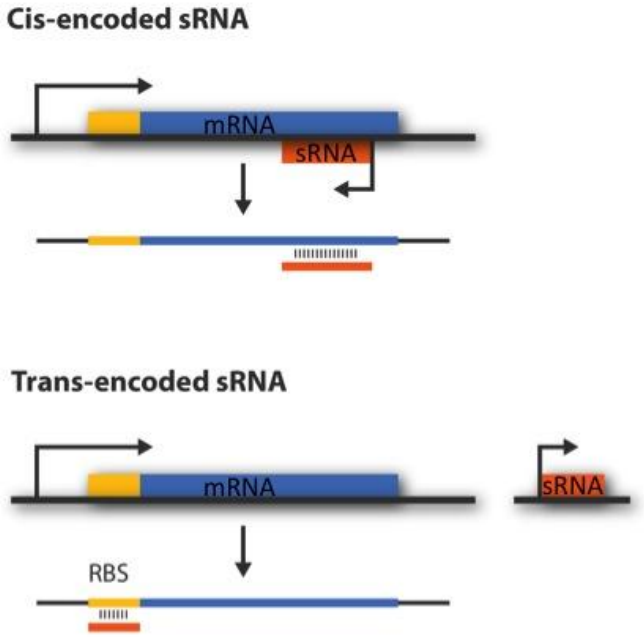

Figure 1.4 Representation of genomic locations of sRNAs.

Cis-encoded sRNAs are found antisense to the mRNA target and possess a high degree of complementarity. Trans-encoded sRNAs are found at different locations on the genome, regulate multiple targets and therefore have limited complementarity. Ribosome Binding Site (RBS)

1.9.1 Translational Repression

MicF was the first example of a *trans*-encoded RNA, it was found to negatively regulate the translation of the outer membrane protein OmpF in *E. coli* [102]. Since this discovery, additional outer membrane proteins, OmpA and OmpC have also been shown to be regulated at the translational level by sRNAs MicA and MicC [103, 104]. The sRNAs MicA and MicC act to inhibit translation by binding to the mRNA (with imperfect base pairing complementarity), to mask the ribosome binding site (RBS) and prevent the mRNA being loaded into the ribosome [105] see Figure 1.5. sRNAs in *E. coli* such as MicA, MicC, Spot42 and OxyS sRNAs were shown by *in vitro* toeprinting experiments to directly interfere with 30S ribosome binding of their target mRNAs *OmpA*, *OmpC*, *galK* and *fhlA* [104, 106-108]. Toeprinting is a method used to study the formation of ribosomal initiation complexes in bacteria, which allows visualisation of how mRNA conformational changes alter ribosome binding at the initiation site *in vitro*. This differs from the method of DNA foot printing where the sequence specificity of DNA-binding proteins *in vitro* is ascertained.

E. coli is not the only organism in which this mode of action has been observed.

sRNAs RNAIII and SR1 in the Gram-positive bacteria *S. aureus* and *Bacillus subtilis,* respectively*,* have also been shown to inhibit translation [87, 109].

As more work on sRNA regulatory mechanisms is performed, variations on the basic theme of translational repression have been discovered. Binding of sRNAs to mRNAs outside the RBS can still inhibit translation

[110-113]. Two such mechanisms include the recruitment of Hfq to bind at a site overlapping the ribosome binding site blocking access to the ribosome [114] or by binding to mRNA sequences that apparently act as translational enhancer elements [115, 116]

Regardless of the precise regulatory mechanism, sRNA-mediated translational repression often results in mRNA degradation by an RNase E degradosome-dependent pathway. The ribosomes protect the mRNA from RNase E degradation by masking the RNase E recognition sites [117], thus sRNA inhibition of translation unmasks these sites and leaves target mRNAs susceptible to ribonuclease attack [118].

However, translational inhibition is not always coupled to mRNA degradation. It has been observed that mutations abolishing RNase E-dependent turnover of sRNA targets can have no impact on translational repression [119-121]. There are also some cases where sRNA-mediated translational repression has no significant effect on mRNA levels [107].

This mode of regulation allows for differential regulation of genes within the same operon. Such is the case in *E. coli*, the spot42 sRNA targets the RBS of *galK* within the *galETKM* polycistronic mRNA (which is involved in galactose metabolism) to prevent translation initiation of *galK* without affecting the other genes of the operon [107].

The reverse is also true, with cases where sRNAs do not directly affect translation but target mRNAs for degradation [122, 123].

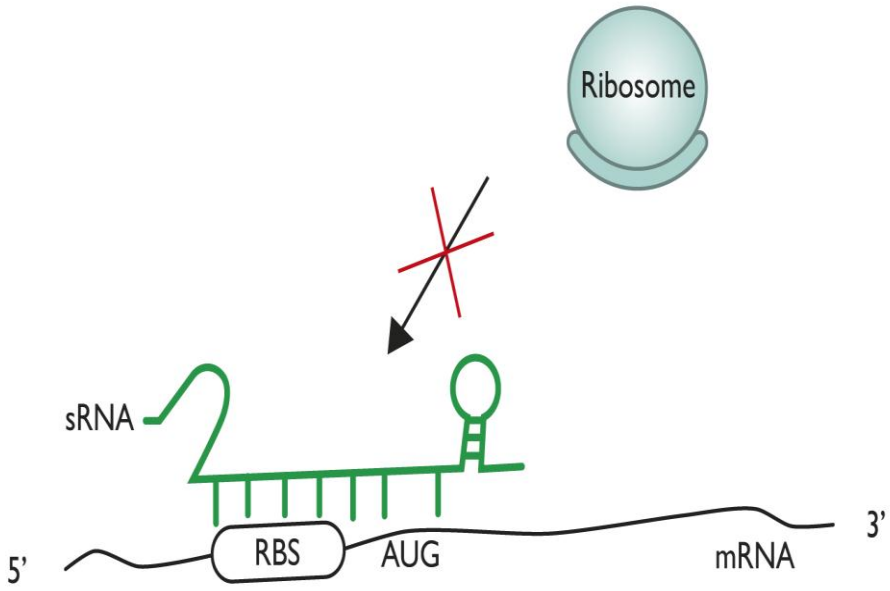

Figure 1.5 Translational inhibition mediated by sRNAs.

Translational Inhibition by sRNAs typically involves base pairing to the mRNA to occlude the ribosome binding site of the mRNA. This prevents ribosome association and thus represses translation. Such as is the case for the sRNA Spot42 which binds to its mRNA targets with imperfect complementarity under glucose stress [107].

1.9.2 Translational Activation

sRNAs are capable of not only repressing translation but also activating translation. The *E. coli* sRNAs DsrA and RprA are induced under low temperature and surface stress, respectively. DsrA and RprA bind to the mRNA of *rpoS*, (the stress sigma factor) and increase translation through a change in secondary structure of *rpoS* to reveal an otherwise masked ribosome binding site [93, 124, 125]. The *rpoS* mRNA has a long highly structured 5' untranslated region (UTR), which can fold to mask the ribosome binding site. Upon pairing of the sRNA with the mRNA the secondary structure is opened to allow access to the RBS (see Figure 1.6). This form of regulation, as with translational repression, is not limited to monocistronic mRNAs. Examples of discordant operon regulation by activation also exist. GlmZ sRNA increases translation of *glmS* in the *glmUS* operon by influencing the action of another sRNA GlmY, in a hierarchical fashion [126, 127]. First GlmZ, together with the chaperone Hfq activates translation of the *glmS* mRNA through the opening of a stem loop secondary structure to reveal the ribosome binding site. Secondly GlmY acts to stabilise the GlmZ sRNA by sequestering the RNA-processing protein YhbJ, thereby indirectly activating expression of *glmS* by increasing the levels of the sRNA GlmZ [47, 128].

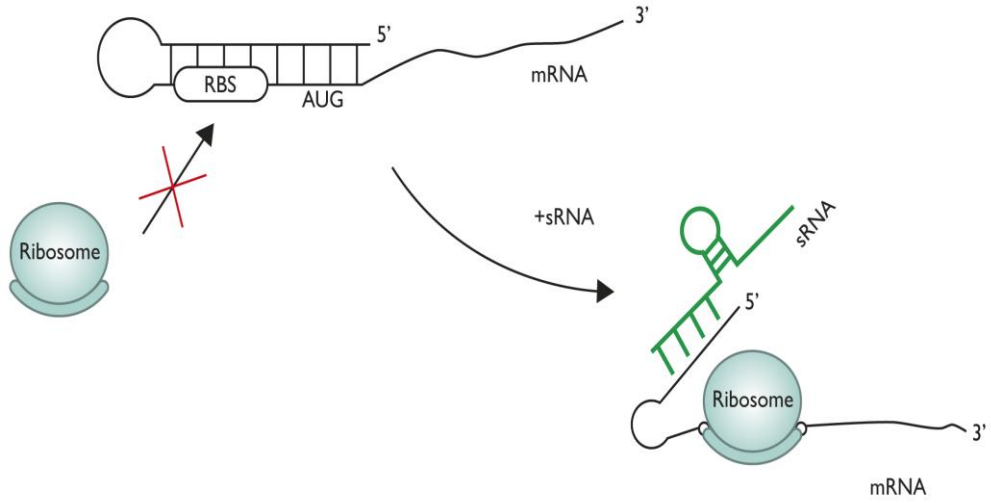

Figure 1.6 Translational activation mediated by sRNAs.

Long 5' UTRs of mRNA can fold into auto-inhibitory stem loop structures, which prevent ribosome access. Interaction of a sRNA with the mRNA results in translation activation by dissolving the fold-back structure, for example *rpoS* mRNA and the sRNA DsrA [129].

1.10 6S RNA

Although the most common mode of action for sRNAs is through base pairing, some sRNAs bind proteins to inhibit their (regulatory) activities. The best studied example is that of *E. coli* 6S RNA, which binds the housekeeping form of RNA polymerase (σ^{70}-RNAP) (reviewed in [130]). This sRNA was first identified in 1967 but its function was not discovered until more than 30 years later.

Co-migration studies demonstrated that 6S sediments with RNAP in glycerol gradients [131] binding tightly to the σ^{70} but not the σ^{s} holoenzyme [132]. The secondary structure of 6S RNA mimics that of DNA during transcription initiation (i.e. an open promoter complex) competing for RNAP, blocking access of the DNA promoter to the RNAP active site [130] thereby broadly down regulating transcription (Figure 1.7). However, down-regulation is only observed for a subset of σ^{70} –controlled genes when 6S is expressed indicating that σ^{70} -RNAP activity is modified in a fine tuning manner and not just inhibited.

In *E. coli* 6S RNA has been shown to regulate transcription of *relA*, which encodes a guanosine (penta) tetraphosphate (p) ppGpp synthase. The decreasing availability of amino acids upon entry into stationary phase is mainly sensed by RelA. The uncharged tRNAs accumulate as a result of decreasing amino acid pools causing RelA to be activated and synthesizes ppGpp.ppGpp binds to RNAP along with the transcription factor DksA [133] to alter transcription of genes with σ(70)-dependent promoters sensitive to ppGpp such as genes involved in amino acid

biosynthesis and rRNA. In gram negative bacteria RelA and SpoT are responsible for the production of (p)ppGpp, but in *M. tb* only the single homolog RelA produces (p)ppGpp [134]. The mechanism of rRNA control in mycobacteria, which lack DksA is unknown but the essential protein CarD has been identified as a regulator of rRNA transcription [135]. It has been observed in *E. coli* that induction of relA leads to increased ppGpp levels in early stationary phase in cells lacking 6S [136].

Deletion of 6S RNA in *E. coli* has no obvious detrimental effects during exponential growth but is important for optimal survival during stationary phase growth when 6S accumulates within the cell [137]. During outgrowth from stationary phase, under conditions of nutritional up shift when NTPs are no longer limiting, the 6S RNA acts as a template for a short product RNA (pRNA). These pRNAs of 14-20 nucleotides destabilize the 6S RNA-RNAP complex, which leads to the ejection of the pRNA-6S RNA hybrid [138] thereby recycling the RNAP for re use.

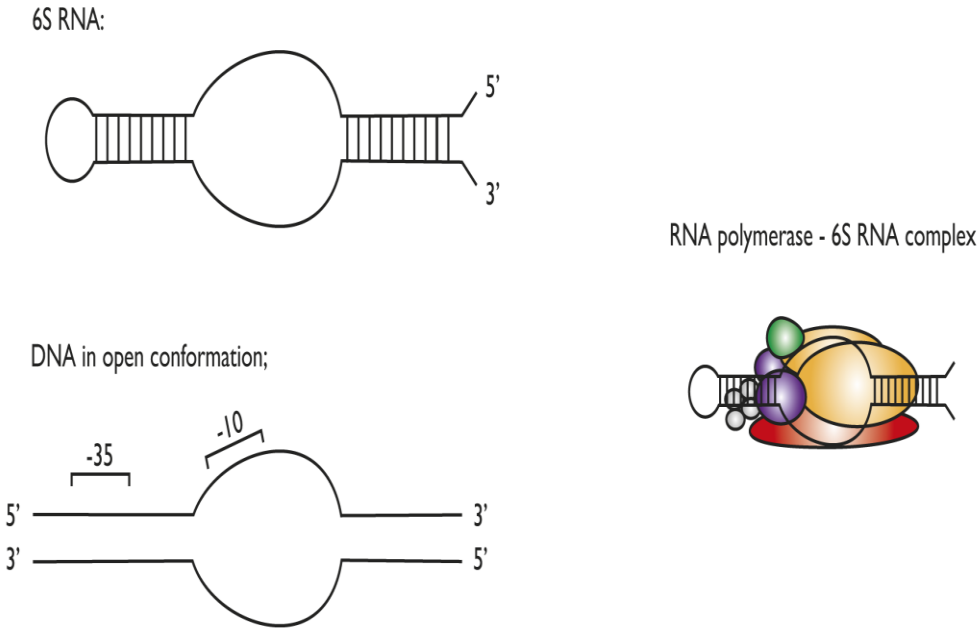

Figure 1.7 Sequestering of RNAP by 6S RNA

6S RNA acts as a mimic of the DNA in open promoter conformation suppressing housekeeping transcription by binding to σ^{70} RNA polymerase holoenzyme (core polymerase + σ^{70}) causing widespread down regulation of σ^{70} genes.

1.11 Dual Function sRNAs

sRNAs are in general considered to be non-coding. However, examples do exist of sRNAs that can both regulate mRNA through base pairing, and encode proteins. In *E. coli* the 227bp sRNA SgrS helps cells recover from glucose phosphate stress. SgrS negatively regulates translation and stability of the mRNA *ptsG,* which encodes a major sugar phosphate transporter, by a base pairing mechanism that requires Hfq [139]. It was found that the sRNA contained a small open reading frame (ORF) of 43 amino acids encoding SgrT [140]. SgrT is encoded upstream of the nucleotides involved in base pairing and is translated under glucose phosphate stress, inhibiting the glucose transporter PtsG. [140]. It was concluded that SgrT reinforces the regulation of SgrS by independently down regulating glucose uptake by interacting directly with PtsG protein to inhibit its activity, possibly by plugging the transporter [140].

1.12 Riboswitches

A 5' UTR is the region from the transcriptional start site to the translational start site of a gene. It is in this region that riboswitches and RNA thermo sensors are usually found. Riboswitches can bind small molecules, which result in an alternative secondary structure of the RNA. This change in structure can lead to either transcriptional or translational repression or activation of the downstream sequence by blocking or revealing the RBS. [141].

Homology searches using the consensus sequence and structural model for the coenzyme B12 class of riboswitches revealed that *M. tb* contains two such

riboswitches. This type of riboswitch is often found upstream of genes involved in the synthesis and transport of cobalamin. One example is that of the B12 riboswitch found upstream of MetE, which codes for the B12-dependent methionine synthase [142]. The other B12 riboswitch is found upstream of the operon containing PPE2, *cobQ1* and *cobU*.

In addition to the above riboswitches *M. tb* also contains two copies of the magnesium sensing riboswitch known as an Mbox. One is found upstream of Rv1535 [3, 143] which is up regulated in response to magnesium starvation [144]. The other Mbox is found upstream of a putative operon containing four PE-PPE genes. The *B. subtilis* Mbox when bound to Mg^{2+} results in attenuation of transcription, and this is the likely mechanism in *M. tb.* Rv1535 is also co-transcribed with a downstream riboswitch that binds uncharged tRNAs, (TBox) [145] this TBox is in the 5'UTR of *ileS* a tRNA synthase.

Gene expression has also recently been demonstrated to be directly affected by c-di-AMP-responsive riboswitches in the 5' UTR's of many mRNAs in bacteria. The important resuscitation promoting factor (*rpfA*) was identified as having one such riboswitch in *M. tb* [146].

1.13 sRNAs in *Mycobacterium tuberculosis* pathogenesis

Many sRNAs are post-transcriptional regulators of gene expression induced in response to external stimuli or stress and they have been found to be differentially regulated under a variety of growth conditions [54]. Stress conditions that have been shown to induce sRNA expression include low iron [147, 148], low temperature [149], changes in glucose concentration [107],

changes in glucose-phosphate levels [49], and outer membrane stress under the control of σ^E [108]. This additional layer of control that complements transcriptional regulation affords the bacteria a method of rapid response to stress.

Regulation of sRNAs has been implicated in the stress response and virulence of many pathogens other than *M. tb* including *Listeria monocytogenes, S. aureus, and Salmonella* [58, 150-152]. It is therefore reasonable to expect that sRNAs play a role in the pathogenesis of *M. tb*.

Until the accessibility of high-throughput sequencing and tiling arrays, the complete potential contribution of non-coding RNA to gene regulation in *M. tb* could not be appreciated. This was due to the fact that techniques such as traditional microarrays focused on annotated, mainly protein coding genes. It had been firmly established from studies in other bacteria that transcriptional control alone was not solely responsible for gene regulation. A post-transcriptional regulatory network exists that is dependent on sRNAs.

The contribution of sRNAs to gene regulation in *M. tb* was first assessed in 2009 with the discovery of nine putative sRNAs found by cDNA cloning [153]. This approach was also taken by another group with the model organism BCG. The study revealed 34 novel sRNAs with putative homologues for many of the sRNAs identified found to exist in *M. tb* and *M. smegmatis* [2] .

In 2011 Arnvig et al, using high throughput sequencing technology found the *M. tb* genome to contain an abundance of non-coding RNA, including 5’ and 3’ UTRs, antisense transcripts and intergenic sRNAs, [3]. Some of these have

shown markedly varied expression profiles in *M. tb* under different *in vitro* growth phases and stress conditions [153]. For example: *M. tb* sRNA ncRv11733 (MTS1338), is highly expressed during stationary phase, nutrient starvation and infection [154]; ncRv12659 is induced by nutrient starvation and during mouse infection [155]; and ncRv13661 (MTS2823) is elevated in stationary phase bacteria and infection [3].

Of the 20 intergenic sRNAs that have been identified and confirmed by northern blotting [153, 155, 156] some are unique to the *M. tb* complex while others are more widely conserved in mycobacteria and actinomycetes [154].

Mcr7 is the first sRNA in *M. tb* to be assigned a function. Mcr7 is expressed under the control of PhoP, and the sRNA binds to the 5' end of the *tatC* mRNA preventing ribosome loading and therefore translation. Proteomic analysis has shown the sRNA to have a role in Tat-dependent secretion of well-known tuberculosis antigens such as Ag85 complex. It was shown that this control was at the post transcriptional level and no impact on the amounts of mRNA was observed [156]. This sRNA completed the link between the PhoPR two-component system and Tat-dependent secretion, demonstrating the importance of mcr7 in the virulence of *M. tb*.

The adaptation of *M. tb* to environmental changes during the course of infection has mostly been monitored at the level of gene expression. To date gene expression studies have concentrated on the expression of mRNA [157, 158], and largely in tissue culture systems [159] and animal models [160] that do not completely replicate all features of *M. tb* infection in humans. Two studies have assessed the issue of *in vivo* adaptation. Garton et al., assessed sputum prior

to patient treatment using PCR based microarrays [161]. Another study looked at the transcripts associated with proteins from infected human lungs [162]. While these studies were very informative, they were concentrated on mRNA and annotated ORFs, so the contribution of sRNAs remains unknown.

Recent work has shown that some *M. tb* sRNAs are highly induced in *M. tb* infected mouse lungs [3, 155] and ongoing studies aim to identify the specific functions of these sRNAs both *in vitro* and *in vivo*.

1.14 Defining sRNA Regulons

The low conservation of sRNAs across bacteria and their reduced complementarity to mRNA targets make it difficult to predict sRNA targets. However, algorithms such as targetRNA2 can aid in the identification of possible targets [163]. TargetRNA2 works by taking the sequence of a sRNA and searching for targets within a specified genome. Features that are taken into account are conservation of the sRNA in other (related) bacteria, the secondary structure of the sRNA, the secondary structure of each candidate mRNA target, and the hybridization energy between the sRNA and each putative mRNA target [163, 164]. The latest version now also allows for integration of RNA seq and microarray data into the prediction of targets by considering differential gene expression therefore improving the accuracy of target identifications.

However, part of the search criteria for sRNA targets relies on conservation of sRNAs in other bacteria, this can make target searches difficult. For example, the *E. coli* RhyB [147] and the *Pseudomonas aeruginosa* functional homologues [165] share very little sequence similarity.

Experimental and computational approaches have been used to define currently known sRNA regulons. The experimental approaches have included studies of sRNA dependent changes in gene expression (microarrays, RNA seq or comparative protein analyses), changes in reporter gene expression or altered growth phenotypes. Both direct targets of sRNAs, along with downstream effects will be detected by approaches that assess altered gene expression complicating the elucidation of sRNA function.

Due to the complete sequence of the *M. tb* genome being available, global analysis of gene expression has become routinely possible through both microarray and RNA seq. Microarrays use gene specific hybridisation probes to quantify the relative abundance of specific transcripts and have been used to assess responses of *M. tb* to different environmental conditions and stages of infection [166] along with strain comparisons [167]. This method has the advantage of being relatively cheap in comparison with RNA seq. The data obtained from RNA seq has the advantage over most microarray technology in providing much more precise and higher resolution levels of transcripts [168]. However, microarrays and RNA seq should be viewed as hypothesis-generating tools from which possible regulons can be inferred [169]; possible interacting partners must be tested in detail by more definitive methods such as electrophoretic mobility shift assays (EMSA) or reporters.

1.15 non coding RNA Nomenclature in *M. tb*

The identification of sRNAs in *M. tb* in recent years has led to a number of different methods of nomenclature. The first identification of non-coding RNA (ncRNA) in *M. tb* resulted in annotation referring to the sequenced clone from

which they were identified e. g B11, C8 and F6 [153]. Later reports numbered the sRNAs by chronological order [2] or by intergenic regions [3, 170], both with different prefixes. This lack of consistency led to a need for a defined method of annotation for ncRNA in *M. tb.* It was suggested that ncRNA were annotated with a prefix of 'nc' for non-coding, followed by a locus identifier that indicates the sRNA location in relation to neighbouring ORFs [171]. sRNAs in this study will be referred to using the new nomenclature.

1.16 Hypotheses & Aims

The focus of this study is to determine the roles of selected sRNAs in *M. tb* pathogenesis, by identifying their function and mode of regulation. Four candidate sRNAs were selected for study and these are detailed in each individual chapter. A summary of their characteristics can be found in Table 1.1

The hypotheses under investigation are

- That sRNAs will control a set of genes in response to a specific stimulus.
- That sRNAs are important in pathogenesis.

To address the hypothesis that sRNAs have regulons and are important in pathogenesis the project aims to

- Identify genes or proteins that are regulated directly or indirectly by the sRNAs under investigation.
- Identify the expression conditions of the selected sRNAs both *in vitro* and *in vivo.*
- Characterise the phenotypes of *M. tb* strains in which the sRNAs are inactivated or over expressed.

Figure 1.8 details the experimental plans to achieve the aims listed above.

sRNA	Method of identification	Known Induction Conditions	Notable Features
ncRv10243	cDNA cloning (Arnvig, 2009)	Starvation and Acid stress	Over expression in *M. tb* results in slow growth
ncRv11690	cDNA cloning (Arnvig, 2009)	Exponential and Stationary Phase	Over expression in *M. tb* is lethal
ncRv13661	RNA seq (Arnvig, 2011)	Stationary Phase and Mouse infection	Most abundant RNA after ribosomal RNA
ncRv12659	RNA seq (Arnvig, 2011)	Stationary phase	Cis-encoded sRNA found antisense to Rv2660c locus induced during starvation

Table 1.1 Key Characteristics of the sRNAs chosen for further investigation

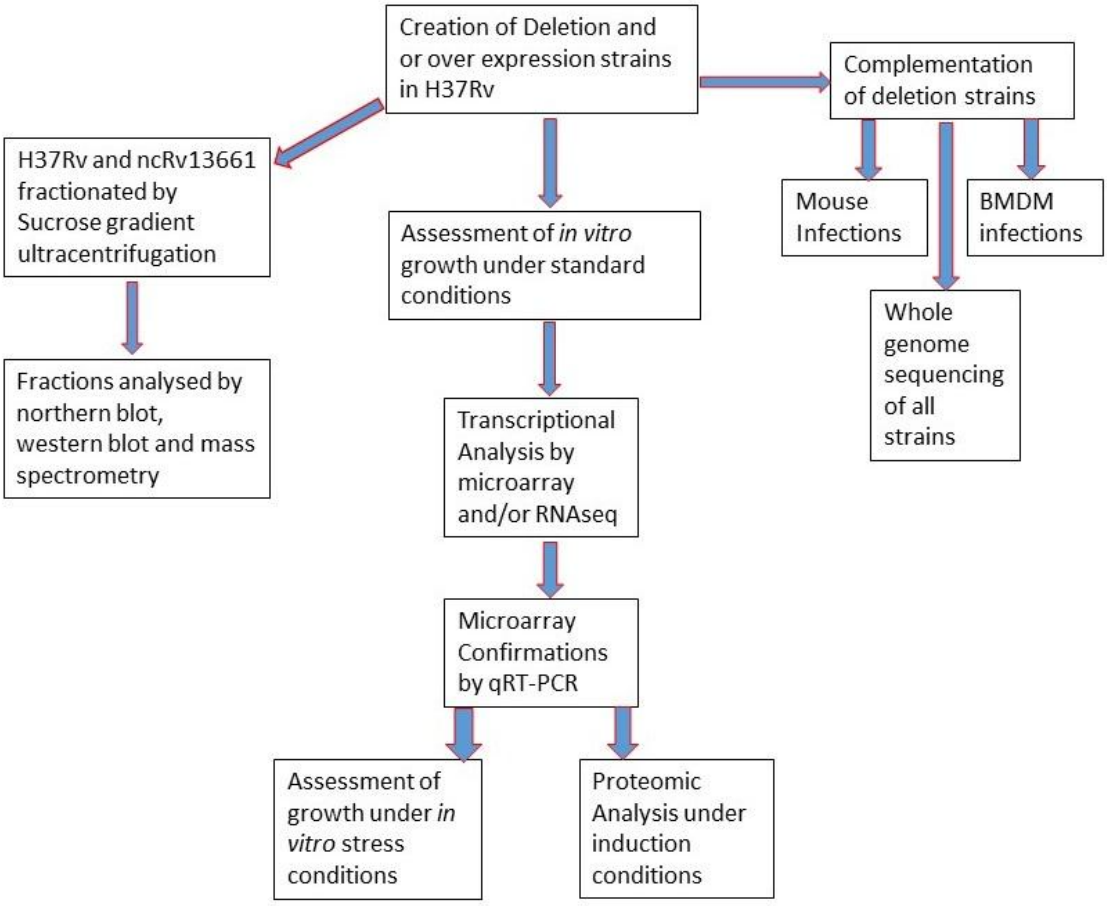

Figure 1.8 Experimental Workflow for elucidating the roles of the sRNAs under investigation.

2 Materials and Methods

Full composition of all media and buffers are listed in Appendix I.

2.1 Bacterial Strains and Growth Media

Mycobacterial strains were grown on 7H11 agar plus 10 % OADC (Becton Dickinson). Liquid cultures were grown in standard Middlebrook 7H9 medium supplemented with 0.5% glycerol, 10% Middlebrook ADC (Becton Dickinson) and 0.05% Tween-80 at 37°C in a roller bottle (Nalgene) rolling at 2 rpm or 50 ml falcon tubes (Corning) in an SB3 Tube Rotator (Stewart) at 28 rpm. For propionate utilisation experiments glycerol, ADC and Tween were replaced with 0.1% sodium propionate 0.5% Albumin fraction V and 0.05% Tyloxapol respectively. Kanamycin was added where required at 25 µg/ml and X-Gal where required at 50 µg/ml.

Escherichia coli (E. coli) strain DH5α was used for plasmid construction and grown in Luria-Bertani (LB) Agar or Broth using kanamycin at 50 µg/ml and X-Gal where necessary at 200 µg/ml. Details of all strains and plasmids used and constructed in this study are listed in Tables 2.1 and 2.2 respectively.

Strain or Plasmid	Relevant Characteristics	Source or Reference
M. tuberculosis strain	*M. tuberculosis* wildtype H37Rv used for the construction of all mutant strains	[172]
M. tuberculosis strain	Clinical isolates N0031, N0052, N0072, N0145, N0153	[173]
M. bovis strain	*M. bovis BCG* Pasteur	NIMR
DH5α sub cloning efficiency cells	*E. coli* cloning strain Genotype F– Φ80*lac*ZΔM15 Δ(*lac*ZYA-*arg*F) U169 *rec*A1 *end*A1 *hsd*R17 (rK–, mK+) *pho*A *sup*E44 λ– *thi*-1 *gyr*A96 *rel*A	Invitrogen

Table 2.1 Bacterial Strains used in this study

Table 2.2 Plasmids used and constructed in this study

Strain or Plasmid	Relevant Characteristics	Source or Reference
pBackbone	Mycobacterial suicide vector (kanamycin^R and ampicillin^R)	Gopaul, (2002)
pGOAL17	Plasmid containing the *sacB*/*lacZ* cassette (ampicillin^R)	Parish & Stoker, (2000)
pKP186	Integrating mycobacterial cloning vector that does not contain integrase (kanamycin^R)	Rickman et al., (2005)
PBSInt	Mycobacterial suicide vector containing integrase, electroporated in conjunction with pKP186 and its derivatives.	Springer et al., (2001)
pMSC12659	ncRv12659 expressed from native promoter	Houghton *et al*., (2013)
pKA302	pMV261 derived replicating over expression vector containing *M. smegmatis* rrnB (-200/-8)	Arnvig et al., (2009)
pKA303	pMV261 derived replicating over expression vector containing *M. smegmatis* rrnB (-80/-8)	Arnvig et al., (2011)
pKA305	XbaI-ClaI fragment from pKA302 cloned into pKP186 giving rise to an integrating over expression vector.	Dr. Kristine Arnvig, unpublished.
pKA306	XbaI-ClaI fragment from pKA303 cloned into pKP186 giving rise to an integrating over expression vector.	Dr. Kristine Arnvig, unpublished.
pJHP01	Targeting plasmid for removal of ncRv12659 in *M. tuberculosis* pBackbone containing ncRv12659 5′ and 3′ flanking regions, and the *sacB*/*lacZ* cassette.	This Study

Strain or Plasmid	Relevant Characteristics	Source or Reference
pJHP02	Targeting plasmid for removal of ncRv13661 in *M. tuberculosis* pBackbone containing ncRv13661 5′ and 3′ flanking regions, and the *sacB*/*lacZ* cassette	This Study
pJHP03	Targeting plasmid for removal of ncRv11690 in *M. tuberculosis* pBackbone containing ncRv11690 5′ and 3′ flanking regions, and the *sacB*/*lacZ* cassette	This Study
pJHP04	Targeting plasmid for removal of ncRv10243 in *M. tuberculosis* pBackbone containing ncRv10243 5′ and 3′ flanking regions, and the *sacB*/*lacZ* cassette	This Study
pJHP05	ncRv13661 complementing plasmid. pKP186 derivative containing 625bp coordinates 4100449-4101296.	This Study
pJHP06	ncRv10243 complementing plasmid. pKP186 derivative containing 448bp coordinates 293428-293876.	This Study
pJHP07	ncRv11690 complementing plasmid. pKP186 derivative containing 381bp coordinates1914888-1915269.	This Study
pJHP09	pKA305 derivative containing XbaI-ClaI fragment cut from pKA302 containing G2 (Arnvig et al., 2009)	This Study
pJHP10	pKA306 derivative containing XbaI-ClaI fragment cut from pKA303 containing G2 (Arnvig et al., 2009)	This Study

2.2 Recombinant DNA techniques

All general molecular cloning techniques were carried out according to standard methods (Sambrook 2001), using commercially available kits/enzymes where stated.

2.2.1 Polymerase chain reaction (PCR)

For PCR reactions where the product was required for downstream use a proofreading DNA polymerase was used. Primers were designed using the DNAstar lasergene program primer select, and synthesised by Sigma-Aldrich. All primers used in the study are listed in Appendix II.

PCR Reactions were performed in a final volume of 50 µl consisting of 1 x *Pfx* buffer, 1 x PCR Enhancer Solution, 1 mM $MgSO_4$, 300 µM each dNTP (Promega), 300 nM each primer (Sigma-Aldrich) and 2.5U of *Pfx* enzyme (Invitrogen).

Colony PCR's were performed in a final volume of 20 µl 1 x REDTaq ReadyMix PCR mix, which includes 1.5 mM MgCl2, 200 µM each dNTP and 1.5 U Taq DNA polymerase (Sigma-Aldrich), 5 % DMSO, 300 nM each primer, a single colony resuspended in the PCR mix as template or 1-2 µl of an instagene matrix preparation (BioRad) from *M. tb*.

DNA amplification was performed in an Applied Biosystems Veriti Cycler using a touchdown cycle. Cycles consisted of denaturation at 95°C for 5 minutes followed by touchdown cycles from 65°C to 56°C for 30 seconds followed by extension at either 68°C (for proofreading DNA polymerase) or 72°C (for non-proofreading DNA polymerase) for one minute per kilobase of product. 25 cycles were performed with the lowest annealing

temperature and completed with a final extension for 7 minutes. PCR products were analysed by agarose gel electrophoresis.

2.2.2 Agarose Gel Electrophoresis

DNA was separated on 0.8-2% agarose gels using 1 X TBE with 0.5 µg/ml ethidium bromide (Bio-Rad) to allow visualisation of the DNA.
1 x loading buffer was added to samples where necessary (30% glycerol, 0.25% bromophenol blue, 0.25% xylene cyanol) and run alongside 10 µl of a 1 kilobase ladder (Hyperladder I, Bioline). Gels were run at 100 V until the DNA had migrated sufficiently by observation of the Dye Fronts. DNA was visualised on a UV transilluminator (BioDoc-It Imaging System).

2.2.3 DNA Gel Extraction and PCR purification

DNA fragments were isolated using QIAquick Gel Extraction Kit (Qiagen) either straight from the PCR reaction or following agarose gel electrophoresis according to the manufacturer's instructions. Agarose pieces containing DNA were excised over a UV light box and solubilised in a binding buffer. This was bound to a silica membrane on a spin column and contaminants washed away. DNA was eluted in 30 µl of dH_20.

2.2.4 Plasmid DNA Extraction

Plasmid DNA was extracted from 5 ml of stationary phase *E. coli* cultures using the QIAprep Spin Miniprep Kit (Qiagen) according to

manufacturer's instructions. Cells were lysed under alkaline conditions with SDS to denature proteins and DNA, and to solubilise phospholipids of the cell membrane. Lysates were neutralised and adjusted to high salt conditions resulting in contaminants precipitating out and plasmid DNA staying in solution. Plasmid DNA was adsorbed to a silica membrane on a spin column and contaminants were washed away. DNA was eluted in 50 µl of dH_20.

2.2.5 Restriction endonuclease digestion of DNA

Restriction digestion of DNA was performed in 30 µl reactions for 30 minutes at 37°C using FastDigest Enzymes (Fermentas). Reactions contained 1 µl of each enzyme, 1 X FastDigest buffer (Fermentas), and 1 µg of DNA. For vector digests reactions also contained Antarctic Phosphatase (Fermentas) to prevent vector re-ligation. The reaction was inactivated by incubation at 65°C for 20 minutes.

2.2.6 Ligation of DNA

Ligations were performed using the Roche Rapid Ligation Kit according to manufacturer's instructions. Briefly 20 µl reactions containing 1 x Ligation buffer, 1 µl Ligase and 1:3 ratio of vector: insert DNA. Ligations were performed at room temperature for 15 minutes.

2.2.7 Transformation of chemically competent *E. coli*

2 µl of ligated DNA was transformed into 25 µl *E. coli* chemically competent sub cloning efficiency cells DH5α (Invitrogen). DNA and cells

were mixed and placed on ice for 30 minutes. Cells were heat shocked for 45 seconds at 42°C and placed back on ice for 2 minutes. Cells were allowed to recover at 37°C before plating on to selective media.

2.2.8 Sequencing of plasmid DNA

All plasmid constructions were sequenced to verify their identity. 100 ng/µl of construct was supplied to BioSource Sequencing Ltd with vector specific sequencing primers.

2.2.9 Site directed mutagenesis (SDM)

SDM oligonucleotides were designed with the desired mutation in the middle with approximately 20 nucleotides of complementary sequence both sides and a melting temperature of approximately 78°C. Primers were synthesised and purified using HPLC by Sigma. PCR amplifications were performed in 50 µl reactions volumes containing *Pfx* Amplification buffer, 1 X Enhancer buffer, 0.3 mM dNTPs, 100 ng of each oligonucleotide, 1 mM $MgSO_4$, 100 ng template plasmid DNA and 2.5 U *Pfx* (Invitrogen). The reaction mixture was incubated in a PCR thermocycler (Veriti applied biosystems) with an initial denaturation step at 95 °C for one minute followed by 18 to 25 cycles of 95 °C for 50 seconds, an annealing step of 60 °C for 50 seconds and a 68oC extension temperature for two minutes per kb of plasmid and then completed by a final extension at 68°C for seven minutes. Original template methylated DNA was then digested by addition of 1 µl DpnI (Fast Digest, Fermentas) and incubated at 37°C for 15 minutes. DNA

was then ethanol precipitated and the resulting plasmid transformed into chemically competent *E. coli* Supercompetent cells (Bioline)

2.3 DNase treatment and purification of RNA

Contaminating DNA was removed from RNA preparations using Turbo DNase (Ambion) according to the manufacturer's guidelines. Briefly, 10 µg of RNA was treated with 2 µl of Turbo DNase for a total of 1 hour as described in the protocol for a heavily contaminated sample. DNase was removed from the sample using acidified phenol: chloroform pH4.5 (Ambion) at a 1:1 ratio, vortexed and centrifuged at 17,100 xg for 10 minutes. The aqueous phase was removed and RNA precipitated with 1/10 volume of 3 M sodium acetate and 2.5 x volume of ethanol.

2.4 cDNA synthesis

First Strand cDNA synthesis was performed using superscript III Reverse Transcriptase (Invitrogen) according to the manufacturer's instructions using a reaction temperature of 50 ºC for 30 minutes followed by 55 ºC for 30 minutes.

2.5 qRT-PCR

Primers (supplied by Sigma-Aldrich) were designed using the Applied Biosystems software Primer Express and sequences listed in Appendix II. After cDNA synthesis, 1:100 and 1:10,000 dilutions were prepared. Each 20 µl qRT-PCR reaction, contained 1 x SYBRgreen (Applied Biosystems) 900 nm each primer and 5 µl of template cDNA of appropriate dilution. A

standard curve of genomic DNA was generated for each experiment to allow absolute quantitation. All genes were normalised to 16S measured using a 1:10,000 dilution of cDNA. mRNA or sRNA was quantified using a 1:100 dilution.

2.6 Northern Blotting

Northern blots were performed using 6-8% denaturing acrylamide gels (Appendix I). Depending on the abundance of the sRNA a total of 500 ng-10 µg RNA was loaded per well. Each sample contained 1 x Gel loading buffer II (Ambion8547) and was heated at 80 °C for 2 minutes before loading. 10 µl of RNA marker low (Abnova) for size determination was loaded alongside the samples. The RNA was transferred onto Ambion's brightstar membrane for 1 hour in 0.5 x TBE by electroblotting at 1.5 mA per cm^2 of membrane. After transfer the RNA was crosslinked to the membrane by UV before visualising using 0.3 M sodium acetate containing 0.03% methylene blue.

Membranes were pre hybridised with Ultrahyb Buffer (Ambion) for at least 30 minutes at 65 °C before the addition of the riboprobe. Riboprobes were made using oligo templates and the mirVana miRNA probe construction kit (Ambion) and left to incubate with the membrane overnight. Membranes were washed twice with 2 X SSC + 0.1% SDS, once with 0.2 X SSC + 0.1% SDS and once with 2 x SSC. Membranes were visualised using a phosphoimager screen and storm860 scanner.

2.7 Rapid Amplification of cDNA ends (RACE)

2.7.1 5' Rapid Amplification of cDNA ends (RACE)

5' RACE was performed using the GeneRacer kit (Invitrogen). 5 µg of *M. tb* RNA was treated with tobacco acid pyrophosphatase to digest the triphosphate group at the 5´ end of all transcripts, generating 5´-monophosphorylated transcripts. The GeneRacer™ RNA Oligo RNA was added to 0.25 µg GeneRacer RNA Oligo and heated at 65 ºC for 5 minutes. The 10 µl ligation reaction was performed in 1 x ligase buffer, with 10 nm ATP, 40 U RNaseOut and 5 U T4 RNA ligase; samples were incubated at 37 ºC for 1 hour. RNA was extracted with acidified phenol: chloroform and ethanol precipitated with 2.5 volumes with 1/10 3 M sodium acetate. RNA was re-suspended in DEPC-treated H_2O, to which 100 ng random primers and 0.5 mM each dNTP were added, and incubated at 65ºC for 5 minutes.

The reverse transcription (RT) reaction was performed with the addition of primer mixture, 1 x First Strand buffer, 5 mM DTT, 40 U RNaseOut and 200 U SuperScript III RT. Incubation was initially at 25 ºC for 5 minutes followed by 1 hour at 50 ºC. RT was inactivated at 70 ºC for 15 minutes, 2 U RNase H was added to remove the RNA/DNA Hybrids and incubated for 20 minutes at 37 ºC.

cDNA was amplified using the GeneRacer 5' Primer and a gene-specific reverse primer (GSP), using Platinum *Pfx* DNA polymerase. The PCR was conducted as a touchdown, starting with a high annealing temperature and decreasing one degree each cycle. Cycle parameters were an initial 94 ºC denaturation step, 5 cycles of 94 ºC for 30 seconds

and 72 ºC for 1 minute/kb DNA, 5 cycles of 94 ºC for 30 seconds and 70 ºC for 1 minute/kb DNA followed by 25 cycles of 94 ºC for 30 seconds, 65 ºC for 30 seconds and 68 ºC for 1 minute/kb DNA. The cycle finished with an elongation step of 68 ºC for 10 minutes. Only cDNA containing the GeneRacer™ sequences will be PCR amplified.

PCR products were analysed by agarose gel electrophoresis, gel extracted, TOPO cloned and sequenced. Transcriptional start sites were identified as directly adjacent to the GeneRacer RNA Oligo sequence.

2.7.2 3' RACE

5 µg of *M. tb* RNA was poly-A tailed using 1 x poly-A polymerase buffer, 2 U poly-A polymerase, 10 nM ATP, and water to 25 µl. The reaction was incubated for 1 hour at 37 °C. 50 µM oligo d (T) primer from the GeneRacer kit was added to the poly-A tailed RNA before precipitating with 1/10 volume of 3 M sodium acetate, and 3 x volume of ethanol.

Reverse transcription was performed on the resulting RNA using Superscript III using a reaction temperature of 50ºC for 30 minutes followed by 55 ºC for 30 minutes.

cDNA was amplified using the GeneRacer 3' Primer and a gene-specific reverse primer (GSP), using Platinum *Pfx* DNA polymerase. The PCR was conducted as a touchdown, starting at 68°C and decreasing one degree each cycle. Cycle parameters were an initial 94 ºC denaturation step, 5 cycles of 94 ºC for 30 seconds and 72 ºC for 1 minute/kb DNA, 5 cycles of 94 ºC for 30 seconds and 68 ºC for 1 minute/kb DNA followed by 25 cycles of 94 ºC for 30 seconds, 62 ºC for 30 seconds and 68 ºC for 1 minute/kb DNA. The cycle finished with an elongation step of 68 ºC for

10 minutes. Only cDNA containing the GeneRacer™ sequences will be PCR amplified.

PCR products were analysed by agarose gel electrophoresis, gel extracted, TOPO cloned and sequenced. Transcriptional start sites were identified as directly adjacent to the poly-A tail.

2.8 Western Blotting

Protein samples were run on a 10% Bis-Tris Gel (Invitrogen) for 50 minutes at 200 V in MOPS buffer. The gel was placed in semi-dry transfer buffer for 5 minutes. The PVDF Immobilon-P membrane (Millipore) was prepared by washing in methanol for a few seconds, then with dH2O before placing in the semi dry transfer buffer for 5 minutes. Proteins were then electro-blotted onto the prepared membrane using a semi-dry blotter at 1 mA per cm^2 for 1 hour. In order to detect specific proteins, the membrane was incubated in blocking buffer (see Appendix I) overnight at 4 ºC. The membrane was washed three times with TTBS for 5 minutes before incubation with the primary antibodies for RNAP β (Santa Cruz 8RB13) and α (Santa Cruz 4RA2) at 1:1000 in blocking buffer for 2 hours. The three wash steps were then repeated and the membrane then incubated in blocking buffer containing the secondary antibody goat anti-mouse-HRP) for 1 hour followed by a further three wash steps.

Detection was via ECL Western blotting detection reagents (GE Healthcare). Equal volumes of reagents 1 and 2 were mixed and poured onto the protein side of the membrane. After 1 minute excess liquid was removed, the membrane was wrapped in Saranwrap™ and exposed to autoradiograph film (GE Healthcare). Films were developed using an automatic developer (Fujifilm).

2.9 Mycobacterial Specific Techniques

All manipulations of *M. tb* were performed in Containment level III facilities in a Class I hood.

2.9.1 Preparation of mycobacterial competent cells

Rolling cultures of mycobacteria were grown to OD_{600nm} of 1.0, 0.1 volumes of 2 M glycine were added and the culture left incubating overnight. The next day the cells were collected by centrifugation at 2,100 xg for 10 minutes at 4°C. They were subsequently washed three times with 0.5 x volume of cold 10% glycerol finally resuspending in 1/10 of the original culture volume. Cells were then electroporated according to published protocols (Jacobs et al., 1991).

2.9.2 RNA Isolation

Exponential phase cultures were harvested at an optical density (OD_{600nm}) of between 0.5-0.8, whilst stationary phase cultures were harvested 1 week after OD had reached 1.0. When ready, cultures were cooled rapidly with addition of ice and pelleted at 2,100 xg for 10 minutes. RNA was isolated from the pellet using the FastRNA Pro Blue Kit from MP Biomedicals following the manufacturer's instructions. RNA concentration was measured by ND-1000 spectrophotometer (nanodrop) and RNA integrity measured by the 2100 Bioanalyzer using a Nano chip.

2.9.3 Genomic DNA Extraction

Half a plate of confluent *M. tb* was scraped into 300 µl of TE Buffer and heat killed at 80°C for 1 hour. Cells were lysed using lysozyme and

lipase at a final concentration of 2 mg/ml each for 2 hours at 37°C with the addition of DNase-free RNase. Samples were snap frozen on dry ice and ethanol before incubating at 75 °C for 10 minutes. Proteinase K was added to a final concentration of 0.5 mg/ml with SDS at 0.5% and incubated for 1 hour at 50°C. DNA was extracted with phenol: chloroform: isoamyl alcohol. The sample was spun to separate the phases and then the aqueous phase was twice extracted with chloroform only. DNA was then precipitated with 1/50 volume 5 M NaCl and 2.5 volumes of ethanol.

2.9.4 Instagene Preparations of *M. tb*

Quick DNA preparations from *M. tb* suitable for PCR were achieved using the BioRad Instagene Matrix solution. The matrix adsorbs cell lysis products that could interfere with the PCR reaction. A loopful of bacteria was picked into 200 µl of Instagene Matrix solution, vortexed, and heated at 56°C for 15 minutes. Finally the each sample is then boiled at 98°C for 8 minutes before spinning at 17,100 xg to remove the cell debris. Approximately 2 µl of the resulting supernatant can then be used in a 50 µl PCR reaction

2.9.5 *M. tb* Cell Free Extract

M. tb exponential phase cultures were grown to an OD_{600} of between 0.5-0.8, whilst stationary phase cultures were grown for 1 week after OD_{600} had reached 1.0. The cultures were pelleted at 2,100 xg for 10 minutes washed twice in PBS before re-suspending in buffer. Cells were lysed in a fast prep instrument at a setting of 6.0 for 30 seconds three times using

150-212 micron glass beads. Lysates were centrifuged at 17,100 xg for 10 minutes and the cleared lysate filtered using a 0.22 µM filter (Millipore) for removal from Cat III.

2.9.6 Sample Preparation for Proteomic Analysis

M. tb was grown to exponential phase and stationary phase as detailed in *M. tb* cell free extract. The cultures were pelleted at 2,100 xg for 10 minutes and washed twice with PBS. Cultures were re-suspended in the same original culture volume of PBS and incubated at 37ºC. At time points 0, 24 and 96 hours 30 mls of cell suspension were pelleted at 2,100 xg before lysing of cells as detailed in *M. tb* cell free extract. The following Lysis Buffer was used; 0.1 M Ammonium bicarbonate buffer containing 8 M Urea and 0.2% Rapigest (Waters).

Samples were sent to ETH, Zurich Institute of Molecular Systems Biology and analysed by Olga Schubert by Mass Spectroscopy.

2.9.7 Sucrose Gradients

M. tb was grown to exponential phase and stationary phase as detailed in *M. tb* cell free extract. Cultures were then treated with 50nM 4-thio uridine and incubated overnight for incorporation. Cells were concentrated into 10 mls by centrifugation at 2,100 xg. The concentrated cells were then placed in a petri dish on ice and cross-linked with ultra violet light 3 times at 1200. Cell pellets were collected at 2,100 xg ribolysed 3 times in a chilled rotor at setting of 6.0 for 30 seconds in a volume of 600 µl. Lysis was performed in the following lysis buffer: 20

mM Tris, 150 mM KCl, 10 mM $MgCl_2$, 1 mM DTT, and 10 µl of Superase Inhibitor (Ambion). The sucrose gradient buffers contained Roche complete protease inhibitor cocktail, 20 mM Tris, 150 mM KCl, 10 mM $MgCl_2$ and 1 mM DTT. 400 µl of lysate was layered carefully onto the top of a 5-30% sucrose gradient in Ultra-Clear tubes and spun in a SW41 rotor for 16.5 hours at 154,000 xg at 4ºC.

600 µl fractions were collected by AKTA connected to a 254 nm and 280 nm filter. Each fraction was divided into 300 µl for RNA extraction and 300 µl for protein extraction as detailed in 2.9.8 and 2.9.9.

2.9.8 RNA extraction from sucrose gradient fractions

RNA was extracted from each fraction using acidified phenol: chloroform pH4.5 (Ambion) at a 1:1 ratio, vortexed and spun down at 17,100 xg for 10 minutes. The aqueous phase was removed and RNA precipitated with 1/10 volume of 3 M sodium acetate and 2.5 x volume of ethanol.

2.9.9 Protein extraction from sucrose gradient fractions

Protein was extracted by adding 1 x volume 50 mM Tris pH8.0 and 25% final volume of Pyrogallol Red-molybdate. Solution was left to precipitate overnight at 4°C and centrifuged at maximum speed of 17,100 xg for 20 minutes to collect the precipitate. The supernatant was aspirated and discarded immediately due to pellet instability.

2.9.10 Creating Deletion Strains in *M. tb*

Allelic replacement techniques were used to generate *M. tb* knockout mutants as per published protocol [174]. Briefly, approximately 1kb flanking each region of deletion was cloned into suicide vector pBackbone containing a kanamycin resistance cassette and a *LacZ/SacB* fragment to allow for selection of single crossover and double cross over events.

2.9.11 Macrophage Infection

Bone marrow derived macrophages (BMDMs) were generated from 6-8 week old Balb/C mice in RPMI-1640 (Gibco) containing 10% foetal calf serum, 20 µM L-glutamine, 1 mM sodium pyruvate, 10 µM HEPES and 50 nM β-mercaptoethanol. The cells were then grown and differentiated in complete RPMI-1640 supplemented with 20% L929 cell supernatant for 6 days at 37°C in 5% CO_2. The differentiated cells were seeded at a density of 2 x 10^5 cells/well in 1 ml complete RPMI-1640 supplemented with 5% L929 cell supernatant and incubated overnight prior to infection.

M. tb strains for infection were grown to an OD_{600} of 0.5-0.8 and inocula prepared by washing and resuspending the cultures in PBS, to produce a single cell suspension. This was used to infect BMDMs at a multiplicity of infection (MOI) of 0.1:1. After 4 hr, the cells were washed to remove all extracellular bacilli, and medium was replaced and incubation continued. Macrophages were lysed with water-0.05% Tween 80 to release intracellular bacteria after 4, 24, 72, 120 and 168 hr post-infection. Bacilli were serially diluted in PBS-Tween and plated on 7H11 with OADC.

Plates were incubated for 3-4 weeks to obtain counts of surviving bacteria.

2.9.12 Aerosol infection of mice with *M. tb*

Strains of *M. tb* for infection were grown to mid log in 7H9 and then supplied to Angela Rodgers (a trained animal licensee) for infection of the mice. Groups of 6–8 week old Balb/C mice were infected by low-dose aerosol exposure with *M. tb* using a Glas-Col (Terre Haute, IN) aerosol generator calibrated to deliver approximately 100 bacteria into the lungs. Bacterial counts from the lungs (n = 5) at each time point were determined by plating serial dilutions of individual lung homogenates on duplicate plates of 7H11. CFUs were counted after 3–4 weeks incubation at 37°C.

Balb/C mice were bred and housed under specific pathogen free conditions at the Medical Research Council, National Institute for Medical Research. Protocols for experiments were performed, under project license number 80/2236, in accordance with Home Office (United Kingdom) requirements and the Animal Scientific Procedures Act, 1986.

2.9.13 Microarray Analysis

Microarray Analysis was performed using arrays on ncRv13661, ncRv10243, and ncRv11690 mutants against H37Rv wild type using RNA extracted from exponential phase cultures. Over expression of ncRv11690 and ncRv12659 was also compared against vector control under exponential conditions. Whole genome *M. tb* microarray slides

were purchased from Agilent Technologies through the Bacterial Microarray Group at St. George's (BμG@S), University of London. For cDNA synthesis 2 μg of RNA was labelled individually with both Cy-3 and Cy-5 dyes (GE Healthcare) using Superscript III reverse transcriptase (Invitrogen). Dye swaps were performed and the cDNA hybridized to an 8-Chamber Agilent slide at 65°C for 16 hours before washing the slide with Oligo aCGH Wash Buffer 1 (Agilent) for 5 minutes at room temperature and Oligo aCGH Wash Buffer 2 (Agilent) for 1 minute at 37°C. Slides were stabilized using Agilent's Stabilisation and Drying Solution according to manufacturer's instructions.

Slides were scanned at 5 microns using an Agilent Technologies Microarray Scanner at BμG@S. Txt files created by the Agilent scanner were analysed using Genespring 12.0 filtering on flags and expression. T-test against zero was performed and p-value selected as $p<0.05$, correcting for multiple comparisons using Benjamini-Hochberg. The array design is available in BμG@Sbase (Accession No. A-BUGS-41; http://bugs.sgul.ac.uk/A-BUGS-41) and also ArrayExpress (Accession No. A-BUGS-41).

3 Investigating a function for the starvation induced sRNA ncRv10243

3.1 Introduction

The sRNA originally termed F6 was first identified from cDNA cloning of size fractionated total RNA from *M. tb*. Out of 192 clones, 3 possessed the intergenic region between fadA2 and fadE5 containing F6 (Figure 3.1), which was isolated from both exponential and stationary growth phases [153]. This study showed by 5' and 3' RACE that a primary transcript of 102 nucleotides existed. Northern blotting revealed a shorter ~55 nucleotide transcript of greater abundance which could be due to processing of the primary transcript. In the same study, reverse transcription PCR (RT-PCR) showed this sRNA to be co transcribed with the upstream gene *fadA2*.

F6 was also identified from a screen in BCG by using a dual approach of cDNA cloning and *in silico* prediction to identify novel sRNAs, and was termed Mcr14. The two names for the same sRNA arose due to the lack of guidelines for sRNA annotation. To avoid confusion a new nomenclature has been suggested [171] and from now on F6 will be referred to as ncRv10243 as per the new guidelines. When ncRv10243 was first discovered, a putative SigF promoter was identified upstream of the 5′ end [153]. This was later confirmed by ChIP-on-chip with SigF which was found to give a very strong signal at the sRNA promoter [175]. Although ncRv10243 and *fadA2* were found to be co transcribed, no expression of the sRNA is observed in a SigF deletion strain by northern blotting indicating that the co transcription observed by RT-PCR was probably read-through from the *fadA2* promoter (Houghton & Arnvig unpublished).

SigF was initially found in BCG to be a stationary phase response sigma factor that is also induced upon cold shock and nitrogen depletion. However in *M. tb*

only nutrient starvation shows some induction of *sigF*. This non-essential sigma factor is conserved in most mycobacteria, and deletion leads to an attenuation in mice and guinea pig models of infection [176-178]. sRNA ncRv10243 is also highly conserved in pathogenic mycobacteria, with the 3′ end being less well-conserved in non-pathogenic mycobacteria.

As bacterial gene expression is differentially regulated in response to stress, it can be useful to model the stresses encountered within the mycobacterial host environment in order to assess whether a particular gene product could be important for pathogenesis. Initial studies of ncRv10243 expression showed a two-fold induction in response to acid stress [153] indicating that this sRNA could indeed be important for pathogenesis, as is the case for other pathogens [151]. In particular *M. tb* encounter acid stress upon phagosome lysosome fusion [179], or through acidification of the phagosome when macrophages are stimulated by IFN-γ [180].

In *M. tb* over expression of ncRv10243 resulted in extremely slow growth with pin prick colonies visible only after 3–4 weeks. The expression of ncRv10243 did not result in any apparent growth defects in *M. smegmatis* although the 5' end and central loop containing part of this sRNA are conserved [153].

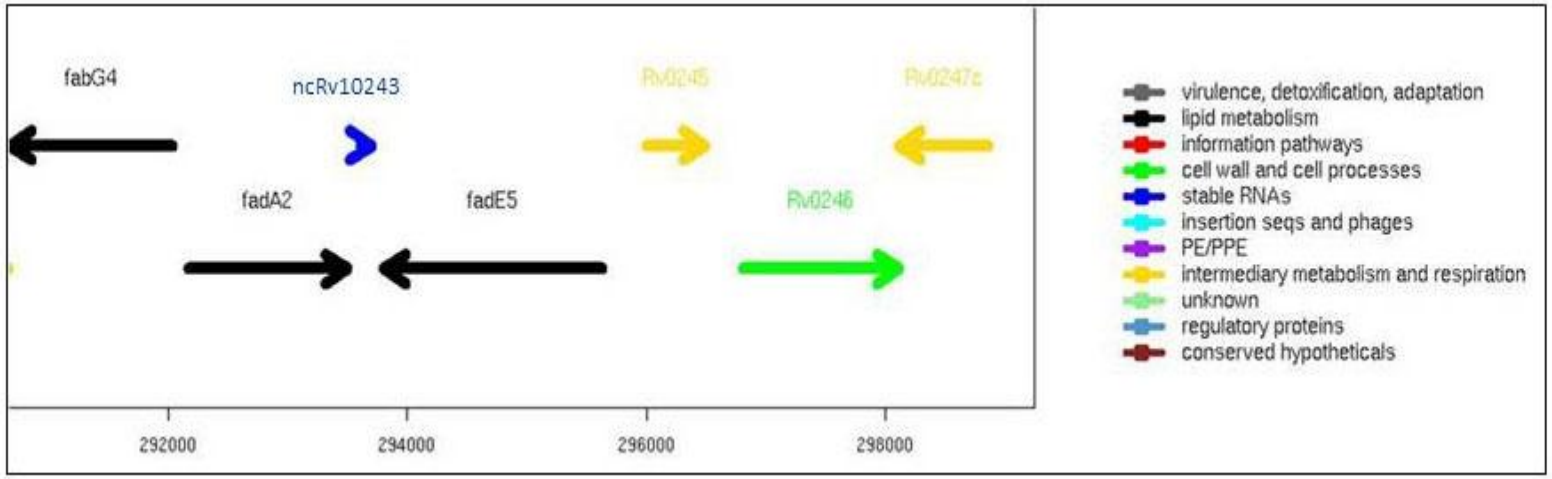

Figure 3.1 Genomic location of sRNA ncRv10243 in the *M. tb* genome as viewed in Tuberculist (http://tuberculist.epfl.ch/)

3.2 Hypotheses and Specific Aims

It is difficult to speculate on possible targets for trans-encoded sRNAs but genome locations can give clues. As well as being co-transcribed with *fadA2*, whose transcription is down regulated in macrophages [181], ncRv10243 is located within a region encoding enzymes involved in lipid metabolism.

Phenotypic changes resulting from experimental manipulation of sRNA expression levels provide an alternative route to target identification. In this study we aimed to take an unbiased approach to identifying the function and possible regulons of ncRv10243 by removing the chromosomal copy from *M. tb* and performing gene expression analysis. This approach was taken due to the previously observed deleterious phenotype of over expression [153].

Many sRNAs regulate their targets by masking the ribosome binding sites in order to inhibit ribosome entry on mRNA (see Section 1). Since the half-life of bacterial mRNAs is strongly affected by the association with ribosomes [182], translation inhibition is often coupled to the decay of the repressed target, e.g., by accelerating RNase E-mediated mRNA turnover. Therefore if a sRNA that represses translation of an mRNA is no longer expressed, the abundance of that message would be increased. Microarrays can be used to assess the relative abundance of mRNAs in both wildtype and deletion strains in order to identify possible sRNA targets.

3.3. *In vitro* and *In vivo* expression levels of ncRv10243

ncRv10243 had previously been shown to be up regulated two-fold in response to acid stress [153]. In order to identify additional stimuli for ncRv10243, quantitative RT-PCR (qRT-PCR) was performed as described in section 2.8, to assess the expression conditions from a variety of growth conditions. RNA extracts from *M. tb* H37Rv were prepared from exponential phase cultures, starvation cultures, and *M. tb* isolated from the lungs of infected mice at 21 days post infection Figure 3.2. The qRT-PCR primers used can be found in Appendix II.

The results show that while ncRv10243 is well expressed in exponential phase, it is up regulated 6-fold in response to infection of mice lungs, and even further up regulated in response to 96 hours starvation in PBS (20-fold on average) when compared to exponential phase expression.

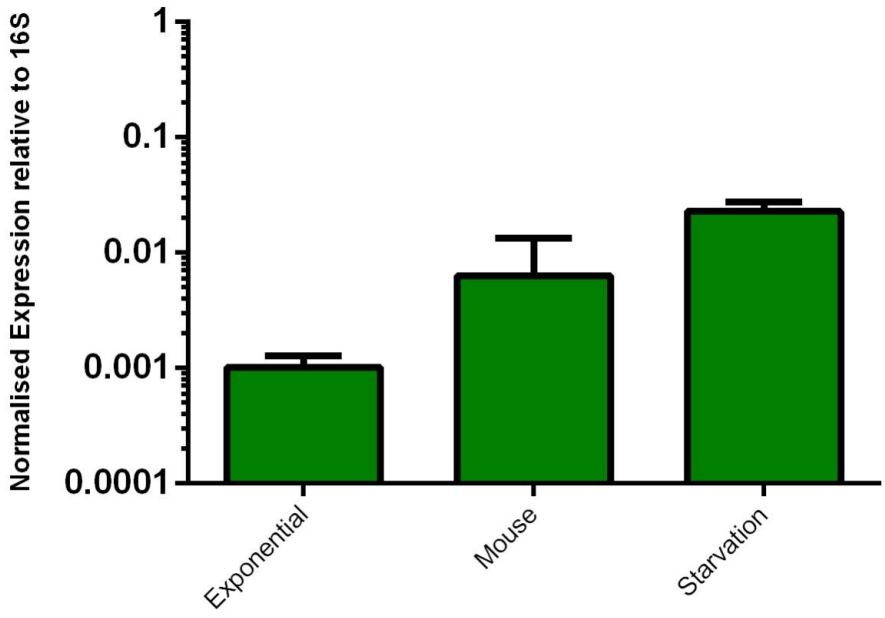

Figure 3.2 Expression levels of ncRv10243 in *M. tb*

ncRv10243 expression levels were measured using qRT-PCR, in each instance ncRv10243 levels are expressed relative to 16S rRNA control. ncRv10243 is a well expressed sRNA in exponential phase that is up regulated upon (96 hours) starvation in PBS. Analysis of *M. tb* RNA from the lungs of three week infected mice showed ncRv10243 to also be up regulated in response to infection. Data represents the mean and standard deviations of three biological replicates for each condition.

3.4 Creation of a ncRv10243 deletion strain

This study set out to identify possible targets of ncRv10243 through the creation of a deletion strain in which the sRNA is entirely removed from the chromosome. Creation of a deletion strain relies on allelic exchange by which homologous recombination causes the chromosomal copy of a gene or genes to be replaced by a mutated/modified version of the gene. The mutation was introduced by using a non-replicating suicide vector [7] in a two-step process. Initially, a single cross-over (SCO) recombinant was isolated from the electroporation of *M. tb* with the targeting construct. These colonies were screened to verify a successful recombination event and only SCO candidates subjected to counter-selection in order to obtain double crossovers (DCO) generated by a second recombination event. PCRs to screen both SCO and DCO are represented in Figure 3.3A. The markers *sacB* and *lacZ* on the targeting construct allow for blue/white screening of colonies and make counter-selection for sucrose sensitivity possible, this ease of screening and selection thereby greatly increases the efficiency of creating deletion mutations in *M. tb* [183].

3.4.1 Design and creation of the deletion plasmid

In order to delete ncRv10243 from the chromosome of *M. tb* the strategy was to remove the sRNA from the chromosome in an unmarked manner. This is to avoid possible effects of an antibiotic cassette which are unrelated to the sRNA. For homologous recombination to occur between the deletion plasmid and the bacterial chromosome, approximately 1.5 kbp from either side of ncRv10243 was cloned sequentially into the suicide vector pBackbone before removing the sRNA by site directed mutagenesis

(SDM). From the 5' flank the bases from coordinates 292520-293605 were first PCR amplified and then cloned, followed by the 3' flank encompassing the bases from coordinates 293709-294600.

In addition to the Kanamycin resistance (Kan^R) cassette already included in the pBackbone plasmid, was the inclusion of the *sacB/lacZ* cassette. The *sacB* gene encodes for levansucrase, responsible for hydrolysis of sucrose to glucose, and the *lacZ* gene encodes for β-galactosidase, which hydrolyses X-Gal in the media to a blue precipitate.

3.4.2 Screening of single and double crossover candidates

The SCO selection uses Kan^R and blue/white screening. Blue colonies on Kanamycin media indicate that the cells express β-galactosidase and are resistant to kanamycin and therefore a possible single recombination event has occurred. After removal of selective pressure by streaking onto non-selective media, SCO candidates can be resuspended and plated to single colonies on 7H11 containing sucrose, which is toxic when *sacB* is expressed. A second recombination event will generate DCOs in which the plasmid backbone containing the Kan^R and *sacB* genes are lost along with the wildtype region targeted for deletion. The result is that the cells are now kanamycin sensitive and sucrose resistant.

After electroporation with the targeting plasmid into *M. tb* H37Rv, cells were plated onto 7H11 containing Kanamycin and X-Gal. After incubation, 4 blue colonies were screened by PCR to identify true SCOs from random integrations Figure 3.3B. As the region of deletion in this instance was only ~150bp, it was difficult to differentiate wildtype bands from SCO bands. Therefore the resulting PCR products were gel extracted and sent for

sequencing. Sequencing revealed 1 SCO, which was then streaked onto non-selective 7H11 for the second recombination event to occur. Full loss of the backbone of the deletion plasmid was confirmed by streaking out onto 7H11 plus Kanamycin and X-Gal, and also 7H11 without antibiotic, plus X-Gal. Only 1 Colony (#4) from DCO selection was white and Kanamycin sensitive. This DCO candidate was screened by PCR amplification and sequencing of the PCR product, which confirmed the deletion of the sRNA from the *M. tb* genome.

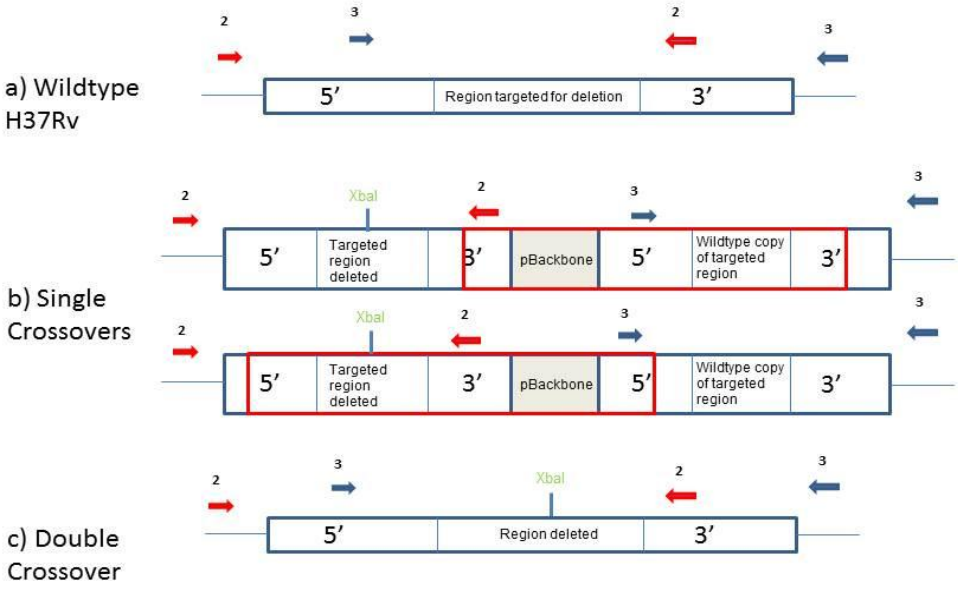

Figure 3.3A Schematic of PCR reactions for screening *M. tb* SCO and DCO strains

Diagram indicates the three PCR reactions used to distinguish between a) wild type *M. tb*, b) single crossovers of either orientation or c) double crossovers. Primer pairs are gene specific, numbered according to the target region and designated either pair2 or pair3. Primer sequences can be found in Appendix II. PCR screening was performed on Instagene preparations from streaked out colonies. PCR reactions are designed so that orientation of a crossover event can be identified. Importantly a random integration can be discerned from a SCO as phenotypically they result in the same characteristics on agar.

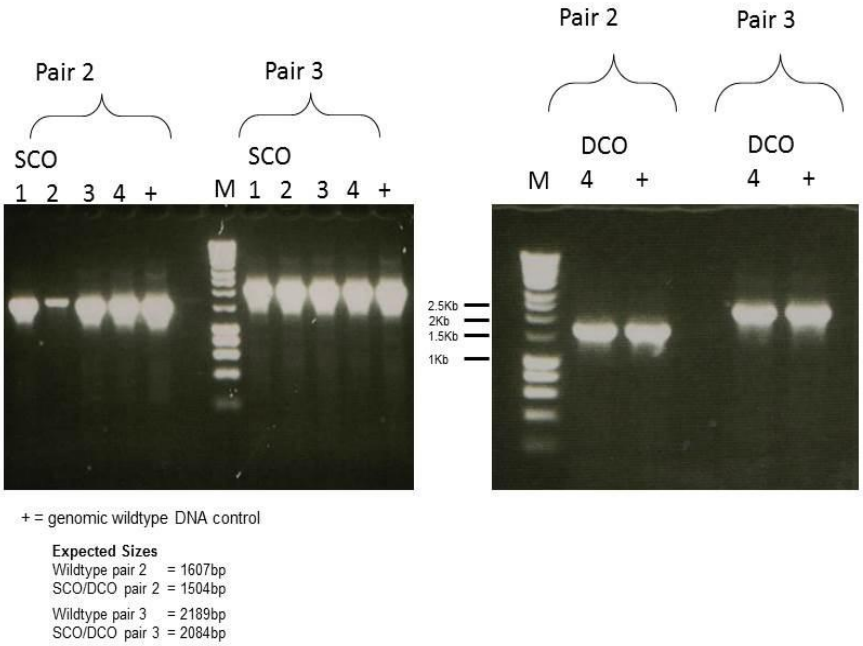

Figure 3.3B PCR screening for the construction of the ncRv10243 deletion strain.

PCR reactions were designed using the strategy outlined in Figure 3.3A. Expected sizes of products for each primer pair are indicated. Due to the small size of deletion, these PCR products were consequently gel extracted as detailed in section 2.2.3 and sequenced directly. SCO = single crossover; DCO = double crossover; M = Bioline Hyperladder I DNA marker.

3.5 Complementation of the ncRv10243 mutant

As the aim of this study was to characterise the phenotype of a ΔncRv10243 deletion strain, it was essential to complement the loss of the sRNA by replacing the lost chromosomal copy.

In order to achieve this the sRNA and its promoter were PCR amplified along with a portion of upstream and downstream sequence (for coordinates see table 2.2), before cloning into pKP186. The resulting plasmid pJHP06 was electroporated into the mutant strain and presence selected for using kanamycin 7H11 agar. Presence of the complementing plasmid was confirmed by PCR from Instagene preparations.

The complementing strain should in theory have the same phenotype as wildtype *M. tb* H37Rv and any non-complemented phenotypes could be due to a secondary mutation elsewhere in the genome or to an antisense effect as a result of the ncRv10243 promoter transcribing across and into *fadE5*. The ΔncRv10243 strain was also whole genome sequenced to identify any possible mutations that would result in a change of expression or amino acid.

3.6 Full Genome sequencing of the ncRv10243 mutant

High Quality genomic DNA was extracted from the mutant and the parental H37Rv strain (as per Section 2.4). Sequencing libraries were prepared from both strains and sequenced by the HTS sequencing facility at NIMR. The resulting reads were aligned to the H37Rv reference genome by Graham Rose (NIMR) and single nucleotide polymorphisms (SNPs) were identified. There are two types of SNPs; a synonymous SNP, which does not change protein function as the nucleotide change does not

result in an amino acid replacement, and a nonsynonymous SNP, which has the potential to alter protein function as the nucleotide change results in an amino acid substitution in the protein.

Alignment of the genomic sequence of ΔncRv10243 identified 6 SNPs in the DCO selected for use (Appendix III). Two of these were due to the *Xba*I site being inserted into the chromosome from the removal of the sRNA. Two SNPs were found in Rv0279c PE_PGRS4, which is a repeat region and therefore could be excluded from analysis due to unreliability. There was 1 nonsynonymous SNP in Rv2541; a hypothetical alanine rich protein, and finally an intergenic SNP at coordinate 4178146 between Rv3728 and Rv3729. As no known function for these regions exist it is impossible to predict the effect of such SNPs on the phenotype of *M. tb*. However, if a phenotype was observed in the deletion strain and it cannot be complemented, it is a possibility that it could be due to these mutations.

3.7 Assessment of ncRv10243 expression in deletion and complement strains

To confirm the removal of the sRNA and to assess the degree of complementation achieved, RNA extracts were prepared from H37Rv, ΔncRv10243, and the complemented strain. cDNA was prepared after removal of contaminating DNA, and expression of ncRv10243 was assessed by qRT-PCR as detailed in the materials and methods section 2.7. Reverse transcriptase negative reactions (RT-) were prepared and assessed in parallel with reverse transcriptase positive reactions (RT+). RT- absolute values were subtracted from RT+ absolute values before normalising to 16S. This allows for any contribution from DNA

contamination to be removed from the final calculation. The normalisation results in a value of relative expression to 16S and provides an internal control for differences in efficiency of first strand cDNA synthesis. 16S was chosen as a suitable gene for normalisation due to its lack of variation in abundance**.** qRT-PCR showed that ncRv10243 was undetectable in the ΔncRv10243 strain (Figure 3.4). There was no statistical significance in the expression level of ncRv10243 between the wild type and complement strain (Figure 3.5; Unpaired t-test, $p>0.05$).

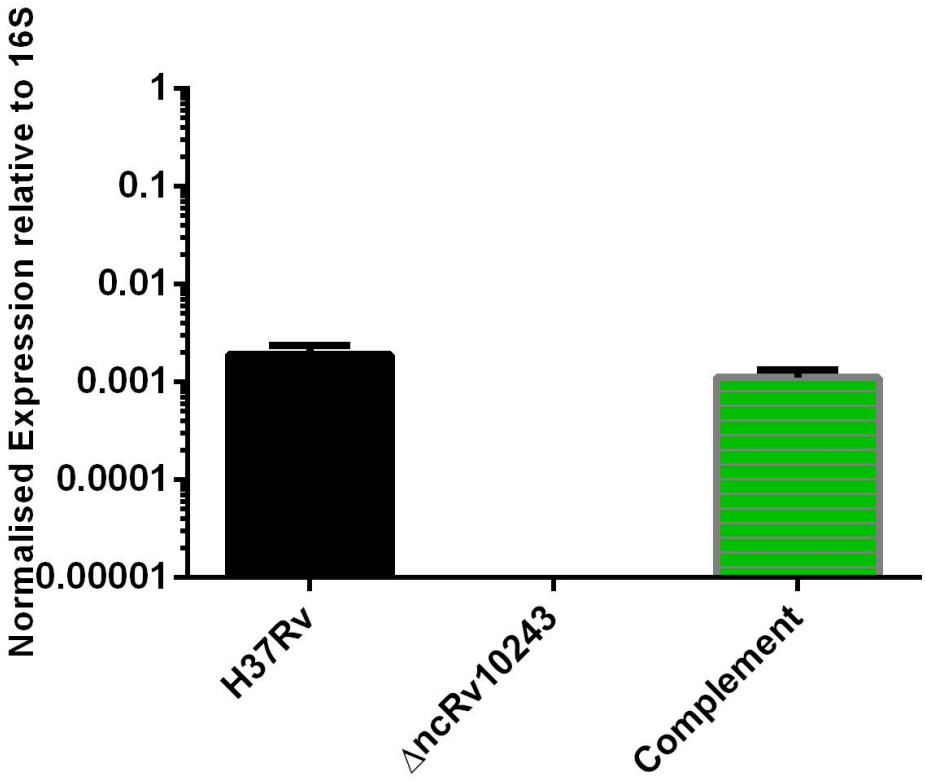

Figure 3.4 qRT-PCR confirmations of ncRv10243 deletion and complementation

Each strain was grown to exponential phase in standard 7H9 media and RNA then extracted. qRT-PCR was performed as described in section 2.8. In each instance sRNA expression is expressed relative to 16S, an rRNA control. Data represents the averages and standard deviations of three biological replicates for each strain.

3.8 *In vitro* phenotype analysis of growth compared to wildtype

In the first instance the ΔncRv10243 strain was assessed for an *in vitro* growth phenotype by comparing growth of the deletion strain against wildtype and complement strain. Cultures were grown to exponential phase (OD_{600} ~0.6) in 7H9 media, and these cultures were used to inoculate fresh media to an OD_{600} = 0.05. The OD_{600} was monitored until a plateau of growth was reached. No significant difference was observed between the doubling times of the three strains (Figure 3.5) as assessed by Linear regression analysis, $p>0.05$, showing that deletion of ncRv10243 has no effect on *in vitro* growth of *M. tb under* these conditions.

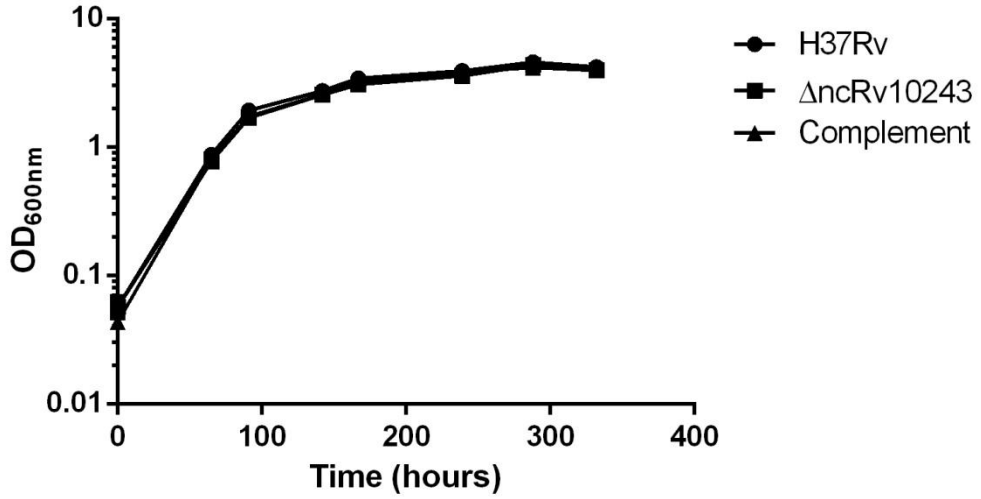

Figure 3.5 Growth of ΔncRv10243 in standard 7H9 media

In vitro growth curves of wildtype *M. tb* H37Rv, the ΔncRv10243 deletion strain and the complement using standard 7H9 media in a rolling culture system. The data represents the averages and standard deviations of three biological replicates. No significant difference was observed between the slopes for each strain as tested by linear regression.

3.9 Growth is inhibited in the Wayne Model

ncRv10243 is known to be under the control of SigF [175] a sigma factor which is induced in the Wayne model, developed by Lawrence Wayne as a simple *in vitro* model of dormancy for *M. tb* through oxygen limitation [30].The lack of growth defect observed in the deletion strain when grown under standard *in vitro* conditions along with the induction of SigF in the Wayne model, led to the hypothesis that a growth defect would be observed under low oxygen tensions (hypoxia). When grown in sealed tubes with slow stirring, tubercle bacilli cease replicating when oxygen concentrations decrease to the micro-aerobic level (1% oxygen saturation, ~100 hours), at which time/stage they enter a state of non-replicating persistence (NRP-1). With continued incubation the oxygen levels decrease to anaerobic levels (0.06% oxygen saturation, ~200 hours) inducing the second state, NRP-2. To allow for differences in respiration rate, depletion of oxygen for each strain is monitored by a methylene blue indicator tube set up for each strain at the start of incubation. Upon depletion of oxygen the methylene blue becomes reduced and turns from blue to colourless. After 14 days, cultures were plated onto 7H11 agar for assessment of survival. Plates were incubated for 3 weeks and colony forming units (CFU) counted. In addition, the anaerobic cells were assessed for their ability to be resuscitated. This was done by diluting the cultures to OD_{600} = 0.05 in fresh media and monitoring growth (OD_{600}). Enumeration of bacteria was necessary to ensure that an equal number of bacteria were inoculated into the growth curves to ensure an accurate phenotype would be observed.

There was no significant difference in CFU after incubation in the Wayne model between the wildtype H37Rv strain and either the ΔncRv10243 or the complemented strain indicating equal numbers of bacteria per unit of OD (Figure 3.6A). This validated the recovery experiment showing that an equal number of bacteria were used in the inoculation of fresh media.

The growth curve however identified that the ΔncRv10243 strain was impaired for recovery following growth in the Wayne model. This phenotype was partially restored in the complemented strain resulting in an intermediate phenotype (i.e. between the wildtype and ΔncRv10243) (Figure 3.6B). It is also possible that the mutant possesses a longer lag phase that the wildtype or complementing strain as the difference in OD's after 300 hours is less marked than at 200 hours post recovery.

The attenuation seen in the Wayne model demonstrates that ncRv10243 is important in recovery from the Wayne model, and is required for the resuscitation of the bacteria in order to recommence active growth.

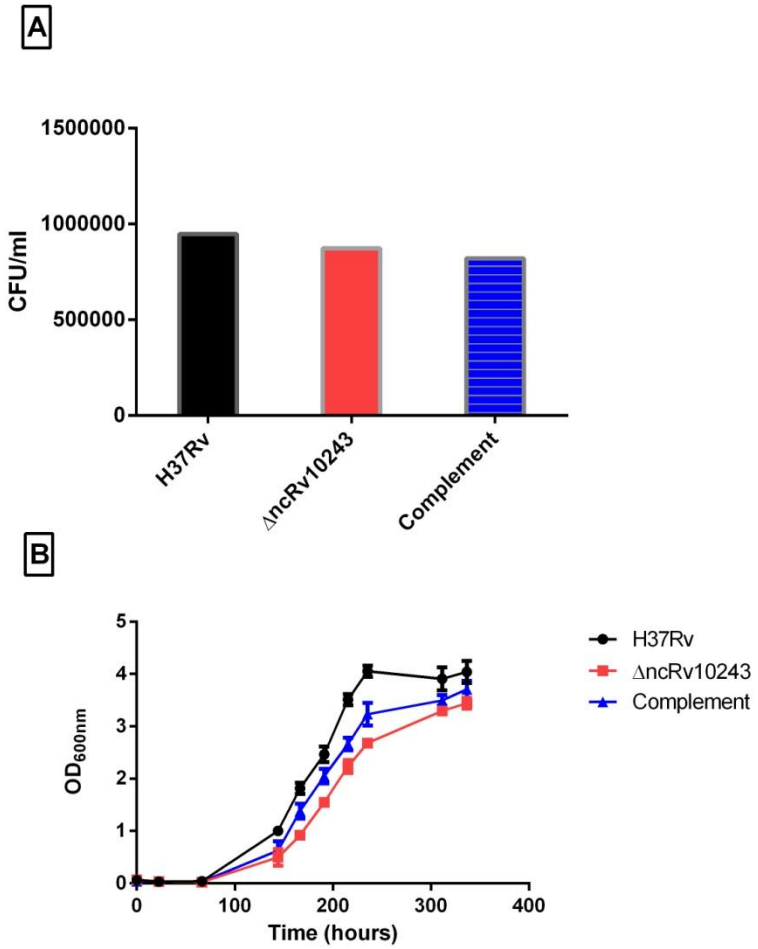

Figure 3.6 Growth in the Wayne Model impairs recovery of ΔncRv10243.

Wildtype *M. tb* H37Rv, ΔncRv10243 and complement strains were grown in the Wayne model until NRP-2 was reached. Cultures were serially diluted and plated for enumeration of viable bacteria. (A) Number of viable bacteria after incubation in the Wayne model. Significance was tested by One-way ANOVA $p>0.05$. All cultures were then adjusted to an OD_{600nm} = 0.05 in fresh media and the growth measured over 14 days (B). All data represents the averages and standard deviation of three biological replicates. It was observed that there was a significant difference between the recovery of the wildtype and that of the deletion strain, as tested by linear regression analysis $p>0.05$. A significant difference was also observed between the slopes for wildtype and complement although the growth observed was an intermediate phenotype of the two.

3.10 Transcriptional Microarray analysis in exponential phase and starvation.

Microarrays can be used as a screening tool to allow comparative analysis of the entire transcriptome in an organism simultaneously. As the targets of ncRv10243 were unknown, an initial unbiased approach was taken to generate a hypothesis as to the functional role of ncRv10243. Since ncRv10243 is strongly induced in starvation as a consequence of SigF induction it was anticipated that deletion of ncRv10243 would result in an altered starvation transcriptome.

Starvation differs from stationary phase markedly. Stationary phase is often due to a growth-limiting factor such as the depletion of an nutrients, and/or the formation of an inhibitory product for example propionate. This results in the growth rate and death rate being equal and this state is reached gradually. Starvation in the model used here however, is the complete deprivation of all nutrients by washing and replacing culture media with PBS. RNA was isolated from exponential cultures as well as from starved cultures (24 hours in PBS was used instead of 96 hours as the latter results in poor RNA quality). Differential gene expression from exponential and starved cultures was investigated by transcriptomics.

cDNA microarrays were used to analyse any differences in global gene expression between ΔncRv10243 and H37Rv.

Briefly, RNA from wild type and mutant was reverse-transcribed and the cDNA labelled before mixing and competitively hybridising against an array. Three biological replicates for each strain were prepared and they were carried out in technical duplicate (dye-swaps) to account for any bias

in the labelling efficiencies of the Cy-dyes. A t-test against zero was performed for each data set and changes were considered to be significant if the p-value was less than 0.05 and changed 2-fold or greater**.** Tables 3.2A and 3.3B show the gene changes observed in the exponential and starvation microarray respectively. Of the genes found to be differentially expressed in both arrays only one, Rv0169 is known to be differentially expressed under starvation conditions. It would have been expected that if ncRv10243 were part of the starvation response that genes known to be involved would be altered in the deletion strain.

Gene Number	Gene Name	Gene Product	Fold Change	P-value
Rv0694	*lldD1*	L-lactate dehydrogenase	2.53	0.008
Rv1130	*prpD*	Methyl citrate dehydratase	2.12	0.017
Rv0169	*mce1A*	Unknown but thought to be involved in host cell invasion	2.08	0.021
Rv0693	*pqqE*	coenzyme PQQ synthesis protein E	2.0	0.031

Table 3.2A Genes down regulated > 2-fold in ΔncRv10243 in exponential phase

Gene Number	Gene Name	Gene Product	Fold Change	P-value
Rv0440	*groEL2*	60 kDa chaperonin 2	4.08	0.035
Rv3418c	*groES*	10 kDa chaperonin GroES	3.38	0.049
Rv0991c		Unknown	2.81	0.032
Rv0990c		Unknown	2.52	0.037

Table 3.2B Genes found to be up regulated > 2-fold in ΔncRv10243 after 24hrs starvation

3.10.1 Confirmation of Microarrays by qRT-PCR

Microarray results were confirmed by qRT-PCR using RNA extracted from three biological replicates of each strain. The complement was included in the analysis in order to assess whether the changes in gene expression could be complemented. qRT-PCR was performed according to section 2.8 and the primers used can be found in Appendix II. Results are shown in Figure 3.7 and 3.8.

All mRNA observed in the exponential microarray showed no statistical significant difference between wild type and deletion strain when tested by qRT-PCR. However, the complement was significantly different to wild type for *Rv1130* although ncRv10243 expression between the strains was not significantly different.

Genes indicated to be differentially expressed between wild type *M. tb* and ΔncRv10243 in the starvation microarray were *groES, groEL2, Rv0990c* and *Rv0991c* which were all found to be up regulated. All but *Rv0990c* could be confirmed by qRT-PCR and found to be at least partially complemented in each case. The transcriptional regulator *Rv0990c,* could not be confirmed by qRT-PCR but has been previously shown to be co transcribed with Rv0991c [184], which was confirmed as up regulated.

GroES, groEL2 and *Rv0991c* are all heat shock proteins known to be under the control of the repressor HrcA (Rv2374c) [185]. The up regulation of all of these genes suggests an indirect effect from a change in this regulator. It was hypothesised that expression of the repressor could be affected in the mutant.

hrcA was measured by qRT-PCR in all strains to identify if the mRNA was changed in the mutant, but had been lost in the filtering analysis of the microarray. Expression levels of *hrcA* were not found to be significantly different between any of the 3 strains Figure 3.8.

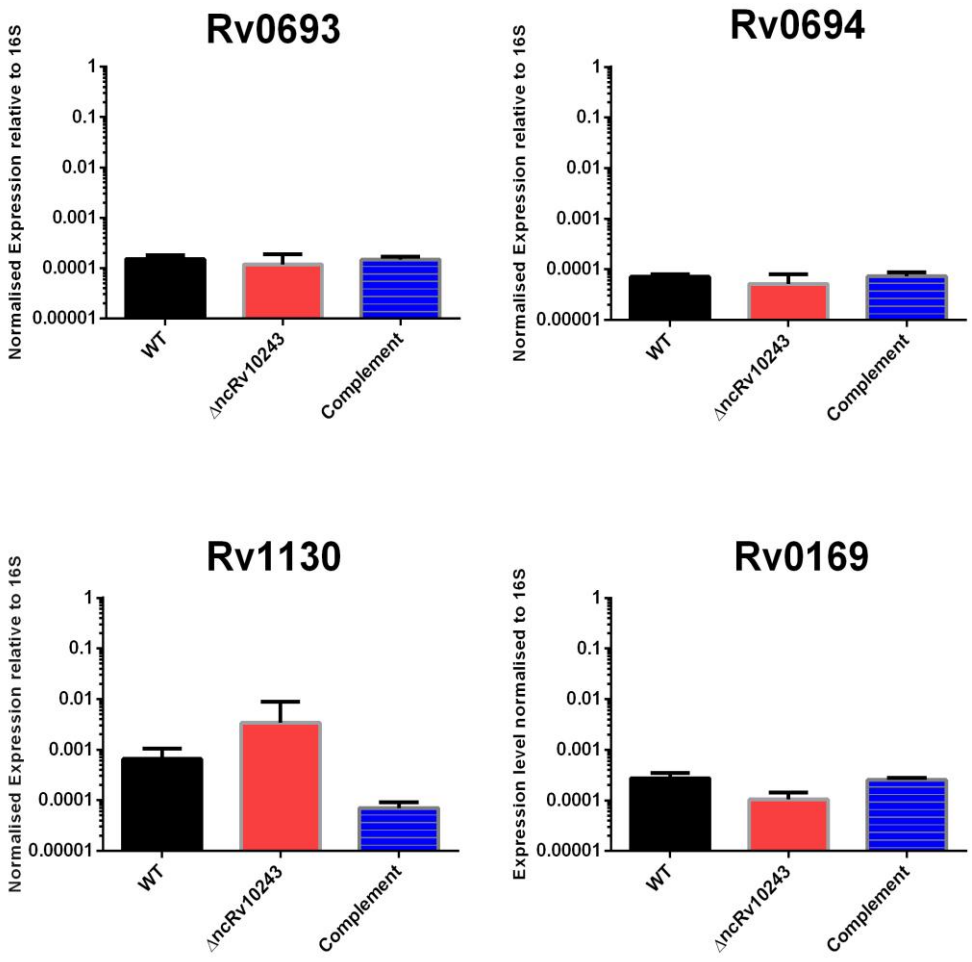

Figure 3.7 qRT-PCR to confirm the gene expression changes observed in the exponential microarray.

qRT-PCR was performed as detailed in section 2.8. Each Figure shows the expression level of the gene normalised to 16S. All data represents the mean and standard deviation of three biological replicates for each strain. Significance tested with one-way ANOVA and only the complement found to be significantly different from the wildtype in Rv1130 expression $p > 0.05$.

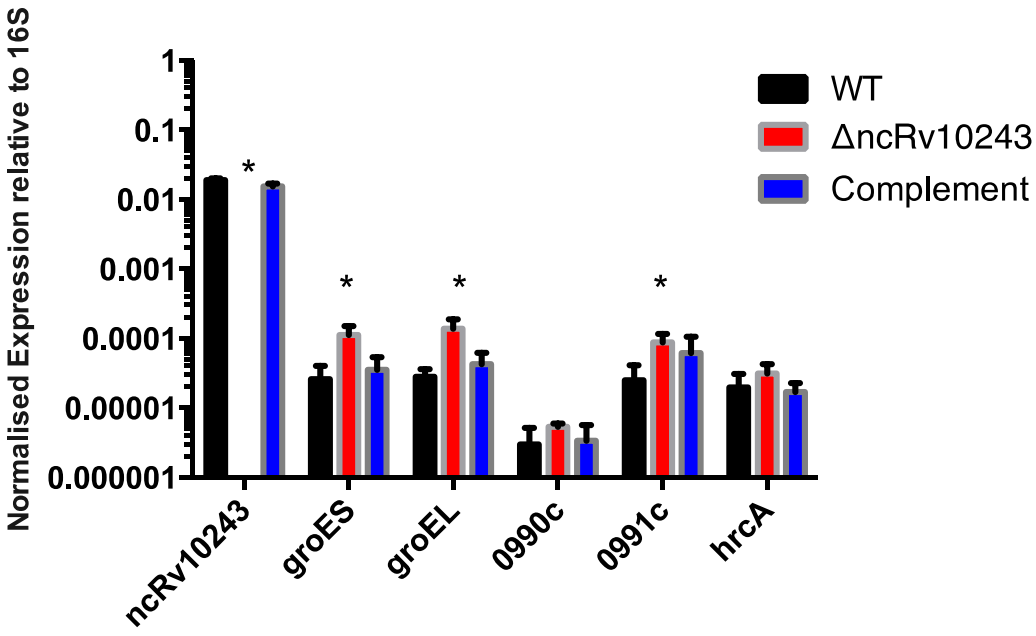

Figure 3.8 qRT-PCR confirmations of gene expression changes observed in the starvation microarray

qRT-PCR was performed as detailed in section 2.8. Each bar shows the expression level of the gene normalised to 16S. All data represents the mean and standard deviation of three biological replicates for each strain. * = p value >0.05 with significance tested with one-way ANOVA.

3.11 Analysis of the ΔncRv10243 proteome

The possibility that the altered expression of the heat shock family genes in the mutant could be as a result of post transcriptional regulation of the repressor HrcA. This was investigated by proteomic analysis of whole cell extracts and analysed by mass spectrometry. If ncRv10243 was responsible for altered expression of heat shock family genes through regulation of HrcA translation then a decrease in the protein abundance would be observed.

Whole cell extracts from 96 hour starved cultures of H37Rv, ΔncRv10243 and the complement were prepared in triplicate and analysed using mass spectrometry by Olga Shubert. Peptide abundance was further analysed using MSstats and fold-changes > = 1 or -1 (in log2 scale) with a p-value < 0.01 were considered statistically significant.

No statistically significant changes were observed in protein abundance between the wildtype and the deletion strain suggesting that the increase in the mRNA transcripts observed in the microarray did not result in increased translation. The observation that HrcA abundance was not significantly reduced leads to the remaining conclusion that ncRv10243 could be acting to sequester the repressor HrcA by binding the protein, or by directly targeting mRNA and stabilising them. This hypothesis remains to be tested in future work.

3.12 *in vivo* Analysis of ΔncRv10243 compared to wildtype *M. tb*

M. tb is an intracellular pathogen that is subjected to a variety of stresses within the host, including but not limited to oxidative stress and nutrient

deprivation. Due to the fact that ncRv10243 is induced under oxidative stress, starvation, and infection in addition to being impaired for recovery from the Wayne model, the effect of its deletion on *M. tb in vivo* survival was assessed. It was expected that the deletion strain would be impaired for growth due to previous *in vitro* phenotypes being observed. It is also of note that loss of the alternative sigma factor SigF, which controls ncRv10243, was found to decrease the virulence of *M. tb* in mice, as well as disease associated tissue damage in mice and guinea pigs [176] [177] [178].

3.12.1 Deletion of ncRv10243 had no effect on the ability of *M. tb* to survive within either naïve or activated macrophages.

The ΔncRv10243 strain, wildtype *M. tb* H37Rv and complement strains, were used to infect both naïve and activated murine BMDMs (as detailed in section 2.13). Macrophages were pre-activated with 10 ng/ml IFN-γ and incubated overnight and infected alongside naive macrophages at an MOI of 0.1:1 (bacteria: macrophages). The infection was allowed to continue for 7 days with five time points. At each time point the macrophages were lysed and plated for CFUs. For both the naive and activated macrophages, there were no significant differences between the three strains (Figure 3.9). This would suggest that ncRv10243 does not result in attenuation in the mouse macrophage model. A lack of attenuation has been observed in a study of a sigF mutant in human monocyte derived macrophages [176]. However, the macrophage model of infection does not completely replicate the conditions encountered by the bacteria in the more complicated whole animal models of infection.

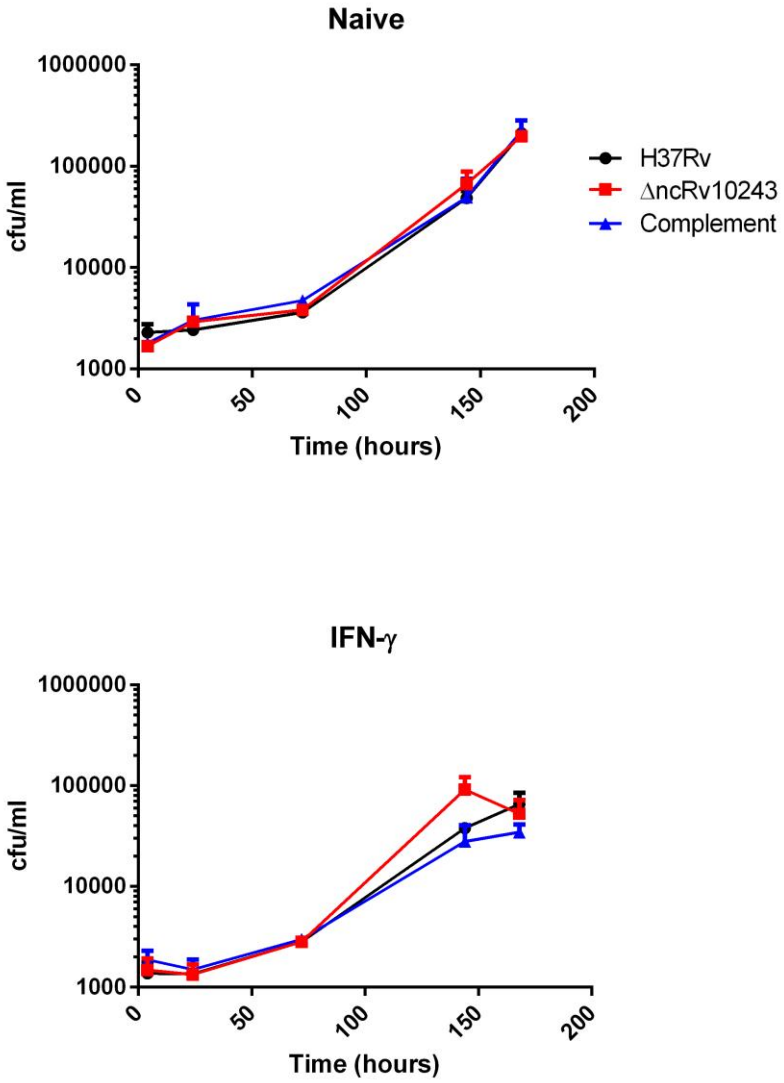

Figure 3.9 Survival of the ΔncRv10243 in a macrophage model of infection

Survival of Wild type *M. tb* H37Rv, ΔncRv10243, and complementing strains within naive and IFN-γ activated BMDM over a time course of infection. Significance was tested with One-way ANOVA $p>0.05$. Data is the mean and standard deviation of triplicate infections. Data is representative of 3 independent experiments.

3.12.2 Deletion of ncRv10243 does not affect the ability of *M. tb* to survive in a mouse model of infection.

In order to assess the role of ncRv10243 in pathogenesis in a more complete model of infection, wildtype *M. tb* H37Rv, ΔncRv10243, and the complemented strain were used in a mouse model of infection. Balb/C mice were infected with approximately 100 CFU via the aerosol route and the infection followed for 143 days. At time points 0, 30, 78, 100 and 143 days, lungs and spleens were harvested for bacterial enumeration. No significant difference was observed in CFUs between the wildtype *M. tb* H37Rv and ΔncRv10243 at any of the time points (Figure 3.11).

The lack of an obvious phenotype observed during the mouse infection does not necessarily mean that ncRv10243 does not play a role during infection and pathogenesis. A phenotype for the sigF mutant (the sigma factor known to control ncRv10243) was only detected through a time to death experiment in mice, along with observations on differences in histology of the lungs of guinea pigs and spleen size in mice [176-178]. No difference in the spleen size was noted for the deletion strain group at any time point during the infection.

It is of note that a mouse model of infection does not replicate that of an *M. tb* infection in a human host. This is mainly apparent in the lack of ability of the mouse to form granulomas. Granulomas provide a unique niche for *M. tb* in which the environment is hypoxic and nutrients are limited. As these are conditions upon which ncRv10243 is induced, it is still possible that ncRv10243 plays a role in pathogenesis during

granuloma formation that could not be replicated in this study. A study in guinea pigs which do develop defined granulomatous lesions may provide an alternative phenotype.

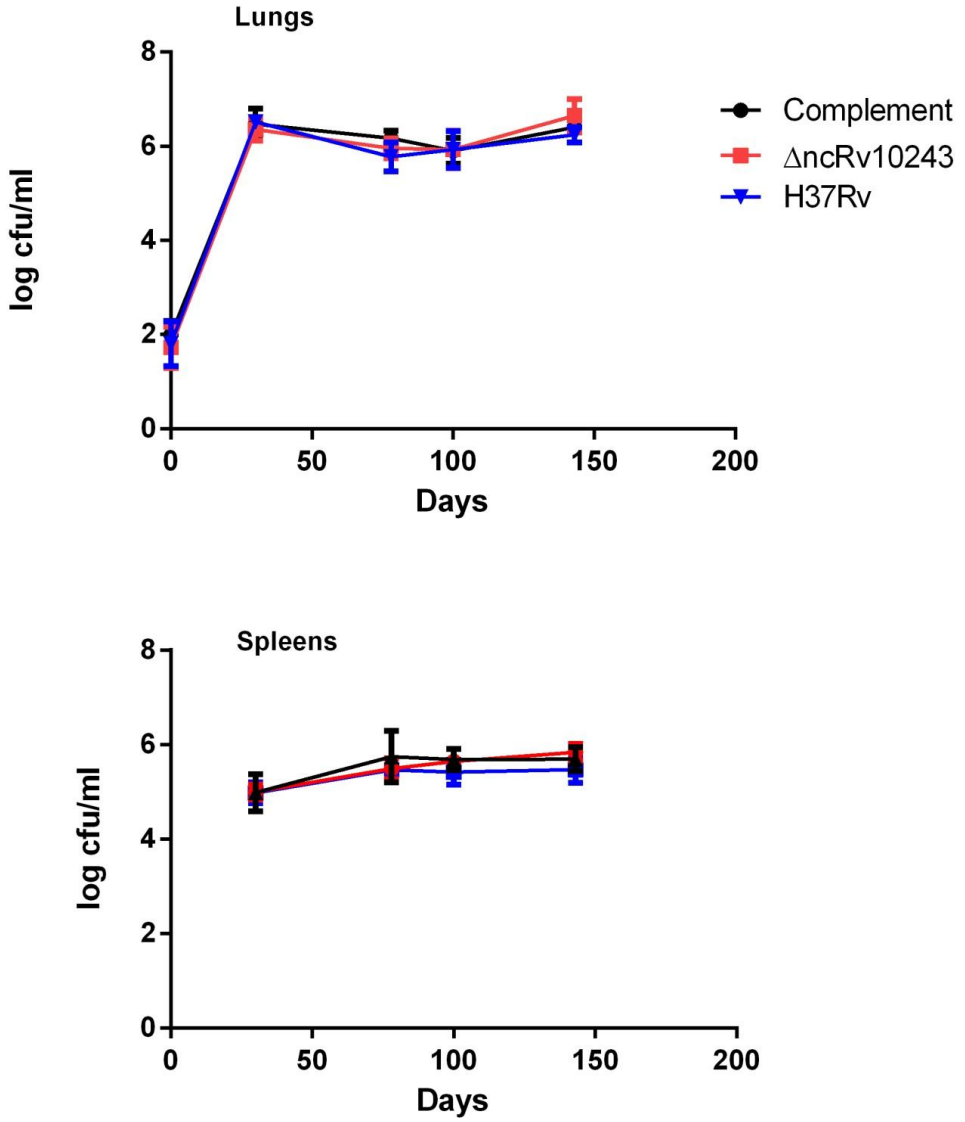

Figure 3.10 Survival of ΔncRv10243 from aerosol infected mice.

Survival of wildtype *M. tb* H37Rv, ΔncRv10243, and complement within the lungs and spleens of Balb/C mice. The data represents the averages and standard deviations from 5 mice per time point. Significance was tested with Two-way ANOVA.

3.12.3 ncRv10243 is expressed in *M. tb* isolated from the granulomas of infected macaques.

To address the importance of ncRv10243 for *M. tb* residing within the granuloma, expression levels of ncRv10243 were measured by qRT-PCR from *M. tb* within macaque granuloma samples (kindly supplied by JoAnne Flynn). Cynamologous macaques were infected with a low dose of *M. tb* (Erdman strain) and infection monitored by Positron emission tomography–computed tomography (PET/CT) imaging and identified granulomas of interest were consequently surgically removed. The samples were immediately flash frozen for RNA and paired samples were plated for CFU estimation. RNA was extracted from the *M. tb* isolated from the granulomas by homogenisation. A summary of the samples can be found in table 3.2.

Although the level of RNA retrieved from the samples was relatively low and contained a large percentage of host RNA (as observed on the Bioanalyzer), qRT-PCR showed ncRv10243 to be detectable in all the 8 samples tested, Figure 3.11. Expression levels observed were found to be comparable with that observed in the mouse even in instances where the estimated CFU's were zero. This indicates that ncRv10243 is important in persistence within the granuloma due to expression in bacteria that are not actively replicating, or cells which lack the ability to be resuscitated. It is possible that the primers had some non-specific binding to macaque sequence producing non-specific amplification. However, qRT-PCR primers were tested on human leukocyte RNA prior

to use and found to result in no amplification. In addition RT- samples for each granuloma also resulted in no amplification.

It was observed that the different types of lesions did not cluster for ncRv10243 expression indicating that the populations within the classified granuloma were not homogeneous.

Macaque Granuloma No.	**Status-CFU**	**Total RNA yield (ng)**
3	Active - 24250	161
4	Active - 282000	831
5	Latent likely sterile	301
6	Latent likely sterile	311
7	Latent -3315	381
8	Latent -0	151
9	4 wk -580000	60
10	4 wk - 211250	641

Table 3.2 Summary of Macaque granuloma status and RNA yield

RNA was extracted from *M. tb* Erdman present in the granulomas of low dose aerosol infected cynomolgus macaques. Granulomas were scored on their status by observations using PET/CT imaging.

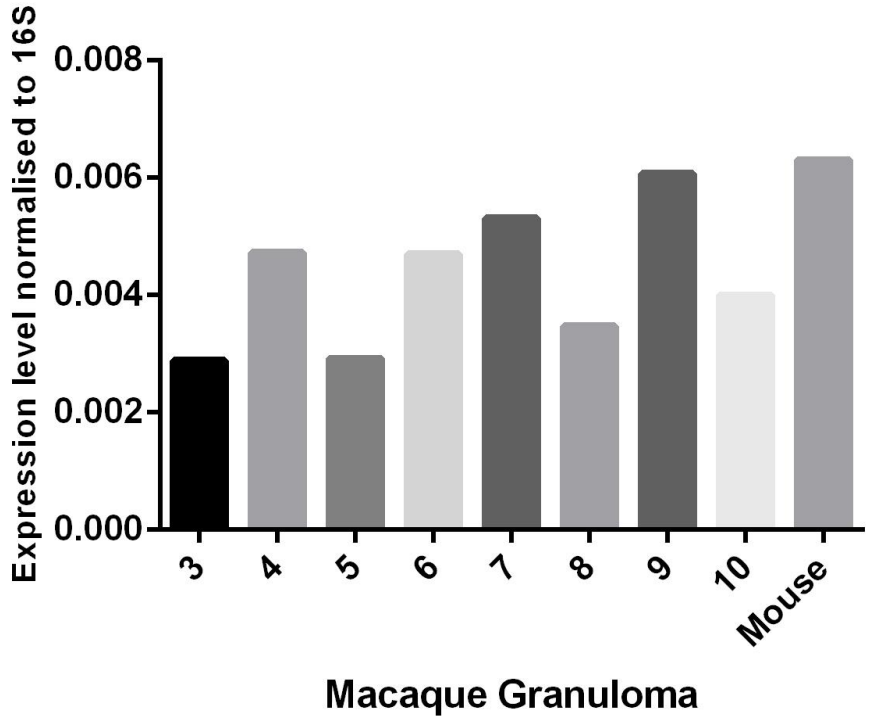

Figure 3.11 Expression of ncRv10243 in the granulomatous lesions of Macaques.

qRT-PCR was performed as detailed in section 2.8. Each bar shows the expression level of ncRv10243 normalised to 16S for each individual granuloma. Expression level of ncRv10243 in the mouse has been included for comparison.

3.13 Discussion

ncRv10243 is a well expressed sRNA in exponential phase that has previously been observed to be up regulated in stationary phase [153]. It was known that this sRNA is under the control of sigF [153, 175] but no function for the sRNA had been determined. In this study we aimed to further assess the expression conditions of this sRNA and to identify a functional role.

Induction of sRNA ncRv10243 was observed to be up regulated during early murine infection (21 days post infection) and upon 96 hours starvation in PBS indicating that this sRNA is important for pathogenesis and in particular could be important for survival within the granuloma. During early infection bacteria are actively replicating and the innate immunity controls the growth of the bacteria through the use of macrophages where upon the *M. tb* is subjected to stresses such as high levels of the bactericidal compound nitric oxide. Around 21 days adaptive immunity begins and bacterial growth plateaus in the mouse. *M. tb* within the granuloma are deprived of nutrients; therefore, bacilli must shift their metabolism to conserve energy up regulating enzymes essential for survival during starvation and hypoxia.

It is assumed that during nutrient starvation conditions; mycobacteria utilize lipids as a sole source of energy [186]. In general, a global metabolic shift is observed when bacilli undergo starvation conditions [187, 188].

M. tb has the ability to survive inside the host environment for decades in a latent state before reactivation. This can be modelled *in vitro* using the

Wayne model of dormancy. The ΔncRv10243 deletion strain was tested in the Wayne model due to the fact that slower growth was observed when oxygen was previously limiting. As predicted the ΔncRv10243 deletion strain was indeed impaired for recovery from the Wayne model (Figure 3.7) but not for growth to NRP-2 (data not shown). As no differences were observed in the level of CFU's post incubation it would indicate that the bacteria were alive but unable to replicate as efficiently in the deletion strain.

Previously it has been observed that the sigma factor which controls expression of ncRv10243 is induced in the Wayne model [189]. SigF was first described in BCG as a stationary phase response sigma factor that is also induced upon cold shock in BCG [189], heat shock, acidic pH and oxidative stress in *M. smegmatis,* and nutrient starvation in *M. tb* [187]. Therefore it is hardly surprising that these are also conditions that induce the expression of ncRv10243.

Microarray investigations of an *M. tb* ΔsigF mutant revealed that Rv3418c (*groES*, which codes for 10-kDa chaperonin) and Rv0991c (a hypothetical protein) were down regulated under exponential phase conditions [176]. 24 hour starvation microarrays on the ΔncRv10243 strain showed up regulation of *groES* and *Rv0991c* along with *Rv0440* (*groEL2*, which codes for 60kDa chaperonin2) as well as *Rv0990c* the downstream gene of Rv0991c. All of these genes except Rv0990c were confirmed by qRT-PCR as being significantly different between the wildtype *M. tb* strain and the ΔncRv10243 deletion strain.

These genes have been shown to belong to the GroE/Hsp60 heat-shock protein family. The GroE chaperonin complex consisting of GroEL and GroES is involved in preventing cellular proteins from misfolding after temperature increase. Up regulation of this family of genes had previously been observed in a Δ*hspR/ΔhrcA* mutant in *M. tb* where they characterised the heat shock response [185].

The heat-shock repressor HrcA acts as the main regulator for the heat shock protein family, controlling its targets through the binding site, controlling inverted repeat of chaperone expression (CIRCE), [185]. The CIRCE binding site can be found in the 5'UTRs of *groES, groEL2* and Rv0991c which is thought to be co transcribed with the adjacent Rv0990c. GroEL2 is preceded by two CIRCE-like elements and both groES and Rv0991c by one. In addition to acting as a transcriptional repressor HrcA has also been shown to play a role in post-transcriptional control of mRNA stability. In *B. subtilis* it was demonstrated that CIRCE elements at the 5' end of a transcript resulted in low stability [190], this was also observed in *Rhodobacter capsulatus* which does not possess a HrcA protein [191]. Therefore it is likely that the heat shock response in *M. tb* is controlled both transcriptionally and post-transcriptionally via the CIRCE element. If regulation of the GroE chaperonin was controlled by ncRv10243 it could be achieved by sequestering HrcA to relieve transcriptional repression. sRNAs binding directly to proteins has been previously reported, for example the CsrB family of sRNAs contain multiple binding sites for the protein CsrA [192]. CsrB RNA functions as a CsrA antagonist by sequestering this protein which functions as an RNA binding protein which

usually prevents translation and thereby activates mRNA decay through endonuclease attack.

As no change in *hrcA* was found by qRT-PCR to evidence this, proteomic analysis of whole cell extracts comparing wildtype *M. tb* H37Rv and the ΔncRv10243 deletion strain were analysed. No difference in abundance of HrcA was observed at the proteomic level leading to the possibility that ncRv10243 directly targets *GroES*, *GroEL* and *Rv0991c* by binding to their 5' ends around the CIRCE element increasing stability of the mRNA. It is also possible that loss of ncRv10243 has some as yet unidentified effect that results in an increase in unfolded proteins resulting in a canonical heat shock response.

As ncRv10243 was found to be induced by nutrient starvation in response to sigF induction, it was reasoned that the ΔncRv10243 deletion strain would be attenuated for growth *in vivo*. Infection of BMDM for 7 days and BALB/c mice for 143 days revealed no attenuation of the ΔncRv10243 deletion strain. Studies of a sigF mutant however showed that ΔsigF can achieve high CFU counts in mice but is attenuated in causing tissue damage and in producing lethality in mice [176, 177].

Using an intravenous infection of mice a time-to-death study was conducted using the ΔsigF mutant. The mutant strain infected mice were able to survive for 334 days whereas the wildtype infected mice lasted only 184 days [176]. This could explain why no phenotype was observed for the ΔncRv10243 deletion strain. Another possibility is that attenuation could have been observed in a different animal system of infection such as the guinea pig model. Mice lack the ability to form granulomas which acts

as a starvation based environment. It was noted that when a ΔsigF mutant was used to infect guinea pigs by the aerosol route it exhibited ill-defined lung granulomas [178] suggesting that sigF responses are important for the bacterial interaction with the host.

Adaptation to nutrient deprivation is essential for long-term survival of persistent bacteria. *M. tb* is capable of surviving under non growing starvation conditions for up to 2 years *in vitro* while maintaining the ability to be resuscitated [193]. In *M. smegmatis* carbon, nitrogen, and phosphorus-starved organisms have been shown to retain viability for over 650 days [194]. Therefore correct adaptation to starvation enables bacteria to survive until conditions become more favourable.

Due to ncRv10243 being identified as important for recovery from the Wayne model, it is possible that the lack of identified targets in this study could be due to the conditions studied. ncRv10243 could be required for the recovery from stress and therefore be accumulated within the bacteria until such time as it is required. This could explain why no targets or strong phenotype was observed for the deletion strain despite over expression of ncRv10243 in *M. tb* leading to reduced growth. However, when ncRv10243 is over expressed in *M. smegmatis* there is no obvious phenotype despite a homolog being present.

4 The constitutively expressed sRNA ncRv11690, may play a role in regulation of EsxA secretion

4.1 Introduction

The sRNA ncRv11690 was originally identified through cDNA cloning of size fractionated RNA and termed G2 after the corresponding clone [153]. It is a *trans*-encoded sRNA found in the intergenic region between lprJ (a probable lipoprotein) and tyrS (an essential tRNA synthase), Figure 4.1a). Further characterisation of the sRNA to identify 5' and 3' ends by RACE led to the calculation of a full-length transcript of 229bp with a possible SigC promoter upstream of one of the 5' ends. Northern blotting shows a predominant transcript of 65 bp indicating substantial processing of this sRNA, Figure 4.1B.

Very little was known about ncRv11690 and no possible function had been elucidated. It was known however that this sRNA was conserved only within the *M. tuberculosis* complex inferring a role in pathogenesis. If this sRNA was indeed also under the control of SigC this would also infer a role in pathogenesis as a SigC deletion mutant was shown to play a central role in the lethality of *M. tb* infected mice [195].

Functional characterisation was attempted through over expression in *M. tb* which proved lethal with two different strength promoters. This prompted the over expression in *M. smegmatis,* which resulted in defective growth, especially in liquid medium [153]. This phenotype was observed in spite of the fact that no obvious homologue of this sRNA is present in the faster growing mycobacterial strain indicating that possible targets are conserved.

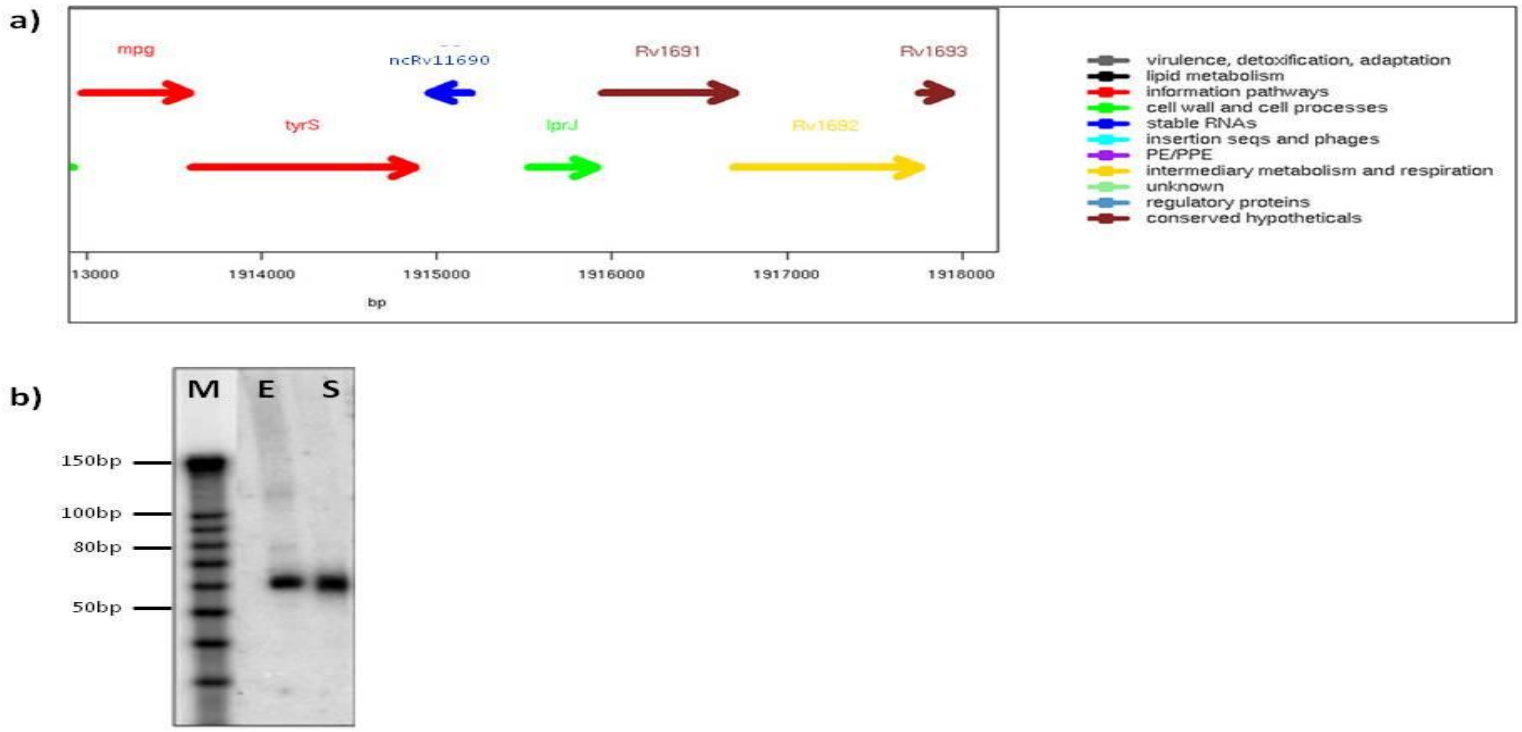

Figure 4.1 Location and transcript size of ncRv11690

a) Genomic position of sRNA ncRv11690 in the *M. tb* genome as viewed in Tuberculist (http://tuberculist.epfl.ch/) b) transcript size of sRNA ncRv11690 by northern blotting (adapted from Arnvig 2009) M = marker, E = exponential phase, S = stationary phase.

4.2 Hypotheses and specific aims

As mentioned previously in 3.2, it is difficult to speculate on possible targets for trans-encoded sRNAs. ncRv11690 is not co transcribed with any other genes as it is divergent to both flanking genes on the genome. Therefore, as with sRNA ncRv10243, an unbiased approach was taken in order to identify possible mRNA targets and therefore elucidate the function of ncRv11690.

As experimental manipulation of sRNA expression levels can provide an alternative route to target identification, the aim of the study was to create both a sRNA deletion strain and an integrating over expression strain. These strains would then be used to perform gene expression analysis by microarray, which would allow the assessment of the relative abundance of mRNA in both the wildtype/vector controls and ncRv11690 deletion/over expression strain.

In addition to this we planned to assess the virulence of *M. tb* upon removal of ncRv11690 from the genome. As this sRNA is potentially under the control of SigC, which was shown to be important in virulence, we predicted that ncRv11690 would also play a role in virulence of *M. tb*.

Results

4.3 *In vitro* and *In vivo* expression levels of ncRv11690

ncRv11690 was known to be a well-expressed sRNA in exponential phase. This study showed that the sRNA is equally well expressed by *M. tb* in the infected lungs of mice after 21 days of infection an early point of infection where the bacteria are actively replicating. The sRNA was also observed in this study to be down regulated in both stationary phase and starvation. This would indicate

that the sRNA is involved in active growth of the bacteria. However, northern blot analysis shows induction of the sRNA in stationary phase, identifying a discrepancy between the two techniques. This is most likely due to the location of the probes for each technique.

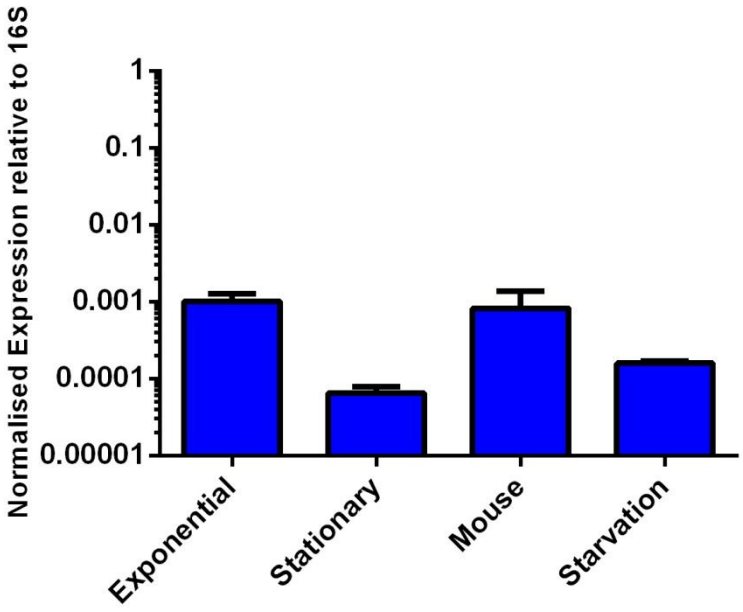

Figure 4.2 Expression levels of ncRv11690 in *M. tb*

ncRv11690 expression levels were measured using qRT-PCR, in each instance ncRv11690 levels are expressed relative to 16S rRNA control. Data represents the mean and standard deviations of three biological replicates for each condition. Expression during stationary phase, mouse infection and 96 hours starvation are significantly different from exponential phase expression when compared by One-way ANOVA, $p<0.05$.

4.4 Creation of a ncRv11690 deletion strain

This study set out to identify possible targets of ncRv11690 through the creation of a deletion strain in which the sRNA and its promoter are entirely removed from the chromosome. The deletion strategy was as described by [183] which uses a non-replicating suicide vector [7] in a two-step process as described in section 2.9.10 and 3.4. Briefly, a single cross-over (SCO) recombinant is isolated from the electroporation of *M. tb* with the targeting construct. SCO are then subjected to counter-selection in order to obtain double crossovers (DCO) generated by a second recombination event. The markers *sacB* and *lacZ* on the targeting construct allow for blue/white screening of colonies and make counter-selection for sucrose sensitivity possible [183] .

4.4.2 Design and creation of the deletion plasmid

In order to remove ncRv11690 from the chromosome of *M. tb* the aim was to remove the entire sRNA and its promoter. For homologous recombination to occur between the deletion plasmid and the bacterial chromosome, approximately 1kb of each of the 5’ and 3’ flanking regions must be included. The targeting constructed was created in this instance by cloning a large fragment of approximately 2.5 kbp encompassing coordinates 1913940-1916496 and the sRNA and its promoter removed by site directed mutagenesis (SDM). This created a deletion strain lacking coordinates 1914961-1915183.

The PCR strategy for screening both SCO and DCO candidates are represented in Figure 3.3A.

4.4.3 Screening of single and double crossover candidates

After electroporation with the targeting plasmid into *M. tb* H37Rv, cells were plated onto 7H11 containing Kanamycin and X-Gal for selection of SCO's. After incubation, 4 blue colonies were screened by PCR to identify true SCOs from random integrations (Figure 4.3). As the region of deletion in this instance was only ~206bp, it was difficult to differentiate wildtype bands from SCO bands. Therefore the resulting PCR products were gel extracted and sent for sequencing. Sequencing revealed 1 SCO, which was then streaked onto non selective 7H11 for the second recombination event to occur. Full loss of the backbone of the deletion plasmid was confirmed by streaking colonies onto both 7H11 plus Kanamycin and X-Gal, and also 7H11 without antibiotic, plus X-Gal. 8 colonies from DCO selection were white and Kanamycin sensitive. These DCO candidates were screened by PCR amplification and sequencing, which showed colony number 5, 6, 8, 11 and 12 to contain the deletion of the sRNA from the *M. tb* genome (Figure 4.3).

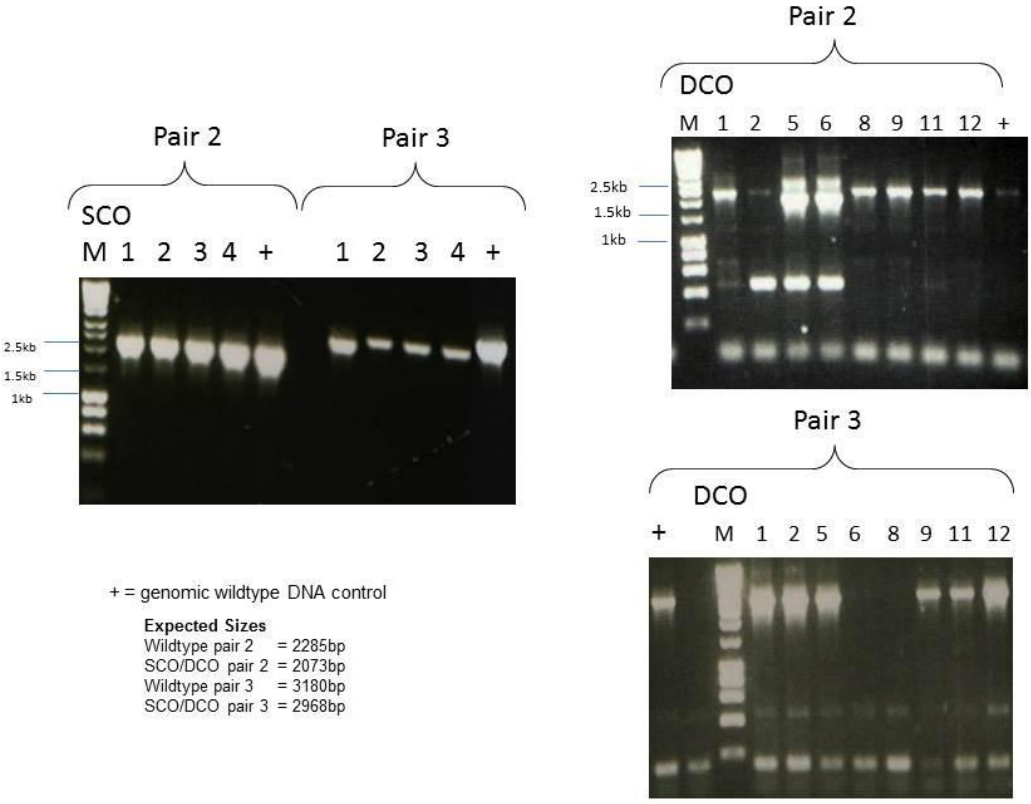

Figure 4.3 PCR screening for the construction of the ncRv11690 deletion strain.

PCR reactions were designed using the strategy outlined in Figure 3.3A. Expected sizes of products for each primer pair are indicated. Due to the small size of deletion, these PCR products were consequently gel extracted as detailed in section 2.2.3 and sequenced directly. SCO = single crossover; DCO = double crossover; M = Bioline Hyperladder I DNA marker.

4.5 Complementation of the ncRv11690 mutant

As the aim of this study was to characterise the phenotype of a ΔncRv11690 strain, it was essential to complement the loss of the sRNA by replacing the chromosomal copy with one supplied on a plasmid. The resulting strain should in theory have the same phenotype as wild type *M. tb* H37Rv.

The sRNA was amplified by PCR with a portion of upstream and downstream region to include any possible regulatory elements and then cloned into the Kan^R plasmid pKP186. The double crossover was electroporated with the complementing plasmid along with a plasmid that separately supplies the integrase. Presence of the plasmid was confirmed by PCR analysis of Instagene preparations.

4.6 Full Genome sequencing of the ncRv11690 mutant

High Quality genomic DNA was extracted from the mutant and the parental H37Rv strain (as per Section 2.4). Sequencing libraries were prepared from both strains and sequenced by the HTS sequencing facility at NIMR. The resulting reads were aligned to the H37Rv reference genome by Graham Rose (NIMR) and single nucleotide polymorphisms (SNPs) were identified.

Alignment of the genomic sequence of ΔncRv11690 identified 1 synonymous SNP in the conserved hypothetical protein Rv1691 (Appendix III). As this was a synonymous SNP, this does not result in a change of the amino acid coded for by the sequence, and therefore should not affect function of the protein.

4.7 Assessment of ncRv11690 expression in deletion and complement strains

To confirm the removal of the sRNA and to assess the degree of complementation achieved, RNA extracts were prepared from H37Rv, ΔncRv11690, and the complemented strain. The cDNA was prepared as previously described in 3.7 and assessed by qRT-PCR before normalising to 16S. qRT-PCR showed that ncRv11690 was undetectable in the ΔncRv11690 strain (Figure 4.4). There was no statistical significance in the expression level of ncRv11690 between the wildtype and complement strain (Figure 4.4; Unpaired t-test, $p>0.05$).

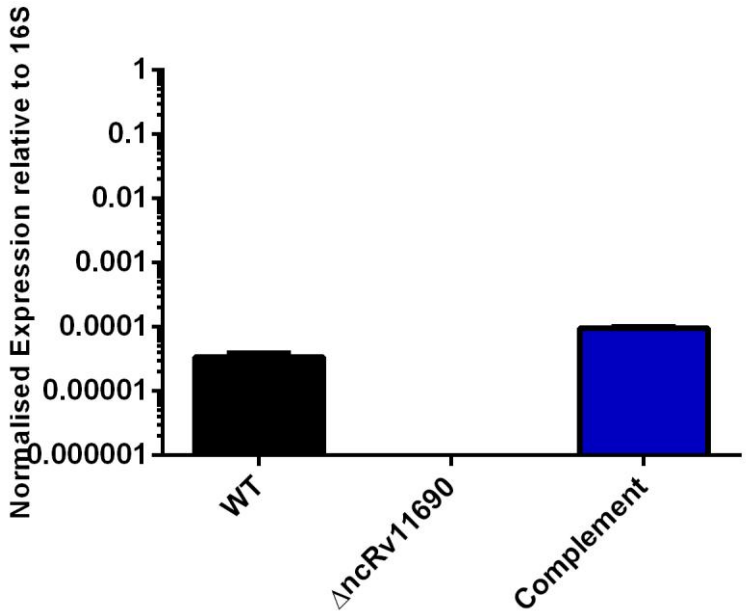

Figure 4.4 qRT-PCR confirmations of ncRv11690 deletion and complementation

Each strain was grown to exponential phase in standard 7H9 media and RNA then extracted. qRT-PCR was performed as described in section 2.8. In each instance sRNA expression is expressed relative to 16S, an rRNA control. Data represents the averages and standard deviations of three biological replicates for each strain. Significance was tested by One-way ANOVA and the complement found to be significantly different from the wildtype with expression on average 2.5 fold that of the wildtype.

4.8 *In vitro* phenotype analysis of growth compared to wildtype

In the first instance the ΔncRv11690 strain was assessed for an *in vitro* growth phenotype by comparing growth of the deletion strain against wildtype and complement strain. Cultures were grown to exponential phase (OD_{600} ~0.6) in 7H9 media, and these cultures were used to inoculate fresh media to an OD_{600} = 0.05. The OD_{600} was monitored until a plateau of growth was reached. No significant difference was observed between the doubling times of the three strains (Figure 4.5) as assessed by Linear regression analysis, $p>0.05$, showing that deletion of ncRv11690 has no effect on *in vitro* growth of *M. tb.* under these conditions.

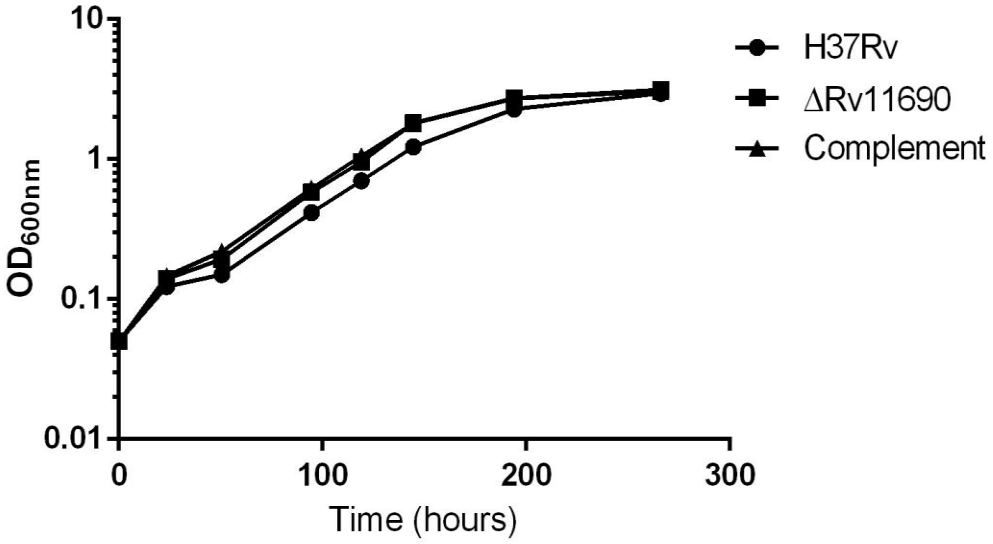

Figure 4.5 Growth of ΔncRv11690 in standard 7H9 media

In vitro growth curves of wildtype *M. tb* H37Rv, the ΔncRv11690 deletion strain and the complement using standard 7H9 media in a rolling culture system. The data represents the averages and standard deviations of three biological replicates. There was no siginificant difference between the growth of the strains as tested by linear regression analysis.

4.9 Transcriptional Microarray analysis in exponential phase

As the targets of ncRv11690 were unknown, an initial unbiased approach was taken to generate a hypothesis as to the functional role of ncRv11690. An *M. tb* whole genome microarray, generated by the Bacterial Microarray Group at St. George's containing 4,410 gene-specific PCR products was used. Since ncRv11690 is most highly expressed in exponential phase, RNA was isolated from mid log cultures for investigation by transcriptomics.

cDNA microarrays were used to analyse global gene expression changes between the ΔncRv11690 and wildtype H37Rv as described in section 2.15 of the materials and methods.

Briefly, 2µg of RNA from wild type and mutant was reverse transcribed to generate cy3 or cy5 labelled cDNA before competitively hybridising against an array. Three biological replicates for each strain were prepared in technical duplicate (dye-swaps) to account for any bias in the labelling efficiencies of the Cy-dyes. Gene expression changes were considered to be significant if the p-value was less than 0.05 and the fold change was 2 or above**.** 65 genes in total were found to be differentially expressed in the ΔncRv11690 and those greater than 2.5 fold are shown in Tables 4.1 and 4.2. The remainder of the list can be found in Appendix IV.

Gene No.	Gene Name	Gene Product	Fold Change	P-value
Rv1535		Unknown protein	3.95	0.048
Rv2699c		Conserved Hypothetical protein	3.53	0.048
Rv3528c		Unknown protein	3.48	0.046
Rv2299c	htpG	Probable chaperone protein	2.97	0.045
Rv0097		Possible oxidoreductase	2.97	0.042
Rv2582	ppiB	Probable peptidyl-prolyl cis-trans isomerise B	2.94	0.041
Rv0634B	rpmG2	50S ribosomal protein L33 RpmG2	2.79	0.042
Rv0846c		Probable oxidase	2.73	0.048
Rv2520c		Conserved membrane protein	2.73	0.046
Rv0761c	adhB	Possible zinc-containing alcohol dehydrogenase NAD dependent	2.66	0.048
Rv2289	cdh	Probable CDP-diacylglycerol pyrophosphatase	2.63	0.042
Rv2288		Hypothetical protein	2.63	0.048
Rv2429	ahpD	Alkyl hydroperoxide reductase D protein	2.59	0.05
Rv2000		Unknown protein	2.59	0.042
Rv1885c	MtCM	Chorismate mutase	2.55	0.042
Rv1515c		Conserved hypothetical protein	2.54	0.048
Rv3790	dprE1	Decaprenylphosphoryl-beta-D-ribose 2'-oxidase	2.53	0.041
Rv1754c		Conserved protein	2.53	0.042

Table 4.1 Genes up regulated > 2.5-fold in ΔncRv11690 in exponential phase

Gene No.	Gene Name	Gene Product	Fold Change	P-value
Rv3229c	desA3	Possible linoleoyl-CoA desaturase	6.70	0.048
Rv3841	bfrB	Bacterioferritin	2.94	0.048

Table 4.2 Genes down regulated > 2.5-fold in ΔncRv11690 in exponential phase

4.9.1 Confirmation of Microarrays by qRT-PCR

A selection of genes was chosen for confirmation of the microarray results by qRT-PCR using RNA extracted from three biological replicates of each strain. The complement was included in the analysis in order to assess whether the changes in gene expression could be complemented. qRT-PCR was performed according to section 2.8 and the primers used can be found in Appendix II. Results are shown in Figure 4.6.

It was apparent from the genes identified in the microarray that there was a trend for genes linked to metal ions, with mRNA from both the Zur and Fur regulons. Furthermore the most up regulated gene Rv1535 is known to up regulated in response to magnesium starvation. This induction is due to the possession of a magnesium responsive riboswitch.

Two genes known to be involved in molybdopterin synthesis Rv3116 and Rv2338c were also shown to be down regulated greater than 2 fold (Appendix IV). Genes of interest were selected for confirmation by qRT-PCR including those with the highest fold changes (desA3, Rv1535 and Rv3841)

From the genes selected for confirmation five were shown to be significantly different in the ΔncRv11690 strain compared to the wildtype as tested by one-way ANOVA. These included *desA3, Rv1535, Rv3841, Rv0761c* and *Rv0846c*. Three genes were found to be either fully or partially restored to wildtype levels in the complement. These were *desA3, Rv1535* and *Rv3841*.

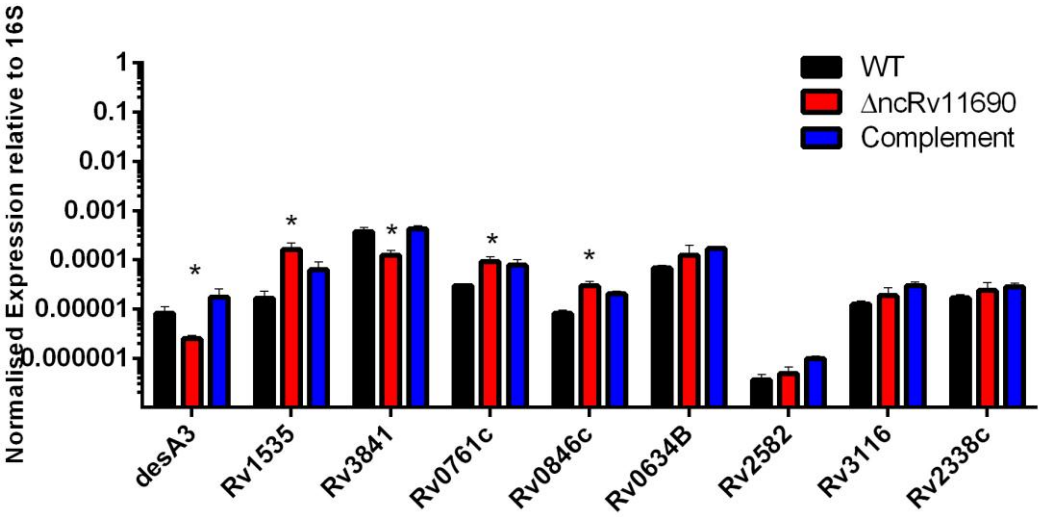

Figure 4.6 qRT-PCR confirmation of the gene expression changes observed in the exponential microarray.

qRT-PCR was performed on a selection of mRNA as detailed in section 2.8. Each bar shows the expression level of the gene normalised to 16S. All data represents the mean and standard deviation of three biological replicates for each strain. * = p value >0.05 with significance tested with one-way ANOVA.

Due to the relatively large numbers of genes shown to be affected in the microarray a common regulator was searched for using the TbDb systems biology database. The TbDb database allows the identification of DNA binding sites for regulators that could affect transcription of mRNA. Therefore if the sRNA was affecting the abundance of a regulator, as opposed to individually targeting an mRNA, then the gene changes observed in the microarray would be due to indirect effects of action on the regulator by the sRNA and not direct targeting.

Regulator candidates generated by TbDb were compared to the microarray results, which identified Rv0891c as a possible regulator of Rv1535 [196]. This mRNA was identified in the microarray as being 2.48 fold down regulated. Therefore mRNA levels were measured to confirm the result (Figure 4.7).

Expression of *Rv0891c* was not found to be significantly different between the mutant and the wildtype. As the level of expression is low in all strains this could have resulted in a false positive in the microarray. It is also possible that the sRNA is acting post transcriptionally on *Rv0891c* in such a way that minimal effects on the abundance of the mRNA are observed.

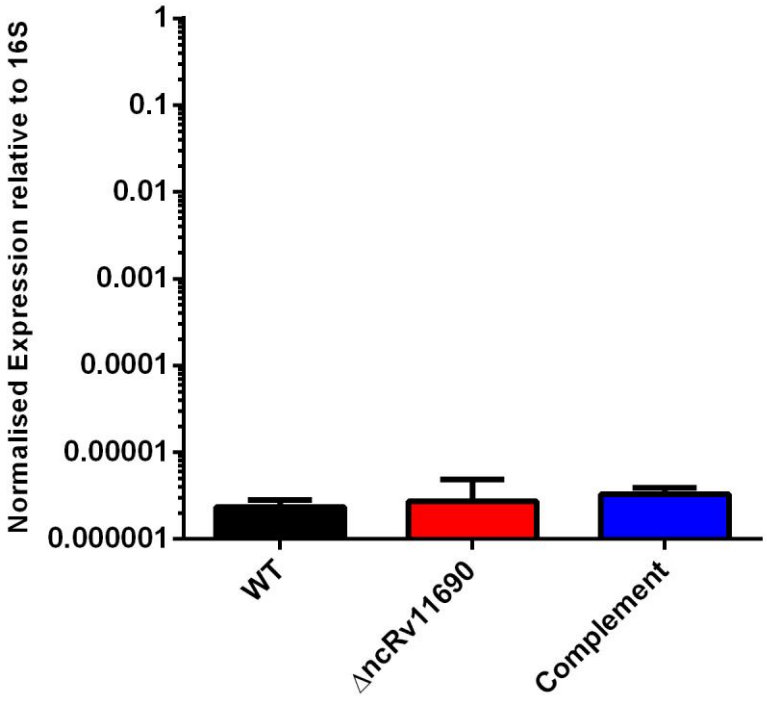

Figure 4.7 qRT-PCR of the regulator *Rv0891c*

qRT-PCR was performed as detailed in section 2.8. Each bar shows the expression level of the Rv0891c normalised to 16S. Data represents the mean and standard deviation of three biological replicates for each strain. Significance was tested with one-way ANOVA.

4.10 ΔncRv11690 is not susceptible to changes in magnesium concentration.

The observation that *Rv1535* was up regulated upon deletion of ncRv11690 could indicate that the sRNA is involved in regulating bacterial homeostasis under magnesium deprivation. This hypothesis is borne from the knowledge that *Rv1535* is up regulated in response to magnesium starvation due to the possession of a magnesium responsive riboswitch. The up regulation that was observed in the microarray could be interpreted as the deletion strain sensing magnesium starvation conditions. If ncRv11690 is responsible for regulating magnesium concentrations that results in an effect on Rv1535, then the deletion strain could be impaired for survival in media lacking magnesium. This hypothesis was tested by growing the wild type H37Rv along in parallel with the ncRv11690 deletion strain and complement in a minimal media (Sautons) with or without the addition of magnesium. No growth defect was observed with or without magnesium in the minimal media indicating that the deletion strain was not suffering from magnesium starvation.

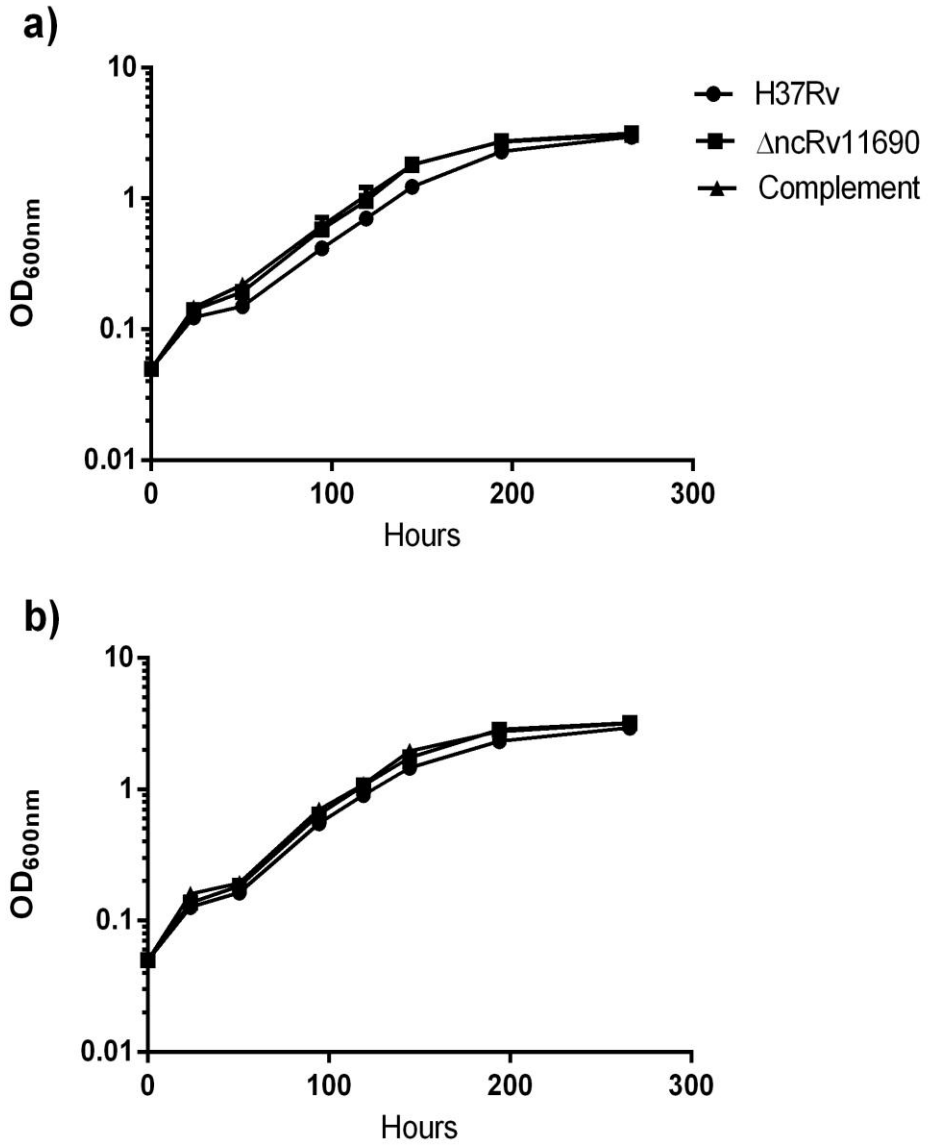

Figure 4.8 Growth of ncRv11690 under different magnesium concentrations

Strains were grown in Sautons media in rolling culture with a) 2 mM magnesium or b) without magnesium and OD_{600} monitored overtime. Data points represent three biological replicates per strain per time point. Slopes were found not to be significantly different from each other by linear regression analysis.

4.11 Over expression of ncRv11690.

In order to gain further insight into the function of ncRv11690, over expression was attempted on an integrating vector in order to achieve a lower level of expression. The promoter, sRNA and synthetic terminator were digested from previous replicating over expression constructs [153] and ligated into the integrating plasmid pKP186. This gave rise to pJHP09 and pJHP10, which were the integrating strong and weak constructs respectively.

The original over expression in a replicating vector proved lethal in *M. tb*. However, when the sRNA under the *rrnB* promoter was placed on an integrating vector, expression was reduced to such an extent that over expression was no longer lethal in wildtype H37Rv *M. tb*. This indicated that a tolerance threshold for the sRNA exists.

No obvious growth defect for any of the strains was observed, and acid fast staining of the over expression revealed no differences in cell morphology by light microscopy. RNA was isolated from both the over expression and the vector control during exponential growth and used to measure the expression level of ncRv11690 Figure 4.9.

It was observed that over expression of ncRv11690 was achieved to an astounding 22,000-fold that of wildtype vector control when expressed from the stronger *rrnB* promoter in pKA305. ncRv11690 expression increases therefore from 0.001% that of ribosomal RNA to approximately 20%. Over expression of this sRNA was still achieved to a large extent in the plasmid with the weaker promoter (pKA306), achieving approximately 18,000-fold over expression when compared to vector control. This would indicate that the expression of ncRv11690 in the replicating over expression background would have reached

or possibly exceeded that of rRNA. This is due to the fact that the plasmid based on pMV261 possessed an estimated copy number of five. Such a high level of expression would indicate that the sRNA was very stable and/or the degradosome (responsible for degradation of the sRNA) was probably saturated. This led us to investigate the stability of ncRv11690.

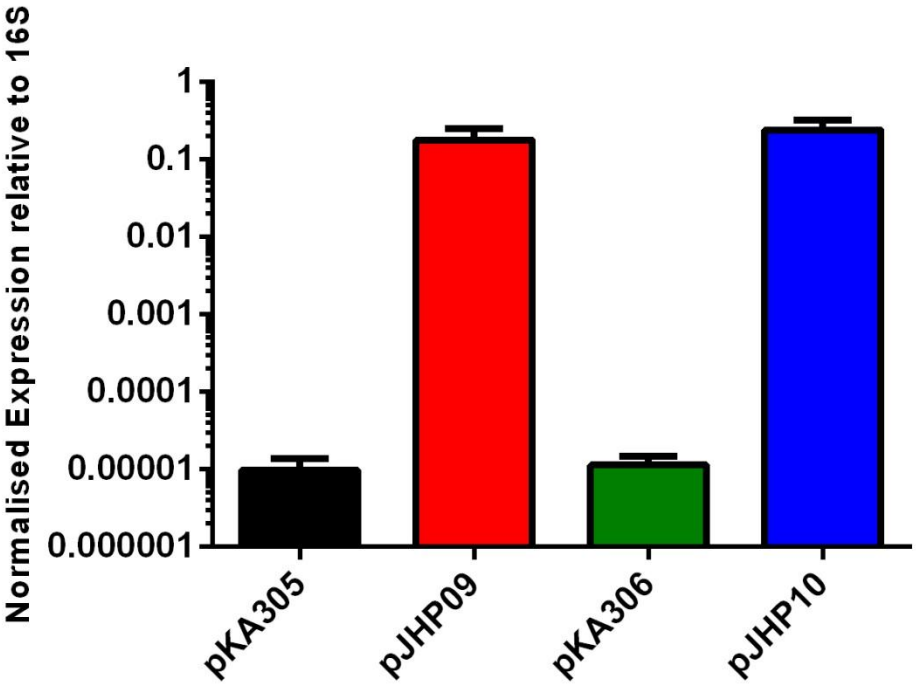

Figure 4.9 Over expression of ncRv11690 in *M. tb*

ncRv11690 expression levels were measured using qRT-PCR and in each instance are expressed relative to 16S rRNA control. Each bar represents the mean of three biological replicates. Vector controls and over expression strains found to differ significantly from each other as tested by t-test, $p<0.05$.

4.12 Stability of ncRv11690

It is important to ascertain the stability of a sRNA as its abundance under different conditions is a reflection of the rate of its synthesis and decay. The drug rifampicin is known to bind the RpoB subunit of RNA polymerase and inhibit new transcription [197]. Therefore the quantity of any RNA species in a cell following exposure to rifampicin is expected to remain unchanged and any changes due to degradation would reflect its stability. To gain insight into the stability of ncRv11690, cultures were grown to stationary phase and Rifampicin was added to the test cultures after diluting to OD_{600} = 0.3. Dilution of the culture back to a starting OD of 0.3 allows the culture to commence exponential growth under which active transcription can be observed.

Samples were taken before and after treatment with rifampicin and at different time points to assess the sRNA stability by northern blotting, Figure 4.10. Northern blotting of rifampicin treated *M. tb* revealed ncRv11690 to be highly stable, with the sRNA being detectable for at least 6 hours. This is in stark contrast to the average half-life of mRNA measured in *M. tb* which was found to be approximately 9.5 min[198]. The increased stability is likely due to the stable secondary structure previously modelled [153]. It is worth remembering however that this is an artificial system. If the sRNA is usually degraded when in a duplex with its mRNA target then lack of target message will artificially enhance the stability of the sRNA due to the specificity of the nuclease required for degradation.

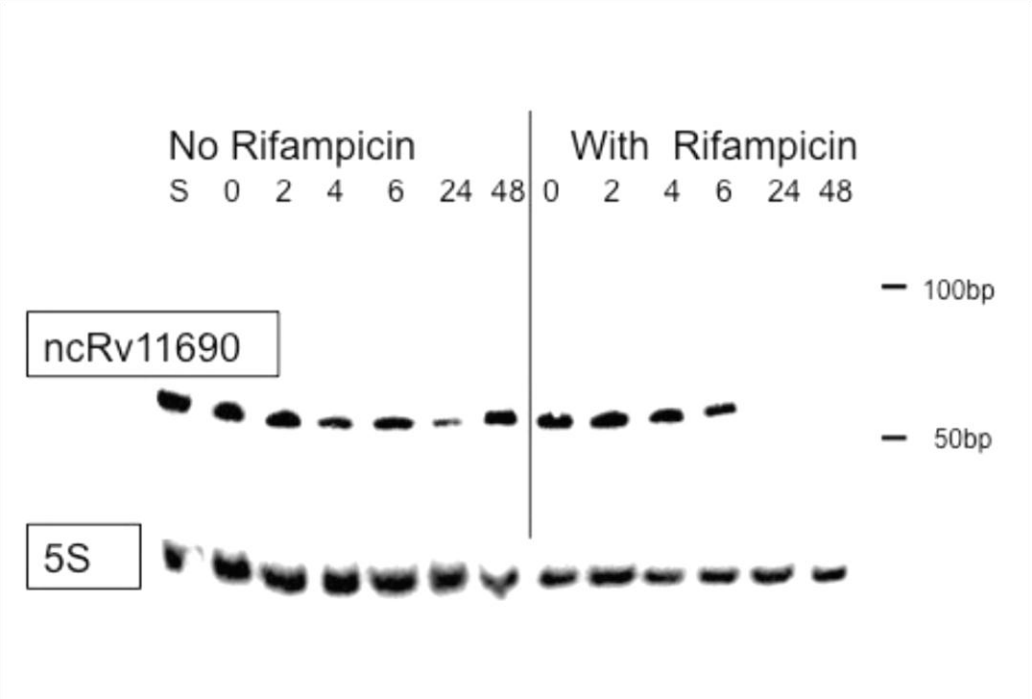

Figure 4.10 Stability of sRNA ncRv11690 +/- Rifampicin.

Cultures were grown to stationary phase, and then diluted to OD_{600} = 0.3 with or without the addition of 1 µg/ml of rifampicin. RNA was extracted for analysis by northern blot as described in section 2.9 using a ^{33}P radiolabelled probe at 0, 2, 4, 6, 24 and 48 hours after dilution.

4.13 Analysis of the ncRv11690 expression proteomes

As sRNAs are known to act on the post-transcriptional level it was of importance to assess the relative abundance of proteins within the various expression strains in order to identify targets of ncRv11690. It was expected that any changes observed in both the over expression and the deletion strain would represent targets for ncRv11690. To test this whole cell extracts were isolated from triplicate exponential phase cultures of H37Rv, ΔncRv11690, complement, ncRv11690 over expression and vector control. Samples were sent to Olga Schubert who performed Mass spectrometry and further analysed the results for statistical significance using MSstats. Protein abundance was considered to be significantly different with a fold change greater than 1 or -1 in log2 scale and with a p value less than 0.01.

18 proteins were found to be differentially expressed between the deletion strain and H37Rv. However, all of these changes were also observed in a comparison of the complement against the wildtype H37Rv, indicating that these changes were not due to the loss of ncRv11690. The induction of DosR and genes belonging to the DosR regulon were observed to be up regulated indicating that the bacteria were under stress.

Analysis of the over expression strain revealed 10 proteins to be differentially expressed between the over expression and vector control strains. 8 proteins were up regulated while 2 were down regulated. Four of these proteins (Rv2007c, Rv3134c, Rv3131 and Rv2629) were also observed to be up regulated in the deletion strain analysis and therefore unlikely to be a specific effect of ncRv11690 expression.

Of the six remaining proteins 3 belong to the functional classification of cell wall and cell processes. These are Rv3866; an Esx-1 secretion associated protein, Rv1496; a possible arginine/ornithine transport system ATPase, and Rv2576c; a possible conserved membrane protein. The observed up regulation of Rv3866 along with the down regulation of Rv2576c could suggest a change in the cell wall upon over expression.

Protein	Δ/H37Rv Fold Change (Log2)	Complement/ H37Rv Fold change (Log2)	Δ/ H37Rv p value	Complement/ H37Rv p value
Rv2007c	6.75	7.17	<0.001	<0.001
Rv2031c	6.54	7.04	<0.001	<0.001
Rv0079	5.32	5.64	0.001	0.003
Rv2626c	5.07	5.09	<0.001	<0.001
Rv3134c	4.72	5.37	<0.001	<0.001
Rv0569	4.56	5.56	0.001	0.008
Rv2030c	4.51	4.91	<0.001	<0.001
Rv1738	4.2	4.93	<0.001	0.001
Rv2623	4.01	4.68	<0.001	<0.001
Rv2032	3.56	4.3	<0.001	0.001
Rv2005c	3.18	3.89	<0.001	<0.001
Rv2629	3.16	3.66	<0.001	<0.001
Rv3131	3.07	3.54	<0.001	<0.001
Rv1996	2.86	3.69	<0.001	<0.001
Rv3133c	2.53	2.91	<0.001	0.003
Rv2383c	1.56	1.52	<0.001	<0.001
Rv0081	1.46	1.48	0.004	0.009
Rv3271c	-0.74	-1.38	<0.001	0.008
Rv3213c	-0.77	-1.09	<0.001	0.009

Table 4.3 Proteins differentially expressed between either wild type and deletion strains or H37Rv and Complement.

Whole cell extracts from exponential phase cultures were analysed by mass spectrometry for differential protein expression. Statistical significance was set at a fold change >1 or -1 in log2 scale with a p value < 0.01

Protein Rv number	Gene name	Over expression/vector Fold change (Log2)	Over expression/vector p value
Rv2007c	fdxA	3.65	0.002
Rv3134c	USP	2.90	<0.001
Rv3131	tgs	1.91	0.001
Rv2482c	plsB2	1.83	0.006
Rv0458		1.27	0.004
Rv2629		1.22	0.008
Rv3866	espG1	1.19	0.001
Rv1496		1.07	0.005
Rv2576c		-1.02	0.008
Rv2782c	pepR	-2.25	<0.001

Table 4.4 Proteins differentially expressed between the over expression and vector control

Whole cell extracts from exponential phase cultures were analysed by mass spectrometry for differential protein expression. Statistical significance was set at a fold change >1 or -1 in log2 scale with a p value < 0.01

4.14 *in vivo* Analysis of ΔncRv11690 compared to wildtype *M. tb*

As ncRv11690 was shown to be well expressed during the early infection of Balb/C mice (Figure 4.2) the possibility that ncRv11690 may play a role in pathogenesis was investigated using *in vivo* models.

4.14.1 Deletion of ncRv11690 had no effect on the ability of *M. tb* to survive within either naïve or activated macrophages.

To investigate the function of ncRv11690 during very early infection we used a cell based model. Both naïve and IFN-γ activated macrophages were infected with wild type H37Rv, and ΔncRv11690 at an MOI of 0.1:1 and the progress of infection was followed, (Figure 4.11).

The wild type H37Rv strain reproducibly replicated to levels corresponding to an increase of approximately 2 logs in naive macrophages during the course of the experiment. Growth and survival of the ΔncRv11690 strain was very similar to that of the wild type with no significant difference detected at any time point.

Growth of both H37Rv and ΔncRv11690 within IFN-γ activated macrophages was less than that observed in naive macrophages. An increase of approximately 1 log would indicate successful activation of the macrophages due to the control of proliferation. However, there was only a significant difference between the two strains at 120 hours, which was not replicated at later time points. This would suggest that ΔncRv11690 is not attenuated for growth in either naive or activated macrophages.

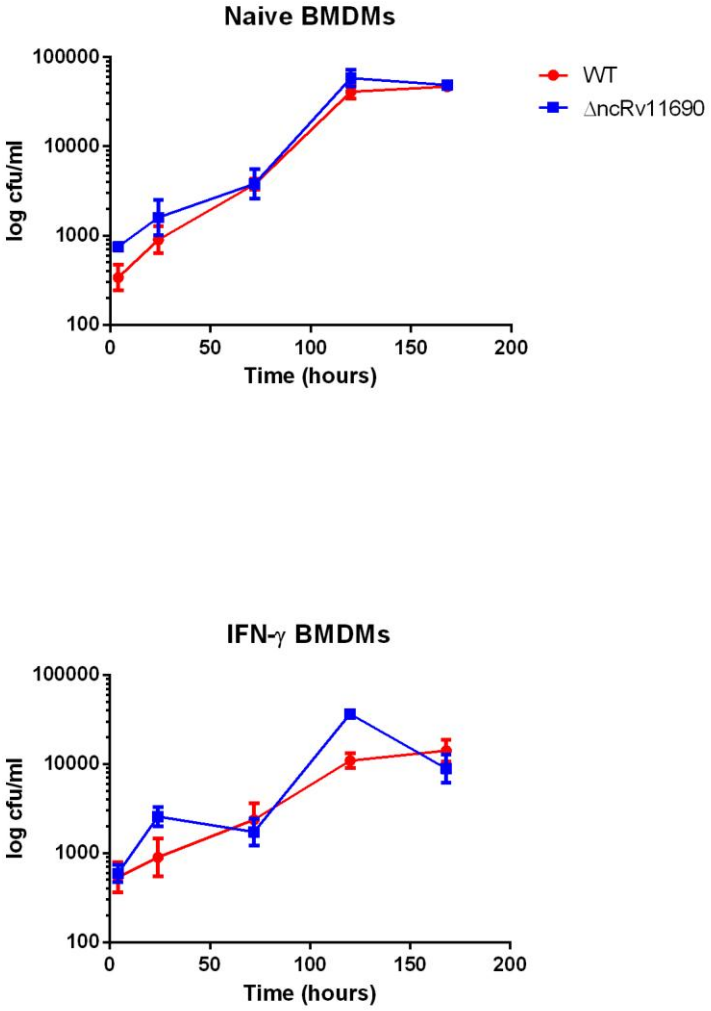

Figure 4.11 Survival of the ΔncRv11690 in a macrophage model of infection

Survival of Wild type *M. tb* H37Rv, ΔncRv11690, and complementing strains within naive and IFN-γ activated BMDM over a time course of infection. Significance was tested with Two-way ANOVA $p>0.05$. Data is the mean and standard deviation of triplicate infections.

4.14.2 Deletion of ncRv11690 had no effect on the ability of *M. tb* to survive in a mouse model of infection

The lack of an attenuation for the mutant strain in macrophages led to the assessment of the importance of the sRNA in establishing an infection in mice. Groups of mice were infected by the aerosol route as described in section 2.8.12, with 5 mice per strain sacrificed at each time point for bacterial enumeration.

Infection of the mice showed that the ncRv11690 deletion strain was not defective in its ability to establish or maintain an infection (Figure 4.12). The first infection hinted at an increase in virulence in the later time points for the ΔncRv11690 strain. However, when the infection was repeated this was not observed.

ncRv11690 in this model of infection does not result in attenuation as measured by CFUs. It remains possible though, that ncRv11690 may still play a role in pathogenesis that does not result in lowered CFUs.

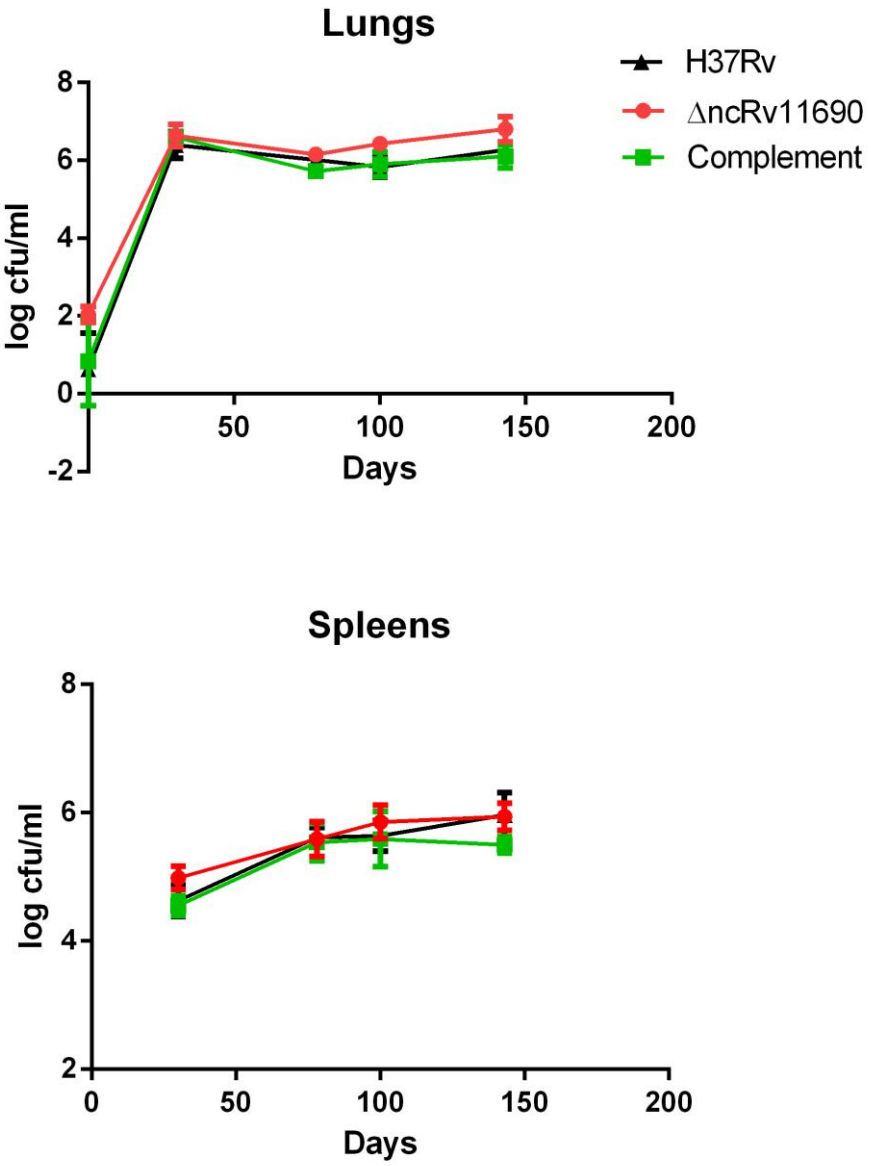

Figure 4.12 Survival of ΔncRv11690 from aerosol infected mice.

Survival of wildtype *M. tb* H37Rv, ΔncRv11690, and complement within the lungs and spleens of BALB/C mice. The data represents the averages and standard deviations from 5 mice per time point and is representative of two independent experiments. Significance was tested with one-way ANOVA.

4.15 Discussion

This study set out to address the role of ncRv11690 in the pathogenicity of *M. tb* by targeting ncRv11690 for inactivation in the wildtype strain H37Rv. Through expression and infection studies the aim was to elucidate a function for ncRv11690 and assess the virulence of the deletion strain.

Successful deletion of ncRv11690 from the *M. tb* chromosome revealed the sRNA to be non-essential *in vitro* despite the sRNA being well expressed in exponential phase. ncRv11690 expression has been observed to be highest in exponential growth and during mouse infection. It is down regulated upon stationary phase and starvation. This suggested that the sRNA was important for active growth. *In vitro* growth in 7H9 however, revealed that the deletion strain was not attenuated for growth under standard conditions. This could suggest that the precise induction conditions are yet to be determined.

Many sRNAs are induced in response to stress [93, 199] yet ncRv11690 is down regulated in both stationary phase and starvation. Therefore in order to explore the possible function of ncRv11690 gene expression microarrays were used.

Transcriptional Analysis of ncRv11690 under exponential conditions revealed *desA3* and *Rv3841* to be down regulated. These genes are from the Zur and IdeR transcriptional regulons respectively [200-202]. These regulons are known to control zinc and iron homeostasis indicating an effect on the intracellular metal concentrations in ΔncRv11690. This was further evidenced in the up

regulation of Rv1535 which possesses a magnesium responsive riboswitch that results in up regulation upon magnesium starvation [154].

Two major mechanisms are involved in metal ion homeostasis and resistance. Firstly the uptake or efflux of heavy metal ions across the membrane [203], secondly the specific chelating of the metals by intracellular chaperones, e.g. metallothioneins [204]. These genes are tightly controlled by the metal sensing transcriptional regulators such as Zur and IdeR which bind iron and then interact with the DNA to control transcription of target genes [205, 206].

Iron is an essential nutrient for most pathogens, and iron limitation at infection sites is an important means of host defence. Expression of a number of *M. tb* genes are regulated in response to reduced iron levels [205, 207, 208]. Importantly *M. tb* virulence has been observed to be reduced in strains that lack the ability to adapt to iron limitation [207, 209, 210].

The ability of the mutant to survive under magnesium starvation conditions was tested to assess the ability of the strain to adapt. No attenuation of the ncRv11690 deletion strain was observed however indicating that it was not suffering from magnesium starvation. The ability of the ΔncRv11690 strain to adapt to iron limiting conditions was not tested in this study but could be included in further studies. However, the reduction of BfrB is most likely compensated for by an increase in expression of the homologue BfrA and therefore unlikely to result in attenuation.

Global analysis of the proteome from the deletion strain during exponential phase showed ncRv11690 deletion resulted in no statistically significant

changes. This would indicate that the induction conditions required for ncRv11690 function were not met under the conditions examined. Analysis of the over expression proteome however, identified three proteins involved in cell wall and cell processes. Rv3866, an ESX-1 secretion associated protein was found to be up regulated while the membrane protein Rv2576c was down regulated. ESX-1 secretion is important for intracellular survival and virulence and is responsible for the secretion of ESAT-6 and CFP-10. The major virulence determinant and ESX-1 substrate, EsxA, arrests phagosome maturation and lyses cell membranes, resulting in tissue damage that ultimately results in spread of the disease.

The EsxA inhibitor BBH7 affects *M. tb* metal-ion homeostasis and revealed zinc stress as an activating signal for EsxA secretion [211]. Interestingly in a bioinformatic search for targets using TARGETRNA2, predicted base pairing to occur upstream of Rv3870 (eccCa$_{1)}$ a conserved ESX component; at bases-12 to -28. This would suggest regulation by translational inhibition. However, target prediction did not identify any of the mRNA highlighted in either the transcriptomic or proteomic analyses.

If ncRv11690 is involved in the regulation of EsxA this could explain why DesA3 from the Zur regulon [200] was found to be down regulated (6.7 fold) upon deletion of ncRv11690.

Deletion of ncRv11690 did not result in attenuation in the macrophage or mouse model of infection when measured by CFUs. It is still possible though that the pathogenicity of the *M. tb* deletion strain was altered. Attenuation of some mutants has only become apparent when tested using a time to death study in

mice, as observed with a sigF mutant [177]. Differences in virulence can also be observed under different host genetic backgrounds. Traditionally, Balb/C mice and C57BL6 mice have been regarded as Th2- and Th1-skewed strains, respectively. Th1 cells are associated with cell-mediated immunity and characteristically produce IL-2, IFN-γ, and TNF-β. Th2 cells regulate humoral immunity, can moderate Th1 responses [212], and produce cytokines IL-4, IL-5, and the anti-inflammatory cytokine IL-10. Therefore the Balb/C mice used for the ΔncRv11690 could influence the *M. tb* phenotype observed, and therefore it is possible that were the infection to be repeated with C5BL6 mice or immune deficient SCID mice, that a different phenotype could have been observed.

5 Deletion of ncRv13661, the most abundant sRNA in *M. tb* has pleiotropic effects on transcription

5.1 Introduction

MTS2823 (or ncRv13661 according to the new nomenclature), was discovered through the full transcriptome analysis of *M. tb* by RNA seq [3]. It is located between Rv3661 and Rv3662c (genome co-ordinates 4100669 - 4100988) Figure 5.1, and was observed to have the highest reads per kilobase of transcript per million reads mapped (RPKM) excluding that of rRNA peaks in exponentially growing cultures. Its expression during stationary phase is increased a further 10-fold reaching approximately 50,000 RPKM in contrast to the most highly expressed mRNA with an RPKM of 6,566 [3].

The abundance of ncRv13661 suggests that this sRNA may be interacting with some major machinery of the cell such as the ribosome or RNAP rather than with low copy number mRNAs. Highly abundant RNAs of known function include for example, 16S and 23S. These are components of the ribosome known as ribosomal RNAs, and are highly conserved between different species of bacteria and archaea [213]. Another abundant regulatory RNA is 6S, which interacts with RNAP under certain conditions to control transcription as described in section 1.10.

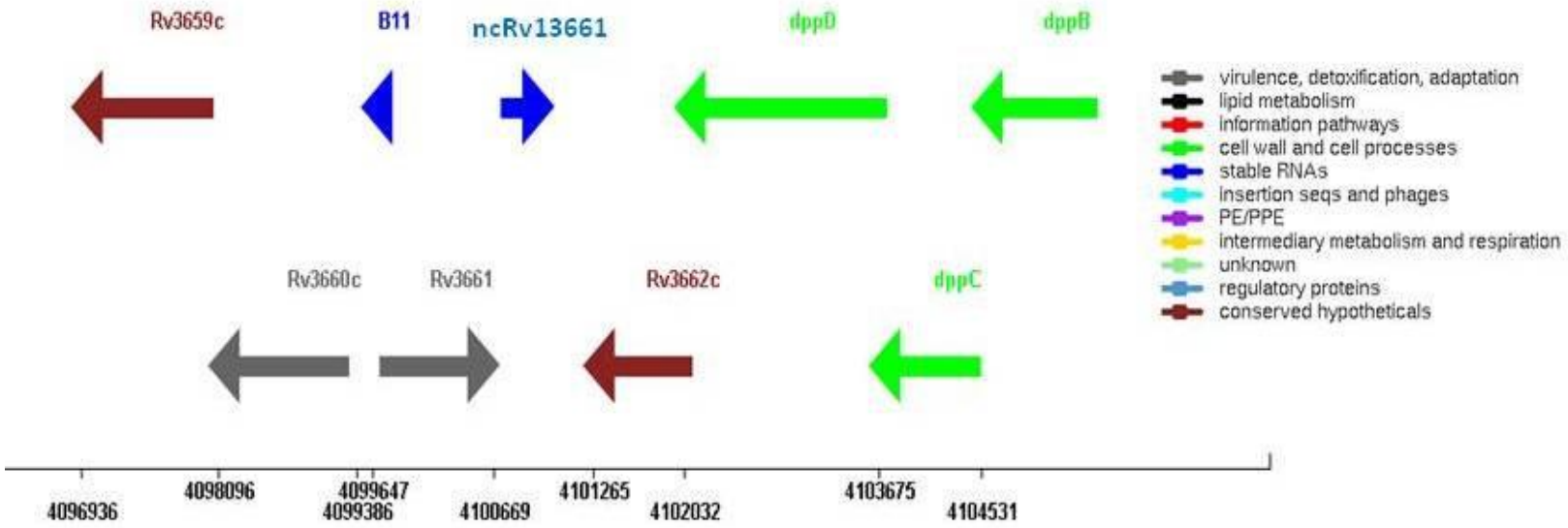

Figure 5.1 Genomic location of ncRv13661 in the *M. tb* genome as viewed in Tuberculist (http://tuberculist.epfl.ch/)

E. coli 6S RNA was the first sRNA shown to inhibit transcription by binding directly to the housekeeping holoenzyme form of RNAP. It is ubiquitously expressed although it is most abundant in stationary phase. No homologue for 6S RNA has been found in *M. tb. S*tructural analysis of ncRv13661 revealed some similarity to the canonical 6S RNA, but failed to match the criteria of a genuine 6S homologue [214]. Ms1, the corresponding sequence in *M. smegmatis*, was initially identified in a bioinformatic screen for 6S RNA but was also found to lack key structural characteristics of 6S RNA [214]. Figure 5.2 shows the predicted secondary structures of the *M. tb* sRNA alongside 6S RNA from *E. coli* for comparison. During the preparation of this thesis, Ms1 was reported to interact with the RNAP core enzyme [215]. This is in contrast to the conventional binding of 6S RNA to the σ^{70} holoenzyme that has been observed in other bacteria [132]. These findings suggest that ncRv13661 may have a functional role related to that of 6S RNA.

Over expression of ncRv13661 in *M. tb* during exponential phase, resulted in a small but significant growth defect [3]. Transcriptional profiling identified down regulation of a panel of genes including those encoding key methylcitrate cycle enzymes PrpC, PrpD and Icl1. The methylcitrate cycle plays an important role in preventing accumulation of toxic intermediates generated during β-oxidation of odd chain fatty acids and growth on cholesterol [216]. The down regulation of these genes suggests that ncRv13661 may be involved in control of lipid metabolism in *M. tb*.

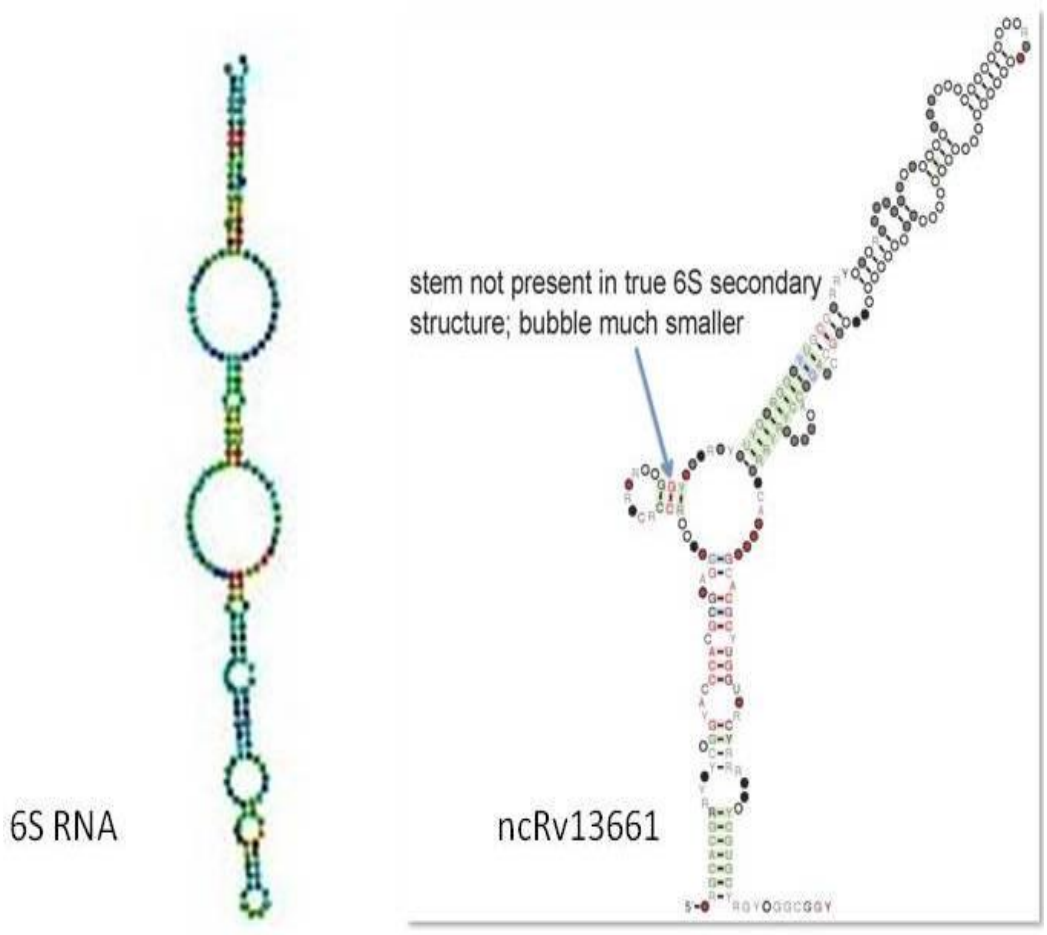

Figure 5.2 Structural comparisons of the highly expressed RNAs

Predicted structure ncRv13661 compared to the canonical 6S RNA structure. Both RNAs are long double-stranded hairpins. However, ncRv13661 has one central bubble that is pinched whereas 6S RNA contains two large central bubbles.

5.2 Hypothesis and specific aims

The abundance of ncRv13661 suggests that rather than base-pairing with specific target mRNAs, it may be performing a regulatory role in conjunction with the major machinery of the cell such as the ribosome or RNAP. Initial transcriptional profiling of an over expressing strain suggests that ncRv13661 may function in the regulation of lipid metabolism. To test the hypothesis that it performs a role resembling that of 6S RNA in transcriptional reprogramming during transition to a non-replicating state, ncRv13661 was assessed for potential interactions with major protein complexes and effects on cell viability and gene expression were characterised in a strain from which ncRv13661 had been deleted.

Results

5.3 Expression of ncRv13661

The abundance of ncRv13661 during exponential growth is approximately 2% that of 16S ribosomal RNA when measured by qRT-PCR. This increased to 20-30% of rRNA in stationary phase and in response to starvation. In a mouse infection model, the level of ncRv13661 was found to be equivalent to that of ribosomal RNA at a three-week time point (Figure 5.3). Over expression of ncRv13661 was measured to be 25% that of rRNA during exponential phase in 7H9 media.

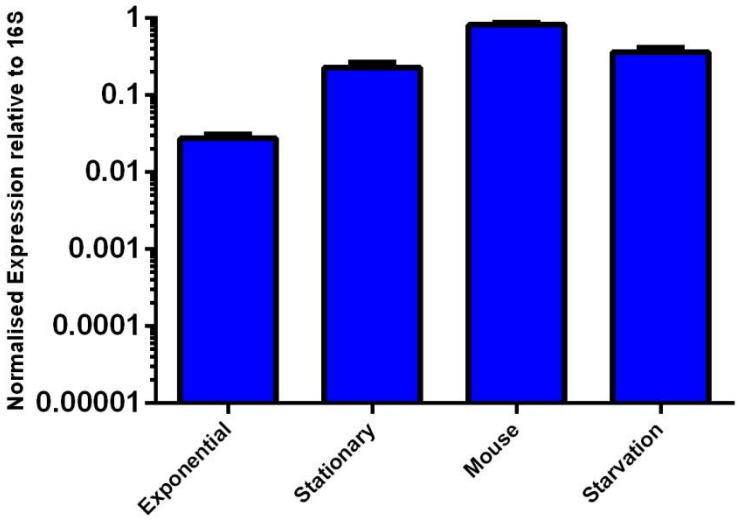

Figure 5.3 Expression levels of ncRv13661 in *M. tb*

ncRv13661 expression levels were measured using qRT-PCR, in each instance levels are expressed relative to 16S rRNA control. RNA was isolated from exponential phase, stationary phase (one week after OD_{600} = 1.0), 96 hours starvation in PBS and from *M. tb* in the lungs of three week infected mice. Data represents the mean and standard deviations of three biological replicates for each condition. Expression levels differ significantly from each other for each growth phase as tested by One-way ANOVA.

5.4 Creation of an ncRv13661 deletion strain

ncRv13661 and its promoter region were deleted from *M. tb* using a non-replicating suicide vector [7] in a two-step process as described in section 2.9.10 and 3.4. Briefly, a single crossover (SCO) recombinant was isolated from the electroporation of *M. tb* with the targeting construct, and subjected to counter-selection in order to obtain double crossovers (DCO) generated by a second recombination event. The markers *sacB* and *lacZ* on the targeting construct allow for blue/white screening of colonies and make counter-selection for sucrose sensitivity possible [183] .

5.4.1 Design and creation of the deletion plasmid

Fragments corresponding to 4099524-4100643 from the 5' flank and 4101050-4102096 from the 3' flank of ncRv13661 were cloned sequentially into the targeting construct. The PCR strategies for screening SCO and DCO candidates are represented in Figure 3.3A.

5.4.2 Screening of single and double crossover candidates

After electroporation of the targeting plasmid into *M. tb* H37Rv, cells were plated onto 7H11 agar containing kanamycin and X-Gal for selection of SCOs. Generation of SCOs for the construction of this particular mutant proved extremely difficult; electroporation of *M. tb* with the targeting construct had to be repeated a total of 8 times.

After incubation, 5 blue colonies along with 3 white colonies as controls were screened by PCR to identify SCOs (Figure 5.4). Only pair 1 PCR reactions resulted in correct PCR products and so at this stage SCOs

could not be distinguished from random integrations, and all potential candidates were taken to the next stage of selection.

SCOs 1 to 5 were plated onto non-selective 7H11 for the second recombination event to occur. After plating on selective media, four of the SCO parents generated potential DCOs that were white and kanamycin sensitive. Five colonies of potential DCOs from each SCO parent were screened by PCR amplification and clone 3.21 was characterised by whole genome sequencing.

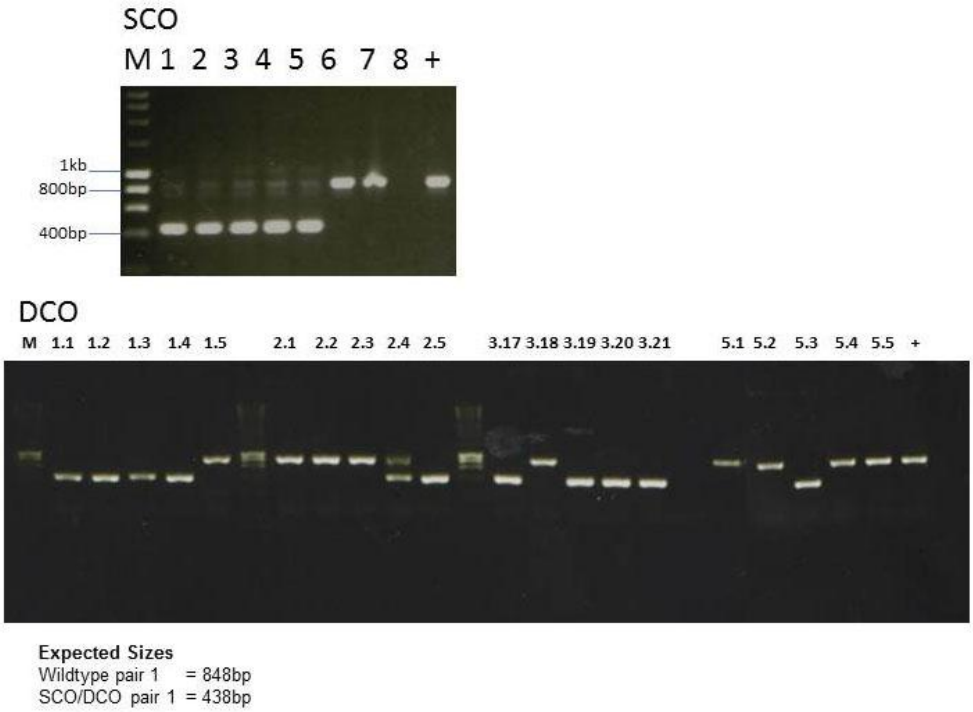

Figure 5.4 PCR screening for the construction of the ncRv13661 deletion strain.

PCR reactions were designed using the strategy outlined in Figure 3.3A. Expected sizes of products for each primer pair are indicated. SCO = single crossover; DCO = double crossover; M = Bioline Hyperladder I DNA marker,

+ = wildtype genomic DNA control.

5.4.3 Whole genome sequencing of DCO 3.21

High quality genomic DNA was extracted from the DCO 3.21 and from the parental H37Rv strain to confirm the deletion and to identify any possible background mutations. Sequencing libraries were prepared from both strains and sequenced by the HTS sequencing facility at NIMR. The resulting reads were aligned to the H37Rv reference genome by Graham Rose (NIMR) (Appendix III). SNPs in repeat regions such as PE_PGRS were discarded due to unreliability along with 2 SNPs created by deletion of the sRNA. This left seven SNPs which mapped to various regions in the genome. Three SNPs mapped to Rv2940c (mycocerosic acid synthase, *mas*); two were synonymous and one was nonsynonymous, causing a change from TTC to TTT at position 3278390 and two changes at positions 3278390 and 3278391 resulting in a change from GTG to GGC. Shotgun proteome analysis of DCO 3.21 by Olga Schubert (ETH Zurich) recorded a 6-fold reduction in Mas (p-value 0.0243 by t test), suggesting that the mutation had a deleterious effect on protein stability. Mas is a polyketide synthase that is responsible for the synthesis of methyl-branched lipids, mycocerosates [217, 218], which are esterified with phthiocerol to generate PDIMs, complex cell wall lipids implicated in the virulence of *M. tb* [219-222]. Spontaneous PDIM mutations have previously been shown to confer an *in vitro* growth advantage for H37Rv [223]. Four other SNPs were identified in intergenic regions of the genome with two mapping upstream of a second polyketide synthase, *pks3*, at positions 1313338 and 1313339, though there was no detectable effect on the level of *pks3* expression measured by microarray profiling (not shown).

SCOs 1-3 and DCO's 1.1-1.4, 2.5, 3.17-3.21 and 5.2 were checked for mutations in *mas* by PCR amplification of a 2kb region surrounding the 3 previously identified SNPs. Consequently these PCR products were sequenced for screening of mutations. It was found that SCO 1 and DCO 1.1, 1.3 and 1.4 were the only clones without any *mas* mutations present. As this method only identifies SNPs in a small region of *mas* and this screening does not identify other possible regions of mutation further sequencing was required. For this reason whole genome sequencing was performed on DCOs 1.1, 1.3 and 1.4.

5.4.4 Whole genome sequencing of DCO 1.1-1.4

High quality genomic DNA was extracted from the DCOs 1.1, 1.3 and 1.4 along with the parental strain to identify any possible background mutations. Sequencing libraries were prepared from all strains and sequenced by the HTS sequencing facility at NIMR. The resulting reads were aligned to the H37Rv reference genome by Teresa Cortes (NIMR) Table 5.1. As with the previous analysis, the SNPs identified in repeat regions were discarded along with 2 SNPs created by deletion of the sRNA.

This left 1 non synonymous SNP in Rv2692c (a glycosyl transferase) that was present in all strains and a synonymous SNP in Rv3661 that was present in DCOs 1.1 and 1.3 only. Due to DCO 1.4 containing only 1 SNP in Rv2692c this clone was selected for further investigation and electroporated with the complementing plasmid. DCO 1.4 was not observed to result in any difference in expression of Rv2692c on the transcript level (Tables 5.2 and 5.3) or protein level Table 5.7. The possibility that this SNP could affect enzyme function however cannot be excluded. Therefore for all experiments the complement was included for comparison and confirmation of ncRv13661 specific effects.

SNP position	H37Rv	1_1	1_3	1_4	Gene	Synonym	Orientation	Change	Type	annotation
336718	A	C	M	M	Rv0279c	PE_PGRS4	-	F786V	nonsynonymous SNV	PE-PGRS
467501	T	G	G	G	Rv0388c	PPE9	-	S167S	synonymous SNV	PPE
3314422	G	A	A	A	Rv2962c	-	-	T234I	nonsynonymous SNV	glycosyl transferase
3934733	G	G	C	G	Rv3508	PE_PGRS54	+			PE-PGRS
3934734	G	G	A	G	Rv3508	PE_PGRS54	+			PE-PGRS
3949383	C	G	C	C	Rv3514	PE_PGRS57	+	A1197G	nonsynonymous SNV	PE-PGRS
4100432	T	A	A	T	Rv3661	-	+	T262T	synonymous SNV	hypothetical protein

Table 5.1 SNP analysis of ΔncRv13661 DCOs 1.1, 1.3 and 1.4.

5.5 Transcriptional profiling of DCO 1.4

The transcription profile of ΔncRv13661 DCO 1.4 in exponential culture was compared to the wildtype parent by oligonucleotide microarray analysis using Cy dye-labelled cDNA. 78 probes, corresponding to 48 genes, were identified as being differentially expressed by greater than 2-fold between wildtype and ΔncRv13661 (Tables 5.2 and 5.3).

The 23 transcripts present at higher abundance in the absence of ncRv13661 including the methylcitrate cycle genes *prpC* and *prpD* that were previously found at decreased abundance when ncRv13661 was over expressed during exponential growth. Six genes from the arginine biosynthesis operon (Rv1652-Rv1659) were also up regulated in ΔncRv13661. The arginine operon is regulated by the ArgR repressor [224] and is markedly down regulated in the starvation model. Rv1813c which is known to be in both the MprAB and DosRST regulons was found to be up regulated [225]. Five genes from the *mas*/*pks15* locus (Rv2940 to Rv2947c) were up regulated in the knockout, though conversely *ppsD* (Rv2934) was down regulated. Other down regulated genes included the mmpSL5 transporter and the associated transcriptional regulator Rv0678 [226]. qRT-PCR validation of the microarrays for the highest ranking transcripts led to the observation that only the up regulated genes could be confirmed and generally complemented (Table 5.2). This pattern of expression would be in agreement with only down regulation observed for the over expression of ncRv13661. A comparison of the over expression and deletion microarrays can be found in Figure 5.5.

Gene	Gene Name	FC Δ/WT Average of probes	p-value	Fold change by qRT-PCR Δ/WT	Fold Change by qRT-PCR Comp/WT
Rv1130	*prpD*	2.7	0.009	5.8	2.3
Rv1131	*prpC*	2.7	0.018	3.6	1.6
Rv2931	*ppsA*	2.4	0.011	2.6	1.2
Rv1813c	-	2.3	0.016	3.1	1.4
Rv2948c	*fadD22*	2.3	0.007	3	1.3
Rv3919c	*gidB*	2.3	0.01		
Rv1656	*argF*	2.2	0.007		
Rv1657	*argR*	2.2	0.004		
Rv2949c	-	2.2	0.005		
Rv3920c	-	2.2	0.011		
TBFG_13135	-	2.2	0.017		
Rv1047	-	2.1	0.012		
Rv1653	*argJ*	2.1	0.007		
Rv1654	*argB*	2.1	0.005		
Rv1655	*argD*	2.1	0.007		
Rv1658	*argG*	2.1	0.009		
Rv2189c	-	2.1	0.005		
Rv2632	*ppsB*	2.1	0.009		
Rv2947c	*pks15*	2.1	0.016		
Rv2666	-	2	0.032		
Rv2782c	-	2	0.007		
Rv2940c	*Mas*	2	0.002		

Table 5.2 Genes up regulated > 2-fold upon deletion of ncRv13661 in exponential phase

Gene	Gene Name	FC Δ /WT Average of probes	p-value	Fold change by qRT-PCR Δ /WT	Fold Change by qRT-PCR Comp/WT
MT3762	*ncRv13661*	147.5	<0.001		
Rv1935c	*echA13*	11.9	0.005	1.1	
Rv2598	-	5.6	0.005	1.1	
Rv0676c	*mmpL5*	2.5	0.007	1.9	2.2
Rv0678		2.5	0.009	1.5	2.3
Rv2428	*ahpC*	2.5	0.005	2.2	1.9
Rv2934	*ppsD*	2.4	0.006	1.1	0.6
Rv0677c	*mmpS5*	2.3	0.005		
Rv1592c	-	2.3	0.005	2.0	3.0
Rv2913c	-	2.3	0.005		
MT1627		2.2	0.006		
Rv1039c	*ppe15*	2.2	0.02		
Rv1040c	*PE8*	2.2	0.023		
Rv2429	*ahpD*	2.2	0.005		
Rv0096	*PPE1*	2.1	0.009		
Rv0410c	*pknG*	2.1	0.007		
Rv1218c	-	2.1	0.004		
Rv2244	*acpM*	2.1	0.007		
Rv2386c	*Mbtl*	2.1	0.014		
Rv2780	*Ald*	2.1	0.034		
Rv3534c	*hsaF*	2.1	0.007		
Rv0097		2	0.007		
Rv0440	*groL2*	2	0.011		

Table 5.3 Genes down regulated > 2-fold upon deletion of ncRv13661 in exponential phase

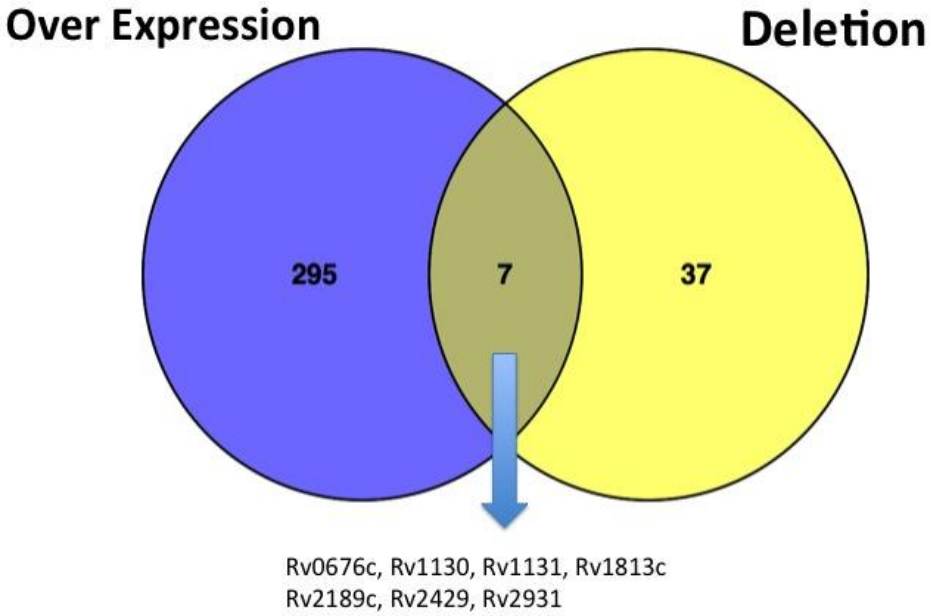

Figure 5.5 Venn diagram representing the common transcriptional changes between over expression and deletion of ncRv13661 during growth on 7H9.

5.6 Transcriptional profiling during growth on propionate

The concordance between down regulation of methylcitrate cycle genes in response to over expression of ncRv13661 and up regulation in the deletion strain could reflect a direct effect of the sRNA on the individual mRNA transcripts or an indirect effect mediated by a metabolic change. The *prpDC* operon (Rv1130-1131) is subject to conventional regulation by the adjacent Rv1129c transcription factor (which is in turn regulated by SigE) and is induced during growth on propionate. To determine whether growth on propionate would override control by the sRNA, the effect of ncRv13661 over expression was assessed by microarray profiling of propionate cultures.

In total 114 probes on the array were found to be differentially expressed between the vector control and the over expression strain with a fold change of 2.5 or greater. This amounted to a change in the mRNA levels of 78 genes (Appendix V). As previously observed during growth on glycerol/glucose [3], the majority of the probes were found to be down regulated in the over expression strain (Appendix V). 29 mRNA were found to overlap with the previous published over expression of ncRv13661 in 7H9 (Figure 5.6). Surprisingly neither *prpDC* nor *icl1* was present in the list of genes with altered expression, as ncRv13661 was previously found to down regulate the genes involved in the methyl citrate cycle. Both assays did identify among others down regulation for *sigB, G* and *sigE* along with the anti-sigma factor E (*rseA*) and Rv1406 (*fmt*) (Appendix V). In addition there were a large number of genes that were down regulated involved in DNA replication and repair. As the overlap

between these arrays is not extensive, it would suggest that ncRv13661 is not targeting a specific set of mRNAs through a standard base pairing mechanism.

In contrast to growth in glycerol/glucose, 41 probes (25 genes) were up regulated when ncRv13661 was over expressed in propionate cultures (Table 5.3). Several of the up regulated genes overlapped with genes that were down regulated in the knockout. In addition to *mmpSL5*, these include a second transporter operon, Rv1216c-Rv1218c, that is regulated by the adjacent transcription factor encoded by Rv1219c (*raaS*) [227]. Up regulation of the *raaS* operon is an indication of intracellular accumulation of fatty acyl-CoA molecules [227].

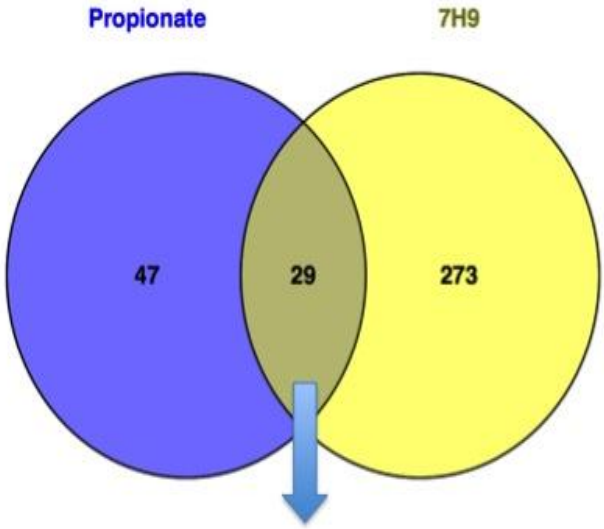

Rv0059, Rv0060, Rv0094c, Rv0182c (SigG), Rv0336, Rv1128c, Rv1221 (SigE), Rv1223 (rseA), Rv1277, Rv1406 (fmt), Rv1588c, Rv1765c, Rv1833c, Rv1945, Rv2015c, Rv2693c, Rv2710 (SigB), Rv2717c, Rv2719c, Rv2974c, Rv3191c, Rv3201c, Rv3270, Rv3370, cRv3466, Rv3585, Rv3776, Rv3839

Figure 5.6 Venn diagram representing the overlapping transcript changes between growth on 7H9 and growth on propionate for the ncRv13661 over expression.

Gene	Gene Name	FC OE/Vector Average of probes	p-value	qRT-PCR Fold Change
MT3630	*ncRv13528*	2.2	0.049	
MT3762	*ncRv13661*	35.2	0.006	30
Rv0118c	*oxcA*	2.7	0.006	
Rv0166	*fadD5*	2.3	0.031	
Rv0167	*yrbE1A*	2.2	0.028	
Rv0169	*mce1A*	2.2	0.046	
Rv0280	*PPE3*	2.3	0.017	
Rv0631c	*recC*	5.9	0.048	
Rv0676c	*mmpL5*	2.3	0.024	
Rv0677c	*mmpS5*	2.5	0.017	
Rv0678	-	2.5	0.006	
Rv0696	-	2.1	0.037	
Rv0697	-	2.0	0.008	
Rv0867c	*rpfA*	3.7	0.022	
Rv0885	-	2.2	0.013	
Rv1216c	-	2.6	0.014	
Rv1217c	-	3.4	0.016	4.7
Rv1218c	-	2.8	0.009	3.5
Rv1219c	*raaS*	2.7	0.009	3.4
Rv1856c	-	2.2	0.017	
Rv2035	-	2.1	0.018	
Rv2406c	-	2.1	0.014	
Rv2485c	*lipQ*	2.3	0.014	
Rv2780	*ald*	2.2	0.016	
Rv3197A	*whiB7*	2.1	0.031	

Table 5.4 Genes up regulated in the over expression strain > 2 fold during growth on propionate

5.7 Transcriptional profiling during stationary phase

The abundance of ncRv13661 increases 10-fold during transition to stationary phase and it might be anticipated that sRNA deletion would result in a more extensive transcriptional phenotype. To address this, microarrays were performed to see if this was the case. In fact, only 40 genes were differentially expressed in a comparison of stationary phase ΔncRv13661 and wildtype cultures (Tables 5.5 and 5.6). Only two genes were differentially regulated in both stationary phase and exponential culture; Rv1935 (*echA13*) and Rv2598. Both genes registered a large fold-change that could not be confirmed by qRT-PCR due to very low baseline expression. Two genes that were down regulated in ΔncRv13661 – Rv0631c (*recC*) and Rv0867c (*rpfA*) – were reciprocally up regulated when ncRv13661 was over expressed (Table 5.4). The highest ranking changes were selected for confirmation by qRT-PCR and fold changes shown in Table 5.5. Fold changes observed by qRT-PCR were not significant for the majority of genes and were low in comparison to those gained in the microarray due to a low baseline expression. Rv2140c and Rv0721 (*rpsE*) were found to be significantly different by t-test but could not be complemented. Again this pattern is inconsistent with a model in which ncRv13661 targets a discrete set of mRNAs.

Gene	Gene Name	FC Δ/WT Average of probes	p value	Fold change by qRT-PCR Δ/WT	Fold change by qRT-PCR Comp/WT
MT3762	*ncRv13661*	206.4	0.006		
Rv0086	*hycQ*	2.5	0.034		
Rv0270	*fadD2*	3.6	0.006	1.87	0.4
Rv0631c	*recC*	3.4	0.034		
Rv0721	*rpsE*	2.2	0.017	1.4	2.4
Rv0845	-	2.2	0.026		
Rv0860	*fadB*	3.4	0.016		
Rv0867c	*rpfA*	12.8	0.01	1.25	0.8
Rv0940c	-	2	0.034		
Rv0941c	-	2.4	0.018		
Rv0942	-	2.2	0.025		
Rv1252c	*lprE*	17	0.006	1.2	0.4
Rv1284	-	2.1	0.019		
Rv1446c	*opcA*	2.2	0.035		
Rv1572c	-	2.5	0.037		
Rv1870c	-	2.3	0.035		
Rv1935c	*echA13*	19.2	0.021		
Rv1937	-	2.9	0.036		
Rv2140c	*TB18.6*	3.4	0.008	2.8	4.8
Rv2342	-	29.6	0.001	1.7	0.4
Rv2598	-	79.2	0.012		
Rv2692	*ceoC*	6.6	0.006	1.3	1.2
Rv2725c	*hflX*	3.6	0.036	1.4	0.4
Rv2884	-	3.1	>0.001	2.72	0.1
Rv3110	*moaB1*	2.2	0.033		
Rv3146	*nuoB*	3.2	0.018		
Rv3389c	*htdY*	2.2	0.043		
Rv3662c	-	2.2	0.03		

Table 5.5 Genes down regulated > 2-fold upon deletion of ncRv13661 in stationary phase

Gene	Gene Name	FC Δ/WT Average of probes	p value
Rv0289	*espG3*	2.1	0.012
Rv0290	*eccD3*	2.7	0.048
Rv0791c	-	2.2	0.018
Rv1255c	-	2.2	0.03
Rv1256c	*cyp130*	3.2	0.024
Rv2053c	*fxsA*	2.1	0.011
Rv2601A	*vapB41*	2.3	0.022
Rv2602	*vapC41*	2.3	0.013
Rv2710	*sigB*	2.1	0.029
Rv3051c	*nrdE*	2	0.016
TBFG_11168	*Rv1146*	3.3	0.007

Table 5.6 Genes up regulated > 2-fold upon deletion of ncRv13661 in stationary phase

5.8 Proteomic analysis of deletion strain during growth on 7H9

Proteomic analysis of whole cell extracts was analysed from exponential phase cultures of the deletion strain, complement and H37Rv in order to ascertain if the changes in the transcriptional profile resulted in altered translation. Only 4 proteins were found to be differentially expressed between H37Rv and ΔncRv13661. Up regulation of *prpD* in the deletion strain, along with 3 proteins from the transcriptional unit Rv2930-papA5 were found to be down regulated in the deletion strain. None of these changes could be complemented meaning that either a mutation existed in the deletion strain, or the replacement of ncRv13661 on a plasmid was insufficient to allow full complementation. This is demonstrated by the complementation that was achieved on the transcriptional level for *prpD*.

Protein	ΔncRv13661/ H37Rv Fold Change (log2)	Comp/ H37Rv Fold Change (log2)	ΔncRv13661/ H37Rv P value	Comp/H37Rv P value
Rv1130- prpD	3.54	3.67	0.005	0.004
Rv2939- papA5	-1.06	-1.03	0.001	0.001
Rv2935- ppsE	-1.90	-1.68	<0.001	<0.001
Rv2933- ppsC	-3.06	-2.68	<0.001	<0.001

Table 5.7 Proteins differentially expressed in ΔncRv13661

Whole cell extracts were prepared and analysed by mass spectrometry and fold changes of deletion strain against either H37Rv or complement was generated by analysis with MSstats.

5.9 Proteomic analysis of over expression during growth on 7H9

Due to the lack of translational effects in the deletion strain it was of interest to ascertain the translational effects of over expression. Over expression of ncRv13661 in exponential phase leads to a massive down regulation of genes involved in exponential growth [3]. It was hypothesised that the transcriptional changes would be reflected in the proteome resulting in a large number of proteins being less abundant in the over expression strain.

Whole cell extracts were analysed by shotgun proteomics and significance was set at a fold change of 0.75 (log2 scale) with a p value of <0.01.

Twenty proteins were differentially expressed between vector and over expression. As expected, more proteins were down regulated than up regulated with only four proteins being up regulated; Rv2576c, Rv3842c (glpQ1), Rv3241c and Rv1865c. Of these, Rv3241c was up regulated 1.26 fold and has been identified as a hibernation factor in *M. smegmatis* named RafS (for ribosome associated factor during stasis) [228]. Of the down regulated proteins, half belong to the classification information pathways. There was a large representative of genes involved in DNA repair including Rv2592c (ruvB), Rv1638 (uvrA) and Rv2737c (recA), with recA being one of the most down regulated genes.

Protein	Over expression/vector Fold Change (log2)	Over expression/vector p value
Rv2576c	1.51	0.003
Rv3842c-glpQ1	1.33	0.002
Rv3241c	1.26	<0.001
Rv1865c	1.09	0.005

Table 5.8 Proteins up regulated in the ncRv13661 over expression

Whole cell extracts were prepared and analysed by mass spectrometry and fold changes of over expression against vector control were generated by analysis with MSstats.

Protein	Over expression/vector Fold Change (log2)	Over expression/vector p value
Rv1638-uvrA	-0.75	<0.001
Rv0412c	-0.79	0.005
Rv2790c-ltp1	-0.82	0.001
Rv3161c	-0.84	0.004
Rv0182c-sigG	-0.84	0.001
Rv2592c-ruvB	-0.86	0.001
Rv3888c	-0.91	<0.001
Rv1316-ogt	-0.92	<0.001
Rv1279	-0.95	<0.001
Rv1833c	-0.98	0.004
Rv0404-fadD30	-1.0	<0.001
Rv1406-fmt	-1.06	<0.001
Rv1527c-pks5	-1.07	<0.001
Rv2737c-recA	-1.23	<0.001
Rv0263c	-1.4	0.004

Table 5.9 Proteins down regulated in the ncRv13661 over expression

Whole cell extracts were prepared and analysed by mass spectrometry and fold changes of over expression against vector control were generated by analysis with MSstats.

5.10 Mechanism of regulation by ncRv13661

Transcriptional profiling of ncRv13661 deletion and over expression strains suggest that the sRNA has a pleiotropic effect on up- and down regulation of multiple mRNA transcripts and that the particular set of transcripts varies during different phases of growth and during growth on different carbon sources. Together with the stoichiometric argument that ncRv13661 is present at a vastly higher copy number than the regulated transcripts, data from transcription profiling are consistent with a model in which ncRv13661 acts in conjunction with some central cellular machinery rather than as a conventional mRNA base pairing sRNA. To test this hypothesis, density gradient sedimentation was used to screen for evidence of interactions between ncRv13661 and protein complexes. Hnilicova et al have recently reported that Ms1, the *M. smegmatis* homologue of ncRv13661, co migrates with RNA polymerase during density gradient fractionation, suggesting a parallel with 6S RNA [215].

Whole cell extracts from stationary phase cultures of *M. tb* were fractionated by centrifugation in 5-35% sucrose gradients at 30,000 rpm for 16.5 hours and ncRv13661 and RNAP were localised in resulting fractions by Northern blot and Western blot staining (Figure 5.7). Both molecules migrated as distinct peaks in the upper half of the gradient but, in contrast to the report of Hnilicova et al, the two peaks were not coincident; with ncRv13661 reaching a maximum in fraction 10, just above RNAP in fractions 11 and 12.

Two peaks for RpoB were observed on the western blot and this could reflect the different sedimentation rates of both free RpoB and that in complex with the rest of RNAP. It is also possible that there is more than one form of RNAP present, with core and holoenzyme having different sedimentation patterns.

Alternatively, if ncRv13661 does not interact with RNAP it is possible that ncRv13661 interacts with some other multimolecular machinery within the cell; other abundant sRNAs interact with ribosomes (*ssrA*), signal recognition particle (*ffs*) and RNase P (*rnpB*), for example. In light of the transcriptional responses described above, it would be attractive to envisage a role in multienzyme complexes. To test this hypothesis, ncRv13661 fractions from the density gradient were screened for other major protein components. A major band was visualised by Coomassie staining (Figure 5.8) and characterised by mass spectrometry; it was identified as the alpha-crystallin chaperone HspX (Rv2031c). To test the possibility that ncRv13661 forms a complex with HspX, density gradient fractionation was repeated using an extract from the ΔncRv13661 strain. The migration pattern of HspX was identical in the absence of the sRNA, suggesting that the native alpha-crystallin multimer [229] is fortuitously co-sedimenting with ncRv13661 rather than forming a protein: RNA complex.

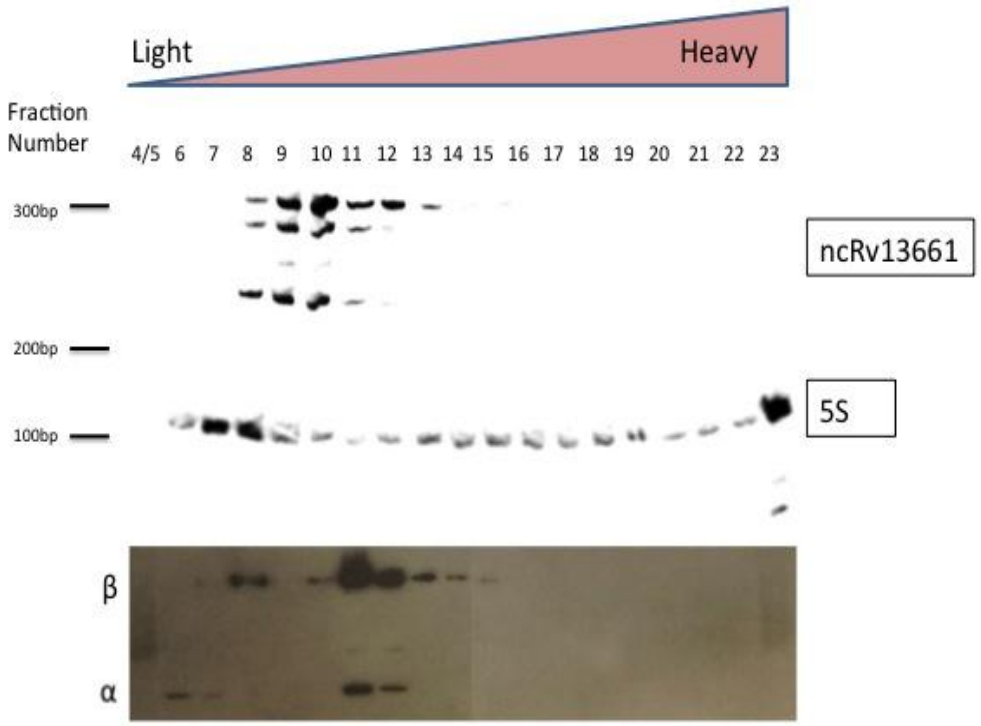

Figure 5.7 Sedimentation of ncRv13661 and RNAP using sucrose gradient ultracentrifugation shows ncRv13661 does not specifically migrate with intact RNAP

Following sucrose gradient ultracentrifugation of whole cell extracts, the gradient was fractionated into 600µl fractions. Each fraction was split and RNA and protein were isolated. Northern blots with ^{33}P were used to detect ncRv13661 and 5S (middle and top panel), while Western blots were used to detect α and β subunits of RNAP (bottom panel). ncRv13661 Appears as multiple bands on the northern blot indicating extensive processing and/or degradation

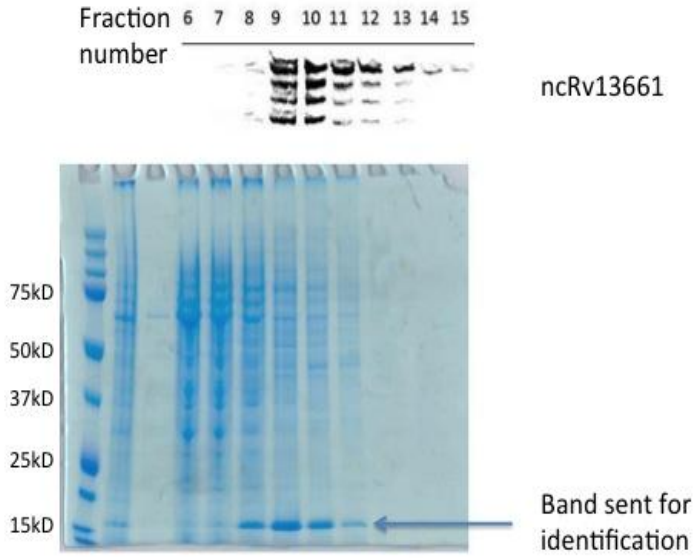

Figure 5.8 Sedimentation of ncRv13661 and *M. tb* proteins using sucrose gradient ultracentrifugation

Following sucrose gradient ultracentrifugation of whole cell extracts, the gradient was fractionated into 600µl fractions. Each fraction was split and RNA and protein were isolated. Northern blots with ^{33}P were used to detect ncRv13661. Isolated protein was run on an SDS-PAGE with a cell free extract control alongside dual precision marker plus before staining using Coomassie.

5.11 Role of ncRv13661 in cell viability

It was previously shown that over expression of ncRv13661 resulted in a decreased growth rate for H37Rv in regular 7H9 culture medium [3]. In contrast, deletion of ncRv13661 had no detectable effect on exponential growth. To test whether loss of ncRv13661 had an effect on stationary phase survival of *M. tb*, cultures of wild type and ΔncRv13661 were maintained over a six-week period, diluted into fresh medium and allowed to re-grow. No difference was observed in the pattern of re-growth (Figure 5.9).

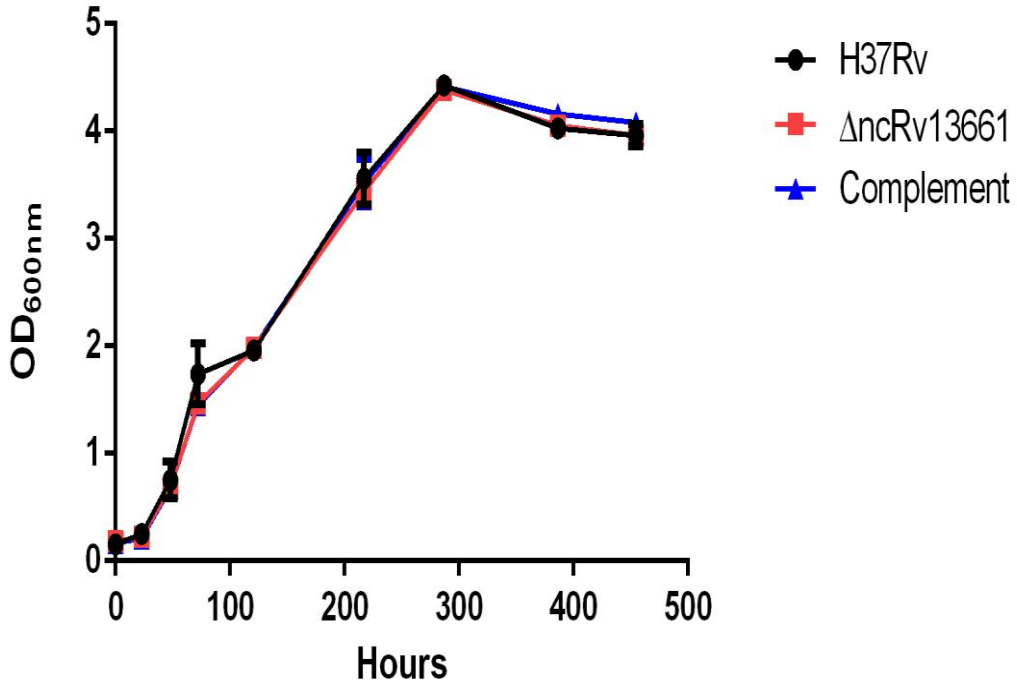

Figure 5.9 Recovery of ΔncRv13661 after six weeks in stationary phase.

In vitro growth curves of wildtype *M. tb* H37Rv, the ΔncRv13661 deletion strain and the complement using standard 7H9 media after six weeks in stationary phase. The data represents the averages and standard deviations of three biological replicates. There was no statistical difference between the growth of the strains as assessed by linear regression analysis.

5.12 Effects of ncRv13661 deletion on *in vivo* survival

It was of interest to determine whether deletion of ncRv13661 had an effect on the ability of *M. tb* to grow in macrophages or in a mouse model. A series of experiments to test this were set up with the original DCO 3.21 prior to identification of the *mas* mutation. The results of these experiments are shown in Appendix VI; no differences were observed in CFUs in either model. While these experiments are clearly flawed by the use of a PDIM mutant, we reasoned that any effect of this mutation was likely to reduce rather than enhance virulence, and that the negative result was strong evidence that deletion of ncRv13661 in a clean background was unlikely to impair virulence. For this reason we decided not to repeat the experiments with DCO 1.4. It is however possible that modulation of the lipid profiles could result in an increase in virulence and/or a change in the pathology of the ncRv13661 deletion strain as has been observed for other pathogen deletion strains [230, 231]. Therefore, if the experiment were to be repeated in the future it would be important to monitor the pathology of the lungs and spleen.

5.13 Discussion

Initial functional characterisation of the sRNA ncRv13661 by over expression, showed a transcriptional response very similar to that of a persister model due to the observation that a large number of genes involved in exponential growth were down regulated [3].

The current study identified transcriptional responses implicating ncRv13661 in long-term mycobacterial survival in agreement with previous

work on the over expression strain. Transcriptomic analysis of the over expression strain would indicate that ncRv13661 contributes to the change in carbon flux associated with transition from replicating to non-replicating culture as seen by Shi and colleagues [232]. It is proposed that ncRv13661 blocks fatty acid degradation for energy and growth promotion and diverts carbon units to form complex storage lipids. When this is activated by over expression in exponential phase, propionate is driven away from the methylcitrate cycle by *prpCD* down regulation [3] which results in the accumulation of fatty acyl-CoAs. This accumulation of acyl-CoAs causes the activation of *raaS*. RaaS is a transcriptional regulator that has been shown to be important in the long-term survival of *M. tb* [227] and has been identified along with its regulon more than once in this study. RaaS has been shown to improve mycobacterial survival after treatment with ethambutol [227], a drug that targets cell wall biosynthesis.

The ATP-dependent efflux pump Rv1218c under the control of the repressor RaaS was found to be up regulated in the over expression strain during growth on propionate and co-ordinately down regulated in the deletion strain indicating that ncRv13661 is involved in persistence through regulation of the cell wall constituents. The repressor RaaS has been shown to use the acyl-CoA oleoyl-CoA as a ligand [227] although it is possible that longer acyl-coAs or complex lipids which contain fatty acids could fit into the binding pocket affecting the DNA binding activity of RaaS. Mycobacteria are able to produce and export many lipids containing fatty acids [233, 234], and interestingly DrrC which may be regulated by RaaS has been implicated in the export of PDIM's in *M. tb*.

The mycolic acid containing PDIM's are an important constituent of the *M. tb* cell envelope. The complex structure of the cell envelope protects against degradation by host enzymes and the action of antibiotics, and toxic molecules produced by the host [235]. The mycobacterial cell envelope is lipid rich and includes the major lipid constituents the mycolic acids [236]. In this study we demonstrated that ncRv13661 has been shown to affect the expression of PDIM associated genes, ppsA-D. The complementation of these changes was not always observed and genome sequencing revealed that the first deletion strain obtained had mutations in *mas*, undoubtedly affecting the PDIM profile in the strain. The second mutant that was isolated, lacked mas mutations but possessed a mutation in a glycosyl transferase which is involved in mycothiol biosynthesis. The apparent role for ncRv13661 in the regulation of cell wall lipids added to the SNPs identified make it difficult to isolate specific effects of deletion. The lack of ncRv13661 could have resulted in compensatory mutations occurring in the genome before the complementing plasmid could be electroporated in. It is also possible that a ncRv13661 deletion strain could only be obtained in a PDIM altered background. Loss of PDIM in laboratory strains of *M. tb* is quite common and arise in the absence of selection pressure, and so complementation is important for assessing deletion specific effects [237]. It is of note however that other sRNA deletion strains were made in parallel during this study using the same electrocompetent cells and/or parental strain and none of those were found to contain SNP's involved in PDIM synthesis, indicating that this could be a specific trait of the *M. tb* lacking ncRv13661.

Proteomic analysis of the over expression strain showed a down regulation of proteins involved in DNA repair, with one of the most down regulated proteins being Rv2737c (recA). In both *M. tb* and *E. coli recA* is involved in homologous recombination and is controlled by the repressor lexA [238]. LexA also regulates *ruvAB* (also identified as down regulated) [239-241]. Interestingly lexA was shown to bind upstream of ncRv13661 in a CHIP seq analysis of lexA binding sites [239]. In a target search for mRNA regulated by ncRv13661 using TargetRNA2, *recA* was identified as the top candidate for sRNA binding with predicted pairing at the 5' end of *recA* at nucleotides 3-18 [164]. This would be indicative of translation repression of RecA by prevention of ribosome binding. Down regulation of DNA damage repair mechanisms upon ncRv13661 deletion could suggest that fewer lesions are being generated due to a slower rate of RNAP.

Sucrose gradient ultracentrifugation revealed that ncRv13661 did not co migrate with intact RNAP contradicting the findings of Hnilicova and co-workers. The deletion of ncRv13661 also did not result in an impaired ability to recover from stationary phase further indicating that it does not function in a 6S manner. The possibility exists however that ncRv13661 could interact with a subpopulation of RNAP. It is difficult to exclude the possibility that ncRv13661 could interact with some particular form of RNAP. The stoichiometry for RNAP core to ribosomes is approximately 1:1. RpoZ and sigma factors have half of that copy number and therefore if ncRv13661 was interacting with a subpopulation of RNAP, it would only be with ~10% of the copies making detection difficult. In contrast when 6S is induced in late stationary phase the majority of $E\sigma^{70}$ is found in a complex

with 6S RNA [132, 137, 138]. When nutrient availability increases the RNAP can then be recycled upon exit from stationary phase by the generation of pRNAs ejecting 6S from the $E\sigma^{70}$ complex [136].

The ability to recommence growth after periods of non-replicating persistence is not only mediated by interactions with RNAP but also by interactions with the ribosome. Down regulation of translation without the need for altering ribosomal numbers have great energy benefits for bacteria. A hibernation-promoting factor rafS (Rv3241c) was identified as being up regulated in the over expression strain and its homologue in *M. smegmatis* (MSMEG_1878) has been shown to associate to the ribosome during hypoxic and carbon starved stasis [228]. It is possible that ncRv13661 could associate with *Rv3241c* to increase translation as a mechanism for ribosome stabilisation. Importantly the expression conditions of *Rv3241c* are also those known to induce the expression of ncRv13661.

In addition to hibernation factors, the survival of *M. tb* during times of nutrient deprivation is aided by mechanisms such as the stringent response [134]. RelA and CarD act in the stringent response to down regulate ribosomal RNA synthesis and RNA ribosomal protein genes to conserve energy at times when nutrients are limiting [135]. The two component system MprAB also allows the regulation of numerous stress responsive genes [242]. When activated, MprAB regulates expression of >200 genes, directly regulating sigma factors *sigB* and *sigE*, and the α-crystallin-like gene *acr2.*

In addition to the potential mRNA base pairing interaction with *recA*, a further role for ncRv13661 must exist. The high level of expression of ncRv13661 during infection and stress conditions suggest that this sRNA is performing a central function, expressed to a high level in preparation for its regulatory requirement. It is possible that ncRv13661 is acting in a stress response mechanism such as the stringent response by some as yet unidentified mechanism.

6 Is ncRv12659 responsible for the starvation-induced signal attributed to Rv2660c?

6.1 Introduction

ncRv12659 (originally termed MTS2048) was identified through the recent study into the transcriptome of *M. tb* [3, 171]. It is encoded opposite the hypothetical protein Rv2660c and flanked by a hypothetical protein and a probable integrase Figure 6.1.

Rv2660c has been reported to be the most highly up regulated gene during starvation using a PCR-based microarray [187]. In addition to this it has also been reported to be up regulated in response to hypoxia-induced non-replicating persistence, and the enduring hypoxic response [243, 244]. It is envisaged that inclusion of antigens expressed by persisting populations in vaccines will result in protection against reactivation of the disease.

H56 is a TB subunit vaccine currently under clinical trials [245]. It was designed to include antigens that are associated with long-term infection and it has been shown that the H56 vaccine gives the best protection of any vaccine to date. H56 contains Rv2660c in addition to Ag85B and ESAT-6, which are two antigens secreted in the acute phase of infection. The increased efficacy of this vaccine over others is considered to be due to the addition of the "latency-associated protein" Rv2660c.

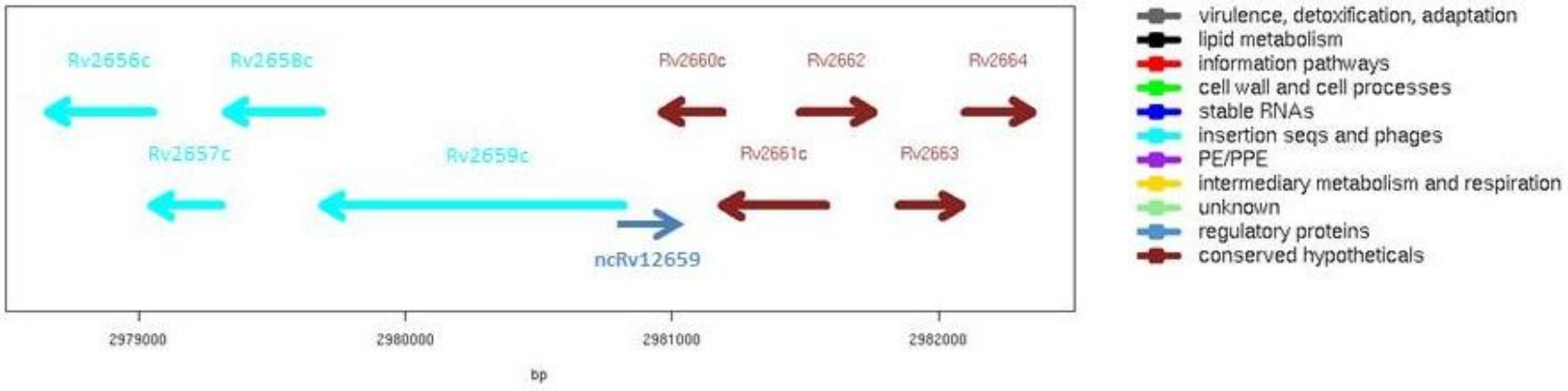

Figure 6.1 Genomic position of sRNA ncRv12659 in the *M. tb* genome

6.2 Hypotheses and specific aims

Due to the overlapping of ncRv12659 with the Rv2660c locus we aimed to characterise the sRNA and assess its contribution to the antigen in the H56 vaccine. As a potential cis-encoded RNA it should function to regulate the target for which it is antisense. Early work has suggested that the starvation-induced signal attributed to Rv2660c arises from the plus strand and not that of Rv2660c encoded on the minus strand (Figure 6.2).

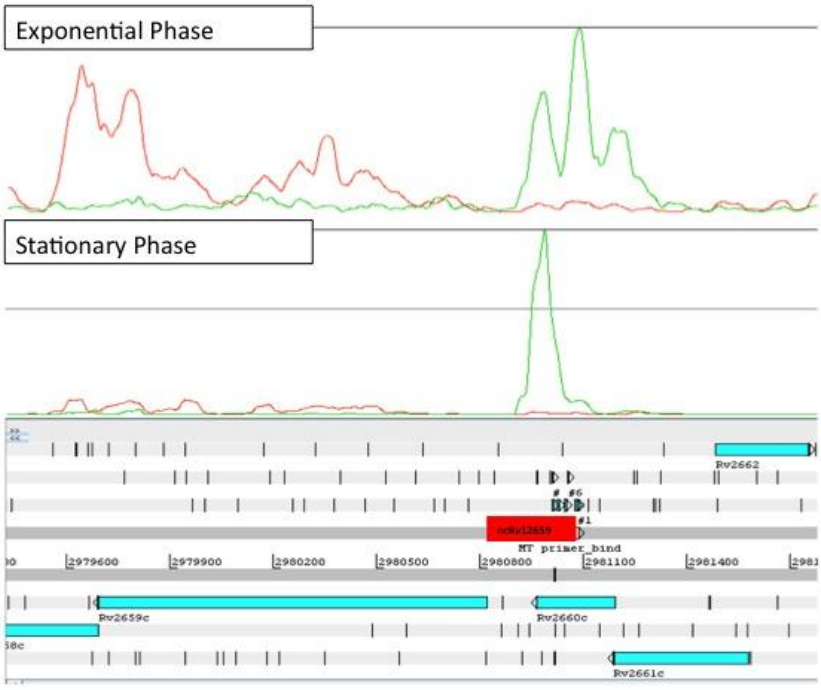

Figure 6.2 RNA seq of the Rv2660c locus as viewed in the genome browser Artemis.

The forward strand is represented in green and the antisense strand in red. The top panel shows expression of ncRv12659 during exponential phase and the bottom panel in stationary phase. Both growth phases lack any detectable expression of Rv2660c on the opposite strand.

Results

6.3 Comparison of RNA sequencing profiles

Rv2660c was originally highlighted as the most up regulated transcript in the microarray analysis of *M. tb* starved for 24 and 96 hours in PBS [187]. It was annotated as a hypothetical protein directly adjacent to a prophage element termed PhiRv2. This prophage is one of two possessed by H37Rv; it is inserted into the *valU* tRNA gene and is present in many strains of *M. tb*. Some of the prophage genes of PhiRv2 including the phage integrase Rv2659c, were also observed to be up regulated in the starvation microarray study [187].

Expression from both strands was investigated by RNA seq profiling comparing exponential growth and 24 hours starvation in PBS**.** Strand-specific sequencing showed that transcription did indeed occur on the forward strand and not the reverse strand where Rv2660c is annotated Figure 6.2A. RNA seq library construction and bioinformatic analysis was carried out by Teresa Cortes.

6.4 Mapping of transcript termini by 5’ and 3’ RACE

The sRNA transcript was mapped by 5’ and 3’ RACE as described in section 2.7 in order to obtain the boundaries of the transcript and establish origin of the sequence. 5’ RACE identified a transcriptional start site (TSS) at position 2980911 which lies between the TSS of the integrase Rv2659c and the boundary of the phage marked by the *attR* duplication. This was confirmed by RNA sequencing based TSS mapping [246]. It was also observed that the peak height of ncRv12659 was increased in response to

starvation as seen in the TSS mapping performed by Teresa Cortes Figure 6.2B.

3'RACE identified seven 3' ends from eight sequenced clones. The primary co-ordinate was at position 2981083 which was identified twice. Other termini were mapped to positions 2981010, 2981011, 2981026, 2981047, 2981055 and 2981077. However, this did not lead to the identification of any canonical intrinsic terminators such as a stem loop followed by a poly-U stretch. These co-ordinates establish the transcript as being 173 nucleotides in length.

In order to confirm the transcript size, northern blotting was performed on RNA extracted from both exponential and stationary phase cultures of *M. tb* as described in section 2.6. Northern blot analysis revealed that the largest prominent transcript was approximately 170 nucleotides in length confirming the RACE results Figure 6.2C. Multiple smaller transcripts were observed on the blot including a dominant one of 120 nucleotides in stationary phase. Due to the identification of a single TSS these smaller transcripts and also possibly the primary transcript are formed as a result of processing at the post-transcriptional level.

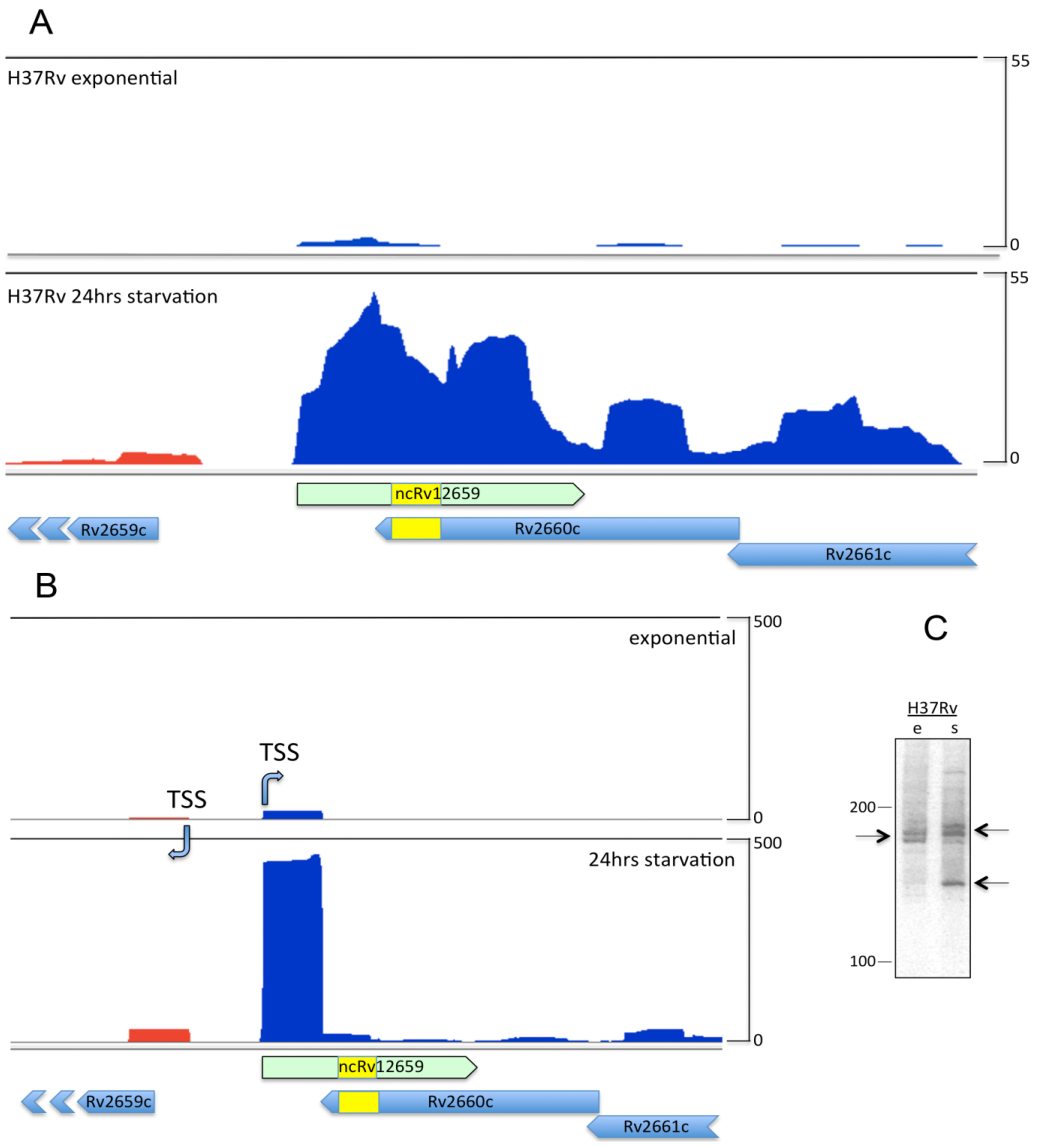

Figure 6.2 Mapping of ncRv12659 in *M. tb* H37Rv (taken from [150])

A. Total RNA seq visualised in the genome browser Artemis. Forward strand reads are blue and reverse strand reads are red. Yellow boxed section on the map of the locus represents the valU tRNA insertion point. B. Transcription start site (TSS) mapping shows the ncRv12659 transcript to begin 62 nucleotides downstream of the TSS of Rv2659c. C. Northern blot analysis of ncRv12659. Expression of ncRv12659 in RNA extracted from (e) exponential and (s) stationary phase cultures of *M. tb* H37Rv using 20µg of total RNA.

Using these coordinates, the transcript ncRv12659 was revealed as consisting of 60 nucleotides of PhiRv2 sequence, followed by 28 nucleotides of duplication from the 3' end of the *valU* in addition to 85 nucleotides of host *M. tb* sequence, Figure 6.3. Further analysis of the region reveals that the 61 bp sequence succeeding the sRNA is duplicated at the *attL* end of PhiRv2, annotated as Rv2645.

Annotations in Tuberculist [247] are based on predictions and therefore a search for alternative annotations in this region was undertaken. It was found that in *Mycobacterium canettii* there is an open reading frame annotated to the forward strand which has homology to part of a protein sequence found in *Salmonella typhimurium* (VBIMycCan 278382_3386) which is marked in blue in Figure 6.3.

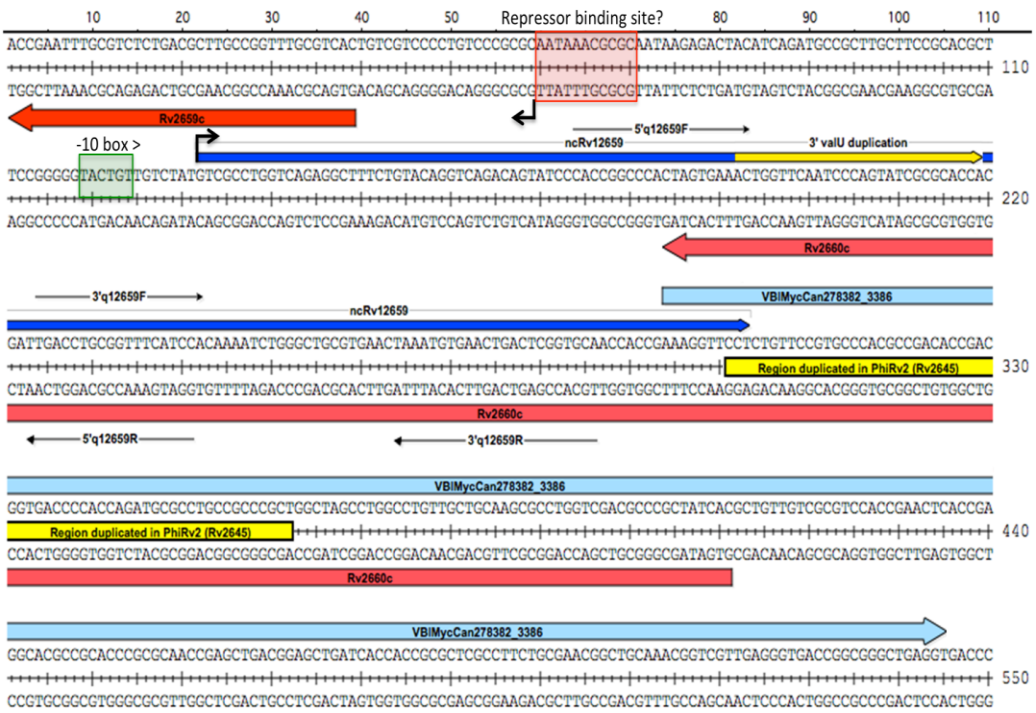

Figure 6.3 Annotation of the ncRv12659 locus (taken from [155])

Sequence detail surrounding ncRv12659 which detail relevant annotations referred to in the text. Repeat regions are shown in yellow. Locations of qRT-PCR primers used in the study are indicated.

6.5 Expression of ncRv12659 in clinical isolates

Analysis of the genomic region of ncRv12659 revealed that the sRNA consisted in part of phage sequence. This suggested that ncRv12659 would only be expressed in strains where the PhiRv2 region was present. This also led to the hypothesis that in PhiRv2 positive strains the creation of an antisense RNA may have led to the silencing of the complementary strand Rv2660c and this repression could be relieved in PhiRv2 negative strains.

To test these theories RNA profiles of five clinical isolates, along with the PhiRv2 negative BCG vaccine strain were compared. N0072 and N0153 were selected as being PhiRv2 negative while N0031, N0052 and N0145 were selected as PhiRv2 positive, (a summary of which can be found in Table6.1).

Strain	Lineage	PhiRv2	TSS	RNAseq	Northern	qRT-PCR
***M. tb* H37Rv**	4	+	Y	Y	Y	Y
***M. tb* N0031**	2	+	N	(Y)	N	N
***M. tb* N0052**	2	+	N	Y	Y	N
***M. tb* N0072**	1	-	N	(Y)	Y	Y
***M. tb* N0145**	2	+	(Y)	Y	N	N
***M. tb* N0153**	1	-	Y	Y	N	N
***M. bovis* BCG**	6	-	(Y)	(Y)	Y	N

Table 6.1 Strains used in this study (adapted from [155])

Y/N indicates yes/no for whether experimental methods were applied to that particular strain, with brackets indicating that the experiment was performed but the data is not shown.

RNA seq profiles of the PhiRv2 positive strains showed no detectable signals from the reverse strand Figure 6.4A. Interestingly, the N0052 strain showed a higher level of expression of ncRv12659. The RNA seq profile of the PhiRv2 negative strain N0153 showed that a low number of reads which could be mapped to the region downstream of the tRNA *valU* Figure 6.4B.

Northern blots were performed in order to confirm the RNA seq findings, probing for the 3' end of the transcript to ensure that detection was possible in both PhiRv2 positive and negative backgrounds, Figure 6.4C. A faint signal of approximately 300 nucleotides was seen however in the PhiRv2 negative background probably corresponding to the unprocessed tRNA transcript. It was observed that there was no signal attributable to Rv2660c in either a PhiRv2 positive or negative background

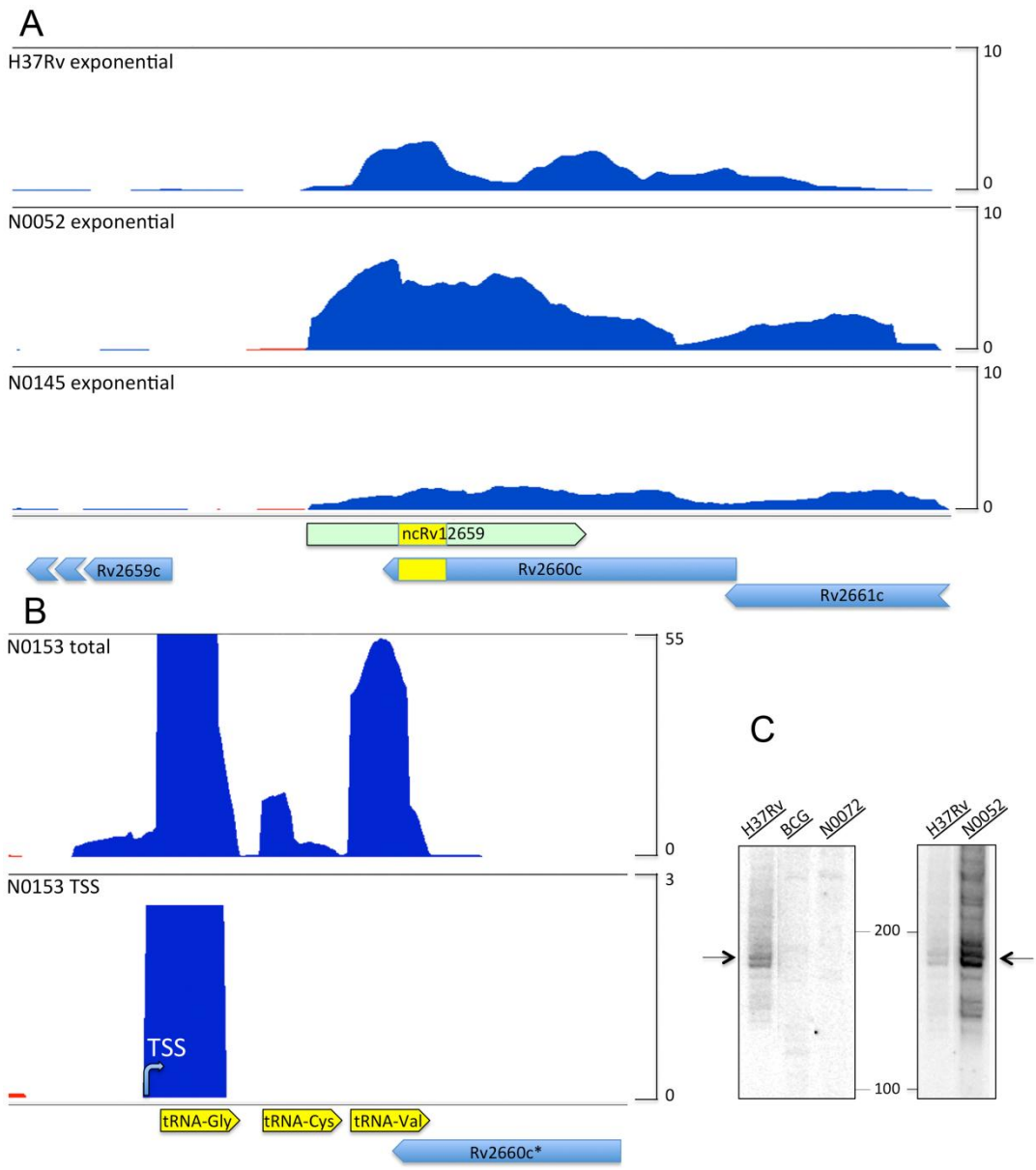

Figure 6.4 RNA profiling of the Rv2660c locus in M. tb clinical isolates (taken from [150])

A. RNA seq profiles of PhiRv2 positive strains indicating no detectable transcriptional signal of Rv2660c. Reads are normalised to the total number of reads

B. RNA seq profiles of PhiRv2 negative isolate shows no Rv2660c transcript even in the absence of a competing antisense ncRv12659 RNA. Only a transcript initiated from the tRNA promoter is evidenced.

C. Northern blot analysis. 20 µg of total RNA from each isolate was used to probe for ncRv12659 at the 3' end to allow detection in the PhiRv2 negative background.

6.6 Proteomic Analysis during starvation

Due to the original up regulation of Rv2660c observed during starvation, protein extracts were analysed to determine expression at the proteomic level. Both exponential and stationary phase cultures were prepared and protein extracts made as described in section 2.8.6. This protocol was optimised for selected reaction monitoring (SRM), which allows the detection of low abundance proteins within mixed populations by mass spectrometry [248]. SRM results in 70% of the proteome being detectable within unfractionated cell lysates from liquid culture, with the detection limit being below 10 copies per cell [249, 250].

With this level of sensitivity we failed to detect any of the three tryptic peptides belonging to Rv2660c that are compatible with the analysis. It is of note that synthetic peptides ran as controls could be detected further indicating the absence of Rv2660c, Figure 6.5.

Taken together the absence of both a detectable transcript and corresponding protein for the hypothetical Rv2660c from either exponential or starved cultures, can only lead to the conclusion that the previously observed starvation signal is attributable to the sRNA ncRv12659 and has little or no contribution from Rv2660c.

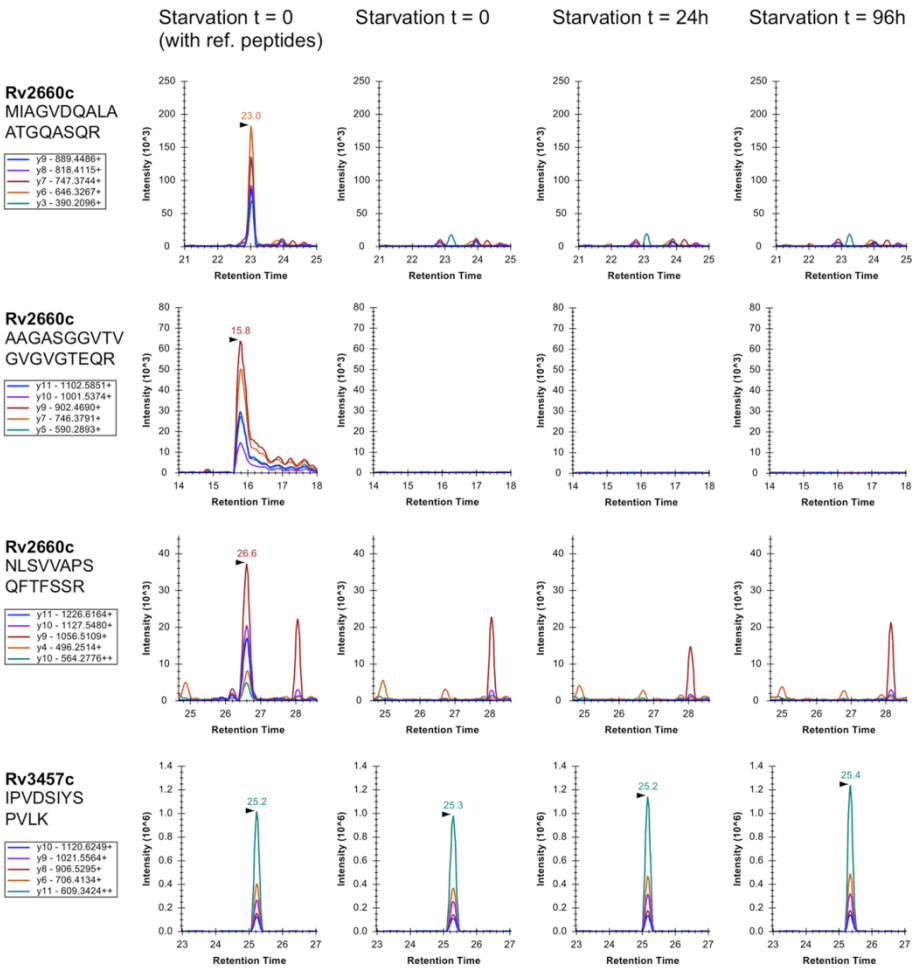

Figure 6.5 SRM analysis of tryptic peptides from Rv2660c. (Taken from [155])

SRM traces over 96 hours of a PBS starvation experiment show three tryptic peptides from Rv2660c and a peptide derived from Rv3457c which acts as a positive control.

The first column shows the SRM signals of the synthetic reference peptides spiked into the first time point. The other three columns show the SRM signals in samples without reference peptides spiked in. No signal for the targeted peptides was detected.

6.7 Expression of ncRv12659 during mouse infection

Due to the success of the H56 vaccine it was important to assess the expression of ncRv12659 during infection using the mouse model employed in the H56 vaccine study [245].

Mice were infected with either the PhiRv2 positive H37Rv or the PhiRv2 negative N0072 for 31 days. Subsequently mice were sacrificed and RNA extracted from the lung tissues and then assessed by qRT-PCR in a comparison with *in vitro* cultures. Two primer sets were used in order to distinguish between the PhiRv2 positive ncRv12659 RNA, and the PhiRv2 negative tRNA. These were termed the 5' and 3' amplicons.

The 5' amplicon consisted of a forward primer within the PhiRv2 derived part of the sequence and hence would only be detected in the presence of the PhiRv2 region such as in H37Rv. The 3' amplicon contains primers downstream of the tRNA repeat and is therefore present in both PhiRv2 positive and negative strains Figure 6.6. The 5' amplicon baseline was set at the level of background detectable in the PhiRv2 negative background as this level was considered noise in the absence of target sequence. Expression of the 5' amplicon was found to increase 50 fold in response to starvation and 6 fold in response to infection when compared against exponential phase levels in *M. tb* H37Rv, Figure 6.6.

The 3' amplicon was observed at much lower levels than the 5' amplicon with a 2 fold reduction observed in comparison to the 5'amplicon for H37Rv in exponential phase. During starvation and infection the 3' amplicon dropped below baseline Figure 6.6. In the PhiRv2 negative N0072 samples the 3' amplicon was detected at very low levels in

exponential phase and reduced further under starvation conditions indicating that read through from the tRNA operon has a minimal contribution to the signals observed and importantly only the PhiRv2 promoter is induced by starvation. Due to the nature of the qRT-PCR design, the amplicons observed also show that there is no detectable Rv2660c transcript in the PhiRv2 negative N0072 strain during infection.

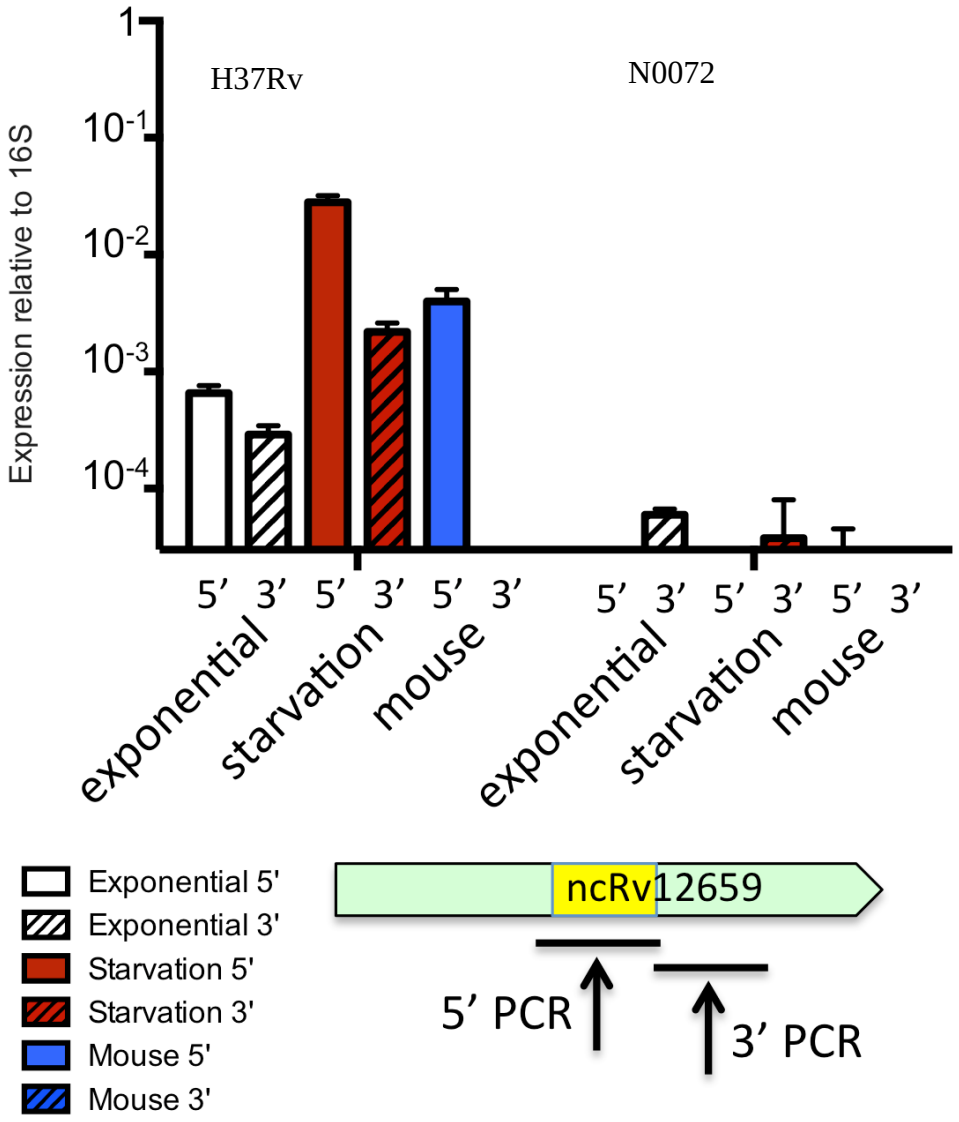

Figure 6.6 Expression of ncRv12659 during infection (taken from [150])

qRT-PCR was performed on RNA extracted from *in vitro* culture in exponential and starvation phase in addition to extraction from the lung tissue of infected mice. Both 5’ and 3’ amplicons were measured as depicted in the schematic. Data represents the mean and standard deviation of three biological replicates

6.8 Over expression of ncRv12659

M. tb H37Rv contains two prophage elements PhiRv1 and PhiRv2 both possessing a similar arrangement of integrase and repressor like proteins; with inward and outward facing promoters, Figure 6.7.

PhiRv2 is a prophage element and therefore lacks the full complement of genes to act as an active phage within *M. tb*. However, analysis with other temperate bacteriophages shows that the promoter of ncRv12659 is probably responsible for driving expression of the phage genes in its circular chromosome, Figure 6.7.

For 51 amino acids from the phage gene ORF of Rv2647 structural homology was identified for a potential binding site of a *korB* repressor from plasmid RP4 [251]. Repeat sequences of 14 nucleotides were identified upstream of several phage genes which represent potential repressor binding sites, and are represented by red boxes in Figure 6.7.

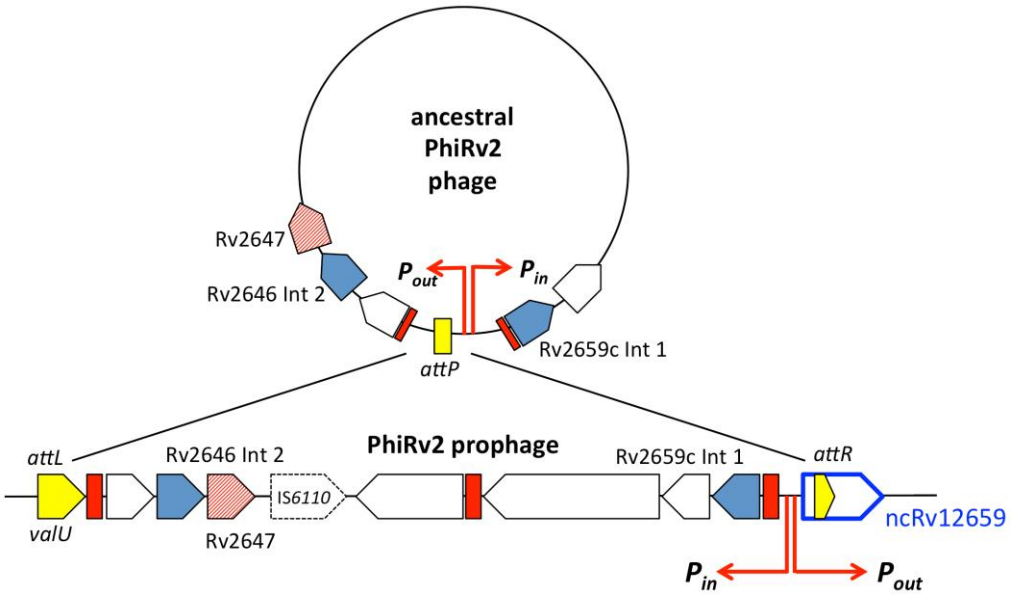

Figure 6.7 PhiRv2 represented as a circular virion (taken from [155]).

After phage integration into the *M. tb* genome at the valU tRNA gene the promoter upstream of Rv2645 drives outward expression of the sRNA. Potential repressor binding sites are shown in red.

As the sRNA is a mixture of both host and phage sequence in addition to the conservation of the sequence within the lysogen it was hypothesised that ncRv12659 could have a functional impact on *M. tb*, especially in light of the activation of the promoter under starvation conditions. To test this hypothesis an over expression strain was constructed using a replicating plasmid that contained the sRNA under its own promoter called pMSC12659. This plasmid contained portions of downstream and upstream sequence in order to include any regulatory elements including potential termination signals (base pairs 1-471 in Figure 6.4).

The plasmid was electroporated into both the PhiRv2 positive H37Rv and PhiRv2 negative N0072. Following successful transformation, cultures were grown to exponential phase and RNA extracted. Analysis of the samples by qRT-PCR showed that over expression of ncRv12659 was around 1000-fold in both strains, reaching around 10% of 16S rRNA levels Figure 6.8A. This resulted in a small but significant reduction in the growth rate of both strains Figure 6.8B.

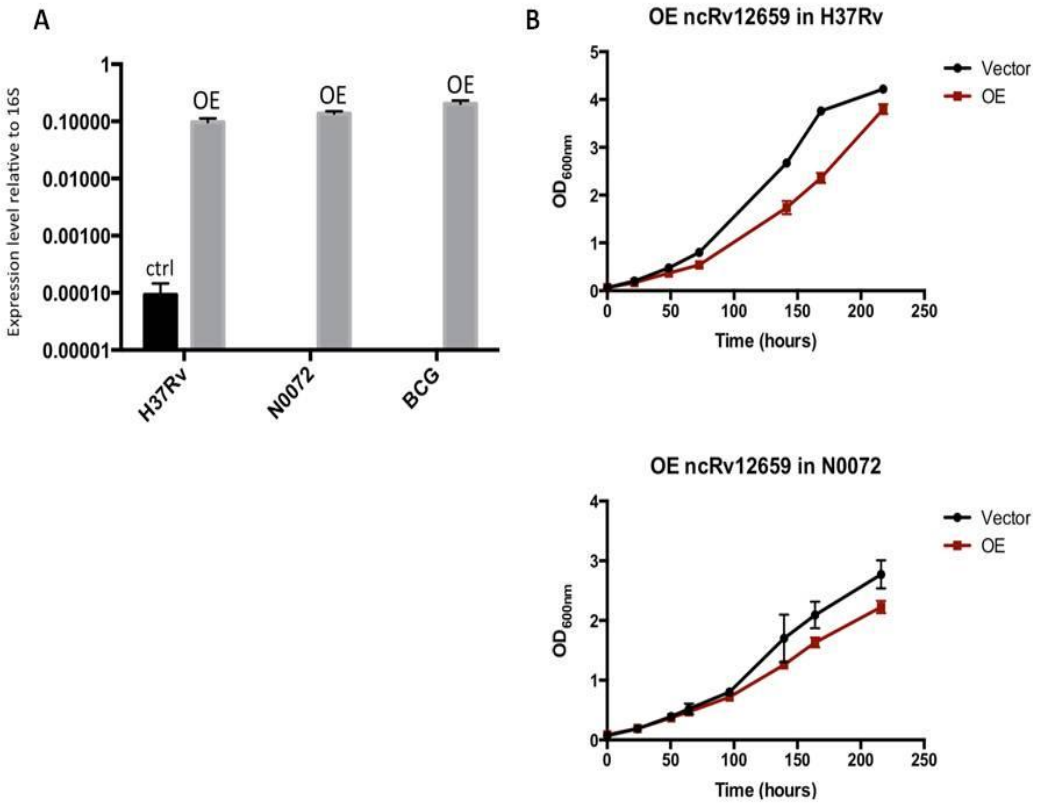

Figure 6.8 Analysis of ncRv12659 over expression (adapted from [155])

A. Expression levels of ncRv12659 in three strains upon over expression of ncRv12659. Expression was normalised to 16S rRNA and data represents the mean and standard deviation of three biological replicates.

B. Growth of the ncRv12659 over expressing strains where H37Rv is a PhiRv2 positive background and N0072 PhiRv2 negative. Each data point represents mean and standard deviation from three biological replicates.

In order to assess the function of ncRv12659, microarray analysis was performed on the H37Rv strain harbouring the over expression using Oligonucleotide arrays, as described in section 2.8.13 using AMADID 027543. A fold change cut off of 2 with a p-value of 0.05 was initially selected and this resulted in differential expression of more than 100 probes. In order to focus our search we increased the fold change to 4 with a p-value of 0.05. This resulted in 27 probes of which 6 corresponded to sequence contained in the over expression construct and so were discarded from the analysis. This left 21 probes which corresponded to 11 genes Table 6.2. Thirteen of the probes identified could be aligned with Rv0257. These repeat loci have been linked to hypothetical protein products in various genomic locations, although frame shifts present indicate that the coding capacity is not conserved between each locus.

Gene Name	Fold Change OE/WT	Average of probes	Regulation	Repeat Locus
MT1650.1	113.3	113	Up	4
MT1560.1	80.5	80	Up	3
MT0270.2	50.3	50	Up	1
Rv1137c	31.8	32	Up	2
Rv3613c	8.3	8	Up	6
MT2423.1	95.8	6	Up	5
MT2423.1	81.5	-	-	-
MT2423.1	62.6	-	-	-
Rv0257	90.4	6	Up	1
Rv0257	86.2	-	-	-
Rv0257	21.9	-	-	-
Rv3612c	5.8	6	Up	6
Rv3612c	5.7	-	-	-
Rv2659c	4.5	4	Up	N/A
Rv2659c	3.8	-	-	-
Rv2658c	4.6	4	Up	N/A
Rv2658c	3.8	-	-	-
Rv2658c	3.6	-	-	-
Rv3229c	4	7	Down	N/A
Rv3229c	8	-	-	-
Rv3229c	9	-	-	-

Table 6.2 Gene expression changes by microarray upon over expression of ncRv12659 (adapted from [155])

Five probes associated with the PhiRv2 region were identified in the array with an observed up regulation of *Rv2659c* and *Rv2658c* 4 and 5-fold respectively, Figure 6.9A. Although over expression resulted in a reduction in growth rate, only one gene, Rv3229c was observed to be down regulated more than 4 fold. Analysis by qRT-PCR confirmed down regulation with a fold change of 8.2.

As *desA3* was the only down regulated gene observed, the PhiRv2 negative strains N0072 and BCG were also used to construct over expression strains using pMSC12659 to determine if this was a phage specific phenomenon. Analysis of *desA3* in the different backgrounds revealed a reduced down regulation of between1.5 - 2 fold in the PhiRv2 negative background of N0072 and BCG, Figure 6.9B. This would suggest that the greater down regulation observed in the PhiRv2 positive H37Rv is due to the presence of PhiRv2 genes other than ncRv12659.

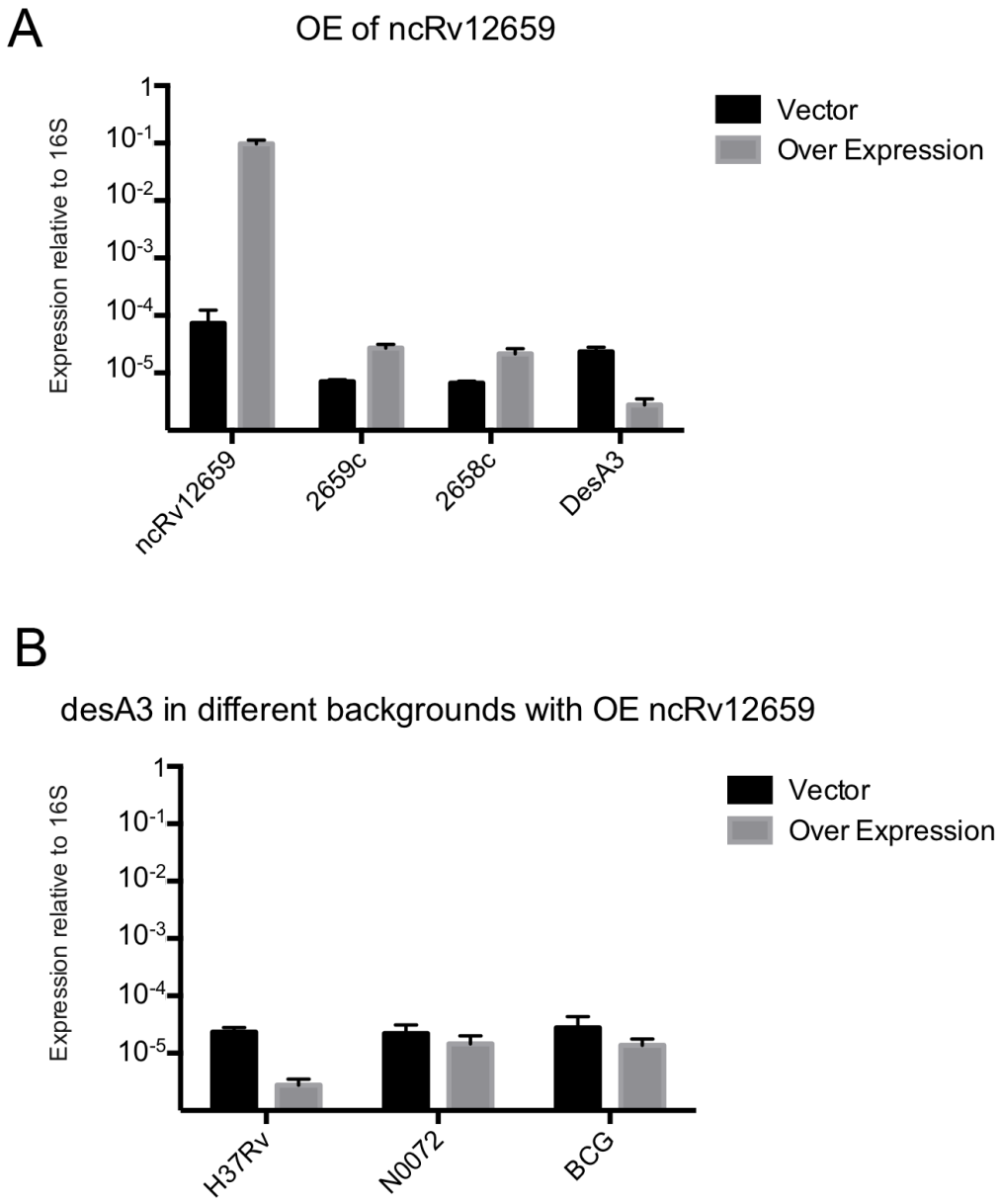

Figure 6.9 Expression analyses by qRT-PCR (taken from [155])

A. Expression level in the over expression strain compared to the empty vector control. Data represents mean and standard deviation of three biological replicates.

B. Expression levels of desA3 in three different PhiRv2 backgrounds over expressing ncRv12659. Data represents mean and standard deviation of three biological replicates. All expression was normalised to 16S rRNA.

6.9 Discussion

Both RNA seq and northern blot analysis have demonstrated that the transcriptional signals previously assigned to Rv2660c are in fact that of a sRNA encoded on the opposite strand of the DNA. This observation has also been observed by others [252]. By assessing a variety of culture conditions and strains we have failed to detect expression of Rv2660c on either the transcript or proteomic level.

Investigations by other groups either during long term starvation [253] or high coverage proteomic mapping [250, 254] also failed to detect Rv2660c on the proteomic level. Only one group have suggested detection of Rv2660c peptides from BCG but only two out of thousands of mass spectra were detected leaving the existence of Rv2660c questionable but highly unlikely.

The sRNA was created by the insertion of PhiRv2 into the genome of *M. tb* and it is therefore only found in strains which are PhiRv2 positive. Due to the loss of many of the genes required for a complete virion it would suggest that PhiRv2 infected an early ancestor. Subsequent selective pressures on *M. tb* have caused specific genes to be deleted which include tail proteins, and hence only the cryptic prophage remains.

The starvation induction of the sRNA ncRv12659 along with the phage integrase Rv2659c is likely due to the release of a repressor that allows the initiation of phage lysis of the cell. The determinants for lysis and lysogeny have been shown by others to be closely linked to nutrient availability to the host and could explain why the induction of ncRv12659 is so marked in response to starvation [255-257].

ncRv12659 was observed to accumulate during infection with the observation that this was only at the 5' end of the transcript suggesting processing, early termination, and or a lack of stability for the 3' end of the transcript. It is possible that the tRNA portion of the sequence stabilises the transcript by increasing its secondary structure.

ncRv12659 is not the only sRNA that has been observed to accumulate during infection [3]. However, the starvation induction of this transcript provides a useful marker for cells that are starved for either nutrients or oxygen and which may be fated to become persisters [187, 243, 244].

Both phage and host sequence are present in the sRNA transcript and it was therefore possible that over expression of ncRv12659 could result in an effect on the physiology of *M. tb*. Over expression did result in a reduction of growth although the transcriptional changes observed showed down regulation of only one gene, *desA3*.

Of the up regulated genes, those belonging to the phage were the most significantly changed along with probes for a novel repeat region. The induction of the phage integrase Rv2659c along with the strong over expression of ncRv12659 could be the result of a repressor being sequestered due to multiple binding sites being available. The novel repeat regions contained no upstream sequence similarity and their functions, whether coding or non-coding are yet to be identified.

The findings of this study suggest that the 5' end of ncRv12659 is a useful starvation marker for analysis of *M. tb* during infection, although this is limited to PhiRv2 positive strains. It seems unlikely that the up regulation

of this starvation induced locus would play a direct role in increasing the efficacy of the H56 vaccine.

This raises the question that if Rv2660c is a misannotation, how does its inclusion in the vaccine enhance protection? It is possible that the recombinant Rv2660c protein elicits a T cell response which results in a cross reaction between an unidentified *M. tb* antigen. This theory is supported by the finding that T cells isolated from infected individuals show responses to stimulation with Rv2660c [258]. Interestingly, a greater response was elicited from T cells isolated from latently infected individuals as opposed to those with active disease [258].

It also remains possible although unlikely; that there is a specific and as yet unidentified condition under which Rv2660c is induced. If this was the case, this expression condition could provide the key to understanding latent infection. It is important to understand how Rv2660c improves the efficacy of the H56 vaccine. Further studies could also help explain why another vaccine candidate containing antigen 85A failed to induce protection [259, 260].

7 Concluding Remarks

The majority of documented sRNAs regulate through base-pairing with a target mRNA resulting in a change in translation and/or stability of the mRNA. It was for this reason that transcriptomic and proteomic profiles were studied upon generation of sRNA deletion mutants. It was expected that microarrays would indicate increases or decreases in mRNA stability, whereas proteomic analysis would show if regulation resulted in translation repression or activation.

Unfortunately the sRNAs selected in this study did not result in clear defined mechanisms of action using these techniques. This study generated mutant strains of the 4 candidate sRNAs and assessed their transcriptomic and proteomic profiles in order to identify their regulatory targets. This approach did not result in the clear identification of targets as hoped. Transcriptomic and proteomic profiles for both ncRv11690 and ncRv10243 deletion strains in particular lacked any discernible targets. A summary of the findings of these studies can be found in Table 7.1

sRNA	Key Findings
ncRv10243	• sRNA is non- essential under the conditions tested. • Expression is induced in mouse infection and starvation • Deletion results in a heat shock signature after 24hrs starvation • ΔncRv10243 is impaired in recovery from the Wayne Model • ΔncRv10243 is not attenuated in a macrophage or mouse model of infection.
ncRv11690	• sRNA is non- essential under the conditions tested. • ΔncRv11690 transcriptional changes indicate a role in metal ion homeostasis • Over expression results changes in cell wall and cell wall process proteins involved in regulation of EsxA • ΔncRv11690 is not attenuated in a macrophage or mouse model of infection
ncRv13661	• sRNA is non- essential under the conditions tested. • Transcriptional responses implicate involvement in long term persistence by diverting carbon from fatty acid degradation to storage lipids • Efflux pump Rv1218c is concordantly regulated in deletion and over expression strain indicating involvement in regulation of cell wall constituents • Deletion affects expression of PDIM associated genes ppsA-D. • Over expression results in a down regulation of DNA repair proteins of which one (recA) is a predicted target. • ncRv13661 does not exclusively co migrate with RNAP and is therefore not acting as a 6S homologue. • ΔncRv13661 is not attenuated in a macrophage or mouse model of infection
ncRv12659	• Induced by starvation and mouse infection • Rv2660c is not starvation induced • Over expression in PhiRv2 positive background results in up regulation of phage genes • Would be a useful biomarker for starvation *in vivo*

Table 7.1 Summary of the key findings of the studies on each sRNA

There is only one sRNA in *M. tb* with an identified target to date. This sRNA is mcr7 which was identified in CHIP seq analysis using PhoP. By using target prediction and proteomic analysis of the secretome mcr7 was identified as regulating *tatC*, through translational repression. This search for a target of mcr7 was very much aided in its focus due to unpublished results from the group suggesting that secretion of Tat-dependent substrates was affected in the *phoP* mutant strain [156]. Importantly, RNA seq analysis of the PhoP mutant in the same study did not identify any differences in the expression levels of *tatC*. If a mcr7 mutant was analysed using the methods employed in this study target identification would not have been possible. The knowledge of a well-defined system allowing very specific investigation of the secretome aided in the target identification for mcr7. This highlights the difficulties in studying sRNAs which is further hindered in *M. tb* where functional identification for a large number of proteins is yet to be ascertained. The characterisation of the functional mcr7 in *M. tb* confirms that sRNA regulation in this important pathogen is comparable to other bacteria. It would therefore seem that the disappointing end points in this study were as a result of the limitations of the tools employed and not poor choice of candidates for investigation.

The findings of the mcr7 study and the proteomic analysis of the ncRv11690 over expression occurred at the end of this project and therefore secretome analysis was not possible. Due to the implication of ncRv11690 in the regulation of the virulence factor EsxA this was unfortunate as such analysis could have proved highly informative. Obviously secretome analysis would not yield the answers to all sRNA

functions but the lessons learned from these studies shows alternate investigation to transcriptional analysis needs to be focused upon.

An approach would be to test viability of mutants in a variety of stress conditions such as the Wayne model, where a phenotype was observed for the ncRv10243. Such survival experiments might be likely to reveal true induction conditions for the sRNA in question and allow target identification.

In addition analysis of mutant strains by sucrose gradient ultracentrifugation can be employed to look at interacting protein partners through proteomic analysis of co-sedimented proteins. Full fractional analysis of mutant compared to wildtype could show differential sedimentation of proteins.

If it were possible to identify essential sRNAs in *M. tb* these would be ideal candidates for study. However, lack of knowledge on essentiality of these RNAs prevents this selection process at present. Due to the size of sRNAs it is difficult to assess essentiality by transposon mapping, as is the case for protein coding genes. If a sRNA lacks a transposon it could simply be due to the lack of attaining one due to its size. It is known from studies in Salmonella however, that few sRNAs are known to be essential.

Many sRNAs have been identified from studies of *E. coli* and *Salmonella* which possess the RNA chaperone Hfq. The importance of Hfq has been demonstrated in these bacteria by the pleiotropic effects of deletion. These phenotypes include decreased motility, attenuation in host cell invasion and decreased replication within macrophages [261, 262]. The strong phenotypes observed led to coIP studies with Hfq employing microarray or

RNA sequencing technologies to identify sRNAs [60, 263]. In addition to this many sRNAs originally identified in *E. coli* were found to be present in *Salmonella* by sequence conservation, and confirmed later in the coIP experiments. This represents another limitation in the study of sRNAs in *M. tb* which lacks the chaperone Hfq preventing this approach from being adopted.

One method of identification employed has been the 'reverse target search' approach in which sRNAs were systematically deleted in *Salmonella* and resulting strains screened for the appropriate phenotype. All outer membrane proteins in *Salmonella* had known sRNA regulators except OmpX. Due to the lack of an identified sRNA regulator for OmpX 35 sRNA deletion strains were created and assessed for effects on OmpX synthesis. This screen identified the Hfq-dependent CyaR sRNA as an OmpX repressor [264]. This approach has major limitations for application to other targets and bacteria. The likelihood of RNA regulation of this outer membrane protein (OMP) was extremely high due to all other OMP having sRNA regulators identified. In addition this extremely laborious process of creating 35 deletion strains especially in a slow growing strain would not viable. The creation of deletion mutants in *M. tb* requires at least 6 months and is not a high throughput technique.

Despite the increase in our knowledge of sRNAs, their contribution to virulence has been much less well established though examples have been demonstrated [58, 265, 266]. Phenotypic investigations for roles of sRNAs and mRNAs deletions in infection have traditionally relied on CFU readouts

to infer virulence. The role of sRNAs in infection is in its infancy but there have been few published studies that have employed RNA seq to monitor the response of the host cell to infection [267]. Exceptions include a study into the eukaryotic miRNA response to bacteria using either macrophage or HeLA cells and enriching for the miRNA fraction. Dual RNA seq would provide a much greater depth of understanding of the complex interplay between bacteria and host [268]. Cytokine readouts from host infections could also provide a route to functional characterisation [269].

sRNAs involved in Hfq-mediated interactions are generally degraded along with their mRNA target [13]. In contrast, we observed accumulation rather than degradation of *M. tb* sRNAs in both stationary phase and starvation induction model. Even higher levels of sRNA accumulation were observed in the lungs of infected mice as seen with other sRNAs [3], with ncRv13661 achieving levels equal to 16S rRNA. This might suggest that the RNA degradation pathways in mycobacteria are distinct from other bacteria such as the model organism *E. coli*.

The lack of phenotypes observed for the sRNA deletion strains along with small changes in mRNA target abundance leads to the conclusion that the sRNAs selected in this study (with the exception of ncRv13661) are either involved in the fine tuning the stress response under particular induction conditions or the specific induction conditions are yet to be identified.

Assays where CFU measurements are used to measure survival of a particular stress are very limited. It is difficult to observe changes in specific stress experiments where more global protein-mediated responses can

mask that of the sRNA. This is especially evident in a whole animal infection model where the pathogenesis of *M. tb* does not rely on the expression of a single response but a coordinated array of responses and as such possess a plasticity that allows the maintenance of virulence. Few cases of deletion strains lead to attenuation and it is these candidate targets that drive drug development and discovery.

However, it is important to understand the riboregulation occurring within *M. tb* for pathways involved in pathogenesis. This greater level of understanding of the biology of *M. tb* could lead to better targeted therapies and rational drug design. The increasing drug resistance in cases of tuberculosis make this all the more important. In fact RNAs could already represent valid targets as antimicrobials. Riboswitches in particular are being pursued as targets due to a high degree of sensitivity and specificity for their ligands [270]. Recently, one compound targeting the guanine riboswitch of *S. aureus* was shown to successfully reduce bacterial load in animals after infection [271].

References

1. Gottesman, S., et al., *Small RNA regulators and the bacterial response to stress.* Cold Spring Harb Symp Quant Biol, 2006. **71**: p. 1-11.
2. DiChiara, J.M., et al., *Multiple small RNAs identified in Mycobacterium bovis BCG are also expressed in Mycobacterium tuberculosis and Mycobacterium smegmatis.* Nucleic Acids Res, 2010. **38**(12): p. 4067-78.
3. Arnvig, K.B., et al., *Sequence-based analysis uncovers an abundance of non-coding RNA in the total transcriptome of Mycobacterium tuberculosis.* PLoS Pathog, 2011. **7**(11): p. e1002342.
4. Daniel, T.M., *The history of tuberculosis.* Respir Med, 2006. **100**(11): p. 1862-70.
5. Schmidt, M., P. Zheng, and N. Delihas, *Secondary structures of Escherichia coli antisense micF RNA, the 5'-end of the target ompF mRNA, and the RNA/RNA duplex.* Biochemistry, 1995. **34**(11): p. 3621-31.
6. Brown, L., *Robert Koch.* Bull N Y Acad Med, 1932. **8**(9): p. 558-84.
7. Smith, I., *Mycobacterium tuberculosis pathogenesis and molecular determinants of virulence.* Clin Microbiol Rev, 2003. **16**(3): p. 463-96.
8. WHO. *World Health Organisation: Tuberculosis Global Facts*. 2014 Accessed on Sept 4th 2014]; Available from: www.who.int/mediacentre/factsheets/fs104/en/.
9. Antoine, D., H. Maguire, and A. Story, *Epidemiology and response to the growing problem of tuberculosis in London.* Euro Surveill, 2006. **11**(3): p. 25-8.
10. England, P.H. *Tuberculosis in the UK 2014 report*. 2014 Accessed on Sept 4th 2014]; PHE publications gateway number: 2014353:[Available from: https://www.gov.uk/government/uploads/system/uploads/attachment_data/file/360335/TB_Annual_report__4_0_300914.pdf.
11. Jagielski, T., et al., *Current methods in the molecular typing of Mycobacterium tuberculosis and other mycobacteria.* Biomed Res Int, 2014. **2014**: p. 645802.
12. Zink, A.R., et al., *Characterization of Mycobacterium tuberculosis complex DNAs from Egyptian mummies by spoligotyping.* J Clin Microbiol, 2003. **41**(1): p. 359-67.
13. Jacobs, W.R., Jr., et al., *Genetic systems for mycobacteria.* Methods Enzymol, 1991. **204**: p. 537-55.
14. Primm, T.P., C.A. Lucero, and J.O. Falkinham, 3rd, *Health impacts of environmental mycobacteria.* Clin Microbiol Rev, 2004. **17**(1): p. 98-106.
15. Beste, D.J., et al., *The genetic requirements for fast and slow growth in mycobacteria.* PLoS One, 2009. **4**(4): p. e5349.
16. Gonzalez-y-Merchand, J.A., et al., *Strategies used by pathogenic and nonpathogenic mycobacteria to synthesize rRNA.* J Bacteriol, 1997. **179**(22): p. 6949-58.
17. Bercovier, H., O. Kafri, and S. Sela, *Mycobacteria possess a surprisingly small number of ribosomal RNA genes in relation to the size of their genome.* Biochem Biophys Res Commun, 1986. **136**(3): p. 1136-41.
18. Asai, T., et al., *Construction and initial characterization of Escherichia coli strains with few or no intact chromosomal rRNA operons.* J Bacteriol, 1999. **181**(12): p. 3803-9.
19. Cole, S.T., *Tuberculosis and the tubercle bacillus*. 2005, Washington, DC: ASM Press. xii, 584 p.

20. Madigan, M.T., *Brock biology of microorganisms*. 13th ed. 2012, San Francisco: Benjamin Cummings. xxviii, 1043, 77 p.
21. Bhatt, A., et al., *Deletion of kasB in Mycobacterium tuberculosis causes loss of acid-fastness and subclinical latent tuberculosis in immunocompetent mice.* Proc Natl Acad Sci U S A, 2007. **104**(12): p. 5157-62.
22. Leemans, J.C., et al., *Depletion of alveolar macrophages exerts protective effects in pulmonary tuberculosis in mice.* J Immunol, 2001. **166**(7): p. 4604-11.
23. Wolf, A.J., et al., *Mycobacterium tuberculosis infects dendritic cells with high frequency and impairs their function in vivo.* J Immunol, 2007. **179**(4): p. 2509-19.
24. Russell, D.G., *Who puts the tubercle in tuberculosis?* Nat Rev Microbiol, 2007. **5**(1): p. 39-47.
25. Kaufmann, S.H., *Protection against tuberculosis: cytokines, T cells, and macrophages.* Ann Rheum Dis, 2002. **61 Suppl 2**: p. ii54-8.
26. Welin, A. and M. Lerm, *Inside or outside the phagosome? The controversy of the intracellular localization of Mycobacterium tuberculosis.* Tuberculosis (Edinb), 2012. **92**(2): p. 113-20.
27. Watson, R.O., P.S. Manzanillo, and J.S. Cox, *Extracellular M. tuberculosis DNA targets bacteria for autophagy by activating the host DNA-sensing pathway.* Cell, 2012. **150**(4): p. 803-15.
28. Simeone, R., et al., *Phagosomal rupture by Mycobacterium tuberculosis results in toxicity and host cell death.* PLoS Pathog, 2012. **8**(2): p. e1002507.
29. van der Wel, N., et al., *M. tuberculosis and M. leprae translocate from the phagolysosome to the cytosol in myeloid cells.* Cell, 2007. **129**(7): p. 1287-98.
30. Wayne, L.G. and C.D. Sohaskey, *Nonreplicating persistence of mycobacterium tuberculosis.* Annu Rev Microbiol, 2001. **55**: p. 139-63.
31. Barer, M.R. and C.R. Harwood, *Bacterial viability and culturability.* Adv Microb Physiol, 1999. **41**: p. 93-137.
32. Kell, D.B., et al., *Viability and activity in readily culturable bacteria: a review and discussion of the practical issues.* Antonie Van Leeuwenhoek, 1998. **73**(2): p. 169-87.
33. Mc, C.R., et al., *Ineffectiveness of isoniazid in modifying the phenomenon of microbial persistence.* Am Rev Tuberc, 1957. **76**(6): p. 1106-9.
34. Lin, P.L., et al., *Sterilization of granulomas is common in active and latent tuberculosis despite within-host variability in bacterial killing.* Nat Med, 2014. **20**(1): p. 75-9.
35. Velayati, A.A., et al., *Totally drug-resistant tuberculosis strains: evidence of adaptation at the cellular level.* Eur Respir J, 2009. **34**(5): p. 1202-3.
36. Naidoo, C.C. and M. Pillay, *Increased in vitro fitness of multi- and extensively drug-resistant F15/LAM4/KZN strains of Mycobacterium tuberculosis.* Clin Microbiol Infect, 2014. **20**(6): p. O361-9.
37. Gagneux, S., et al., *The competitive cost of antibiotic resistance in Mycobacterium tuberculosis.* Science, 2006. **312**(5782): p. 1944-6.
38. Webb, V.D., J., *Antibiotics and antibiotic resistance in Mycobacteria*, in *Mycobacteria: Molecular biology and Virulence*, C.D. Ratledge, J., Editor. 1999, Blackwell Science.
39. Shi, W., et al., *Pyrazinamide inhibits trans-translation in Mycobacterium tuberculosis.* Science, 2011. **333**(6049): p. 1630-2.

40. Calmette, A., et al., *Report of the Technical conference for the study of vaccination against tuberculosis by means of BCFG, held at the Pasteur Institute, Paris, October 15th-18th, 1928*. 1929, Geneva,: Imp. d'Ambilly. 147 p.
41. Andersen, P. and T.M. Doherty, *The success and failure of BCG - implications for a novel tuberculosis vaccine.* Nat Rev Microbiol, 2005. **3**(8): p. 656-62.
42. Borukhov, S. and E. Nudler, *RNA polymerase holoenzyme: structure, function and biological implications.* Curr Opin Microbiol, 2003. **6**(2): p. 93-100.
43. Gomez, M., et al., *sigA is an essential gene in Mycobacterium smegmatis.* Mol Microbiol, 1998. **29**(2): p. 617-28.
44. Kazmierczak, M.J., M. Wiedmann, and K.J. Boor, *Alternative sigma factors and their roles in bacterial virulence.* Microbiol Mol Biol Rev, 2005. **69**(4): p. 527-43.
45. Weiss, L.A., et al., *Interaction of CarD with RNA polymerase mediates Mycobacterium tuberculosis viability, rifampin resistance, and pathogenesis.* J Bacteriol, 2012. **194**(20): p. 5621-31.
46. Liu, J.M. and A. Camilli, *A broadening world of bacterial small RNAs.* Curr Opin Microbiol, 2010. **13**(1): p. 18-23.
47. Reichenbach, B., et al., *The small RNA GlmY acts upstream of the sRNA GlmZ in the activation of glmS expression and is subject to regulation by polyadenylation in Escherichia coli.* Nucleic Acids Res, 2008. **36**(8): p. 2570-80.
48. Wassarman, K.M., *6S RNA: a small RNA regulator of transcription.* Curr Opin Microbiol, 2007. **10**(2): p. 164-8.
49. Gottesman, S., *The small RNA regulators of Escherichia coli: roles and mechanisms*.* Annu Rev Microbiol, 2004. **58**: p. 303-28.
50. Waters, L.S. and G. Storz, *Regulatory RNAs in bacteria.* Cell, 2009. **136**(4): p. 615-28.
51. Kroger, C., et al., *The transcriptional landscape and small RNAs of Salmonella enterica serovar Typhimurium.* Proc Natl Acad Sci U S A, 2012. **109**(20): p. E1277-86.
52. Kroger, C., et al., *An infection-relevant transcriptomic compendium for Salmonella enterica Serovar Typhimurium.* Cell Host Microbe, 2013. **14**(6): p. 683-95.
53. Gottesman, S., et al., *Small RNA regulators of translation: mechanisms of action and approaches for identifying new small RNAs.* Cold Spring Harb Symp Quant Biol, 2001. **66**: p. 353-62.
54. Wassarman, K.M., et al., *Identification of novel small RNAs using comparative genomics and microarrays.* Genes Dev, 2001. **15**(13): p. 1637-51.
55. Altschul, S.F., et al., *Basic local alignment search tool.* J Mol Biol, 1990. **215**(3): p. 403-10.
56. Livny, J., et al., *Identification of 17 Pseudomonas aeruginosa sRNAs and prediction of sRNA-encoding genes in 10 diverse pathogens using the bioinformatic tool sRNAPredict2.* Nucleic Acids Res, 2006. **34**(12): p. 3484-93.
57. Liu, J.M., et al., *Experimental discovery of sRNAs in Vibrio cholerae by direct cloning, 5S/tRNA depletion and parallel sequencing.* Nucleic Acids Res, 2009. **37**(6): p. e46.
58. Papenfort, K. and J. Vogel, *Regulatory RNA in bacterial pathogens.* Cell Host Microbe, 2010. **8**(1): p. 116-27.
59. Romby, P. and E. Charpentier, *An overview of RNAs with regulatory functions in gram-positive bacteria.* Cell Mol Life Sci, 2010. **67**(2): p. 217-37.

60. Sittka, A., et al., *Deep sequencing analysis of small noncoding RNA and mRNA targets of the global post-transcriptional regulator, Hfq.* PLoS Genet, 2008. **4**(8): p. e1000163.
61. Sun, X., I. Zhulin, and R.M. Wartell, *Predicted structure and phyletic distribution of the RNA-binding protein Hfq.* Nucleic Acids Res, 2002. **30**(17): p. 3662-71.
62. Moller, T., et al., *Hfq: a bacterial Sm-like protein that mediates RNA-RNA interaction.* Mol Cell, 2002. **9**(1): p. 23-30.
63. Wagner, E.G., *Cycling of RNAs on Hfq.* RNA Biol, 2013. **10**(4): p. 619-26.
64. Vogel, J. and B.F. Luisi, *Hfq and its constellation of RNA.* Nat Rev Microbiol, 2011. **9**(8): p. 578-89.
65. Schumacher, M.A., et al., *Structures of the pleiotropic translational regulator Hfq and an Hfq-RNA complex: a bacterial Sm-like protein.* EMBO J, 2002. **21**(13): p. 3546-56.
66. Brennan, R.G. and T.M. Link, *Hfq structure, function and ligand binding.* Curr Opin Microbiol, 2007. **10**(2): p. 125-33.
67. Arluison, V., et al., *Spectroscopic observation of RNA chaperone activities of Hfq in post-transcriptional regulation by a small non-coding RNA.* Nucleic Acids Res, 2007. **35**(3): p. 999-1006.
68. Chao, Y. and J. Vogel, *The role of Hfq in bacterial pathogens.* Curr Opin Microbiol, 2010. **13**(1): p. 24-33.
69. Gottesman, S., *Micros for microbes: non-coding regulatory RNAs in bacteria.* Trends Genet, 2005. **21**(7): p. 399-404.
70. Bohn, C., C. Rigoulay, and P. Bouloc, *No detectable effect of RNA-binding protein Hfq absence in Staphylococcus aureus.* BMC Microbiol, 2007. **7**(10): p. 10.
71. Liu, Y., et al., *Hfq is a global regulator that controls the pathogenicity of Staphylococcus aureus.* PLoS One, 2010. **5**(9).
72. Jousselin, A., L. Metzinger, and B. Felden, *On the facultative requirement of the bacterial RNA chaperone, Hfq.* Trends Microbiol, 2009. **17**(9): p. 399-405.
73. Gaballa, A., et al., *The Bacillus subtilis iron-sparing response is mediated by a Fur-regulated small RNA and three small, basic proteins.* Proc Natl Acad Sci U S A, 2008. **105**(33): p. 11927-32.
74. Pandey, S.P., et al., *A highly conserved protein of unknown function in Sinorhizobium meliloti affects sRNA regulation similar to Hfq.* Nucleic Acids Res, 2011. **39**(11): p. 4691-708.
75. Jacob, A.I., et al., *Conserved bacterial RNase YbeY plays key roles in 70S ribosome quality control and 16S rRNA maturation.* Mol Cell, 2013. **49**(3): p. 427-38.
76. Pandey, S.P., et al., *Central role for RNase YbeY in Hfq-dependent and Hfq-independent small-RNA regulation in bacteria.* BMC Genomics, 2014. **15**: p. 121.
77. Morita, T., K. Maki, and H. Aiba, *RNase E-based ribonucleoprotein complexes: mechanical basis of mRNA destabilization mediated by bacterial noncoding RNAs.* Genes Dev, 2005. **19**(18): p. 2176-86.
78. Marcaida, M.J., et al., *The RNA degradosome: life in the fast lane of adaptive molecular evolution.* Trends Biochem Sci, 2006. **31**(7): p. 359-65.
79. Vanzo, N.F., et al., *Ribonuclease E organizes the protein interactions in the Escherichia coli RNA degradosome.* Genes Dev, 1998. **12**(17): p. 2770-81.

80. Callaghan, A.J., et al., *Studies of the RNA degradosome-organizing domain of the Escherichia coli ribonuclease RNase E.* J Mol Biol, 2004. **340**(5): p. 965-79.
81. Py, B., et al., *A protein complex mediating mRNA degradation in Escherichia coli.* Mol Microbiol, 1994. **14**(4): p. 717-29.
82. Silva, I.J., et al., *Importance and key events of prokaryotic RNA decay: the ultimate fate of an RNA molecule.* Wiley Interdiscip Rev RNA, 2011. **2**(6): p. 818-36.
83. Kovacs, L., et al., *Mycobacterial RNase E-associated proteins.* Microbiol Immunol, 2005. **49**(11): p. 1003-7.
84. Arraiano, C.M., et al., *The critical role of RNA processing and degradation in the control of gene expression.* FEMS Microbiol Rev, 2010. **34**(5): p. 883-923.
85. Carpousis, A.J., *The RNA degradosome of Escherichia coli: an mRNA-degrading machine assembled on RNase E.* Annu Rev Microbiol, 2007. **61**: p. 71-87.
86. Viegas, S.C., et al., *Regulation of the small regulatory RNA MicA by ribonuclease III: a target-dependent pathway.* Nucleic Acids Res, 2011. **39**(7): p. 2918-30.
87. Huntzinger, E., et al., *Staphylococcus aureus RNAIII and the endoribonuclease III coordinately regulate spa gene expression.* EMBO J, 2005. **24**(4): p. 824-35.
88. Boisset, S., et al., *Staphylococcus aureus RNAIII coordinately represses the synthesis of virulence factors and the transcription regulator Rot by an antisense mechanism.* Genes Dev, 2007. **21**(11): p. 1353-66.
89. Lasa, I., et al., *Genome-wide antisense transcription drives mRNA processing in bacteria.* Proc Natl Acad Sci U S A, 2011. **108**(50): p. 20172-7.
90. Lioliou, E., et al., *Global regulatory functions of the Staphylococcus aureus endoribonuclease III in gene expression.* PLoS Genet, 2012. **8**(6): p. e1002782.
91. De Lay, N. and S. Gottesman, *Role of polynucleotide phosphorylase in sRNA function in Escherichia coli.* RNA, 2011. **17**(6): p. 1172-89.
92. Andrade, J.M., et al., *The crucial role of PNPase in the degradation of small RNAs that are not associated with Hfq.* RNA, 2012. **18**(4): p. 844-55.
93. Majdalani, N., C.K. Vanderpool, and S. Gottesman, *Bacterial small RNA regulators.* Crit Rev Biochem Mol Biol, 2005. **40**(2): p. 93-113.
94. Griffin, B.E., *Separation of 32P-labelled ribonucleic acid components. The use of polyethylenimine-cellulose (TLC) as a second dimension in separating oligoribonucleotides of '4.5 S' and 5 S from E. coli.* FEBS Lett, 1971. **15**(3): p. 165-168.
95. Ikemura, T. and J.E. Dahlberg, *Small ribonucleic acids of Escherichia coli. I. Characterization by polyacrylamide gel electrophoresis and fingerprint analysis.* J Biol Chem, 1973. **248**(14): p. 5024-32.
96. Tomizawa, J., et al., *Inhibition of ColE1 RNA primer formation by a plasmid-specified small RNA.* Proc Natl Acad Sci U S A, 1981. **78**(3): p. 1421-5.
97. Stougaard, P., S. Molin, and K. Nordstrom, *RNAs involved in copy-number control and incompatibility of plasmid R1.* Proc Natl Acad Sci U S A, 1981. **78**(10): p. 6008-12.
98. Tomizawa, J., *Control of ColE1 plasmid replication: the process of binding of RNA I to the primer transcript.* Cell, 1984. **38**(3): p. 861-70.
99. Tomizawa, J.I. and T. Itoh, *The importance of RNA secondary structure in CoIE1 primer formation.* Cell, 1982. **31**(3 Pt 2): p. 575-83.

100. Gerhart, E., H. Wagner, and K. Nordstrom, *Structural analysis of an RNA molecule involved in replication control of plasmid R1.* Nucleic Acids Res, 1986. **14**(6): p. 2523-38.
101. Mizuno, T., *[Regulation of gene expression by a small RNA transcript (micRNA): osmoregulation in E. coli].* Seikagaku, 1984. **56**(2): p. 113-9.
102. Mizuno, T., M.Y. Chou, and M. Inouye, *A unique mechanism regulating gene expression: translational inhibition by a complementary RNA transcript (micRNA).* Proc Natl Acad Sci U S A, 1984. **81**(7): p. 1966-70.
103. Udekwu, K.I., et al., *Hfq-dependent regulation of OmpA synthesis is mediated by an antisense RNA.* Genes Dev, 2005. **19**(19): p. 2355-66.
104. Chen, S., et al., *MicC, a second small-RNA regulator of Omp protein expression in Escherichia coli.* J Bacteriol, 2004. **186**(20): p. 6689-97.
105. Storz, G., J.A. Opdyke, and A. Zhang, *Controlling mRNA stability and translation with small, noncoding RNAs.* Curr Opin Microbiol, 2004. **7**(2): p. 140-4.
106. Argaman, L. and S. Altuvia, *fhlA repression by OxyS RNA: kissing complex formation at two sites results in a stable antisense-target RNA complex.* J Mol Biol, 2000. **300**(5): p. 1101-12.
107. Moller, T., et al., *Spot 42 RNA mediates discoordinate expression of the E. coli galactose operon.* Genes Dev, 2002. **16**(13): p. 1696-706.
108. Udekwu, K.I. and E.G. Wagner, *Sigma E controls biogenesis of the antisense RNA MicA.* Nucleic Acids Res, 2007. **35**(4): p. 1279-88.
109. Heidrich, N., I. Moll, and S. Brantl, *In vitro analysis of the interaction between the small RNA SR1 and its primary target ahrC mRNA.* Nucleic Acids Res, 2007. **35**(13): p. 4331-46.
110. Darfeuille, F., et al., *An antisense RNA inhibits translation by competing with standby ribosomes.* Mol Cell, 2007. **26**(3): p. 381-92.
111. Sharma, C.M., et al., *A small RNA regulates multiple ABC transporter mRNAs by targeting C/A-rich elements inside and upstream of ribosome-binding sites.* Genes Dev, 2007. **21**(21): p. 2804-17.
112. Bouvier, M., et al., *Small RNA binding to 5' mRNA coding region inhibits translational initiation.* Mol Cell, 2008. **32**(6): p. 827-37.
113. Holmqvist, E., et al., *Two antisense RNAs target the transcriptional regulator CsgD to inhibit curli synthesis.* EMBO J, 2010. **29**(11): p. 1840-50.
114. Desnoyers, G. and E. Masse, *Noncanonical repression of translation initiation through small RNA recruitment of the RNA chaperone Hfq.* Genes Dev, 2012. **26**(7): p. 726-39.
115. Bandyra, K.J., et al., *The seed region of a small RNA drives the controlled destruction of the target mRNA by the endoribonuclease RNase E.* Mol Cell, 2012. **47**(6): p. 943-53.
116. Desnoyers, G., M.P. Bouchard, and E. Masse, *New insights into small RNA-dependent translational regulation in prokaryotes.* Trends Genet, 2013. **29**(2): p. 92-8.
117. Dreyfus, M., *Killer and protective ribosomes.* Prog Mol Biol Transl Sci, 2009. **85**: p. 423-66.
118. Prevost, K., et al., *Small RNA-induced mRNA degradation achieved through both translation block and activated cleavage.* Genes Dev, 2011. **25**(4): p. 385-96.

119. Morita, T., Y. Mochizuki, and H. Aiba, *Translational repression is sufficient for gene silencing by bacterial small noncoding RNAs in the absence of mRNA destruction.* Proc Natl Acad Sci U S A, 2006. **103**(13): p. 4858-63.
120. Rice, J.B. and C.K. Vanderpool, *The small RNA SgrS controls sugar-phosphate accumulation by regulating multiple PTS genes.* Nucleic Acids Res, 2011. **39**(9): p. 3806-19.
121. Rice, J.B., D. Balasubramanian, and C.K. Vanderpool, *Small RNA binding-site multiplicity involved in translational regulation of a polycistronic mRNA.* Proc Natl Acad Sci U S A, 2012. **109**(40): p. E2691-8.
122. Desnoyers, G., et al., *Small RNA-induced differential degradation of the polycistronic mRNA iscRSUA.* EMBO J, 2009. **28**(11): p. 1551-61.
123. Pfeiffer, V., et al., *Coding sequence targeting by MicC RNA reveals bacterial mRNA silencing downstream of translational initiation.* Nat Struct Mol Biol, 2009. **16**(8): p. 840-6.
124. Morfeldt, E., et al., *Activation of alpha-toxin translation in Staphylococcus aureus by the trans-encoded antisense RNA, RNAIII.* EMBO J, 1995. **14**(18): p. 4569-77.
125. Prevost, K., et al., *The small RNA RyhB activates the translation of shiA mRNA encoding a permease of shikimate, a compound involved in siderophore synthesis.* Mol Microbiol, 2007. **64**(5): p. 1260-73.
126. Kalamorz, F., et al., *Feedback control of glucosamine-6-phosphate synthase GlmS expression depends on the small RNA GlmZ and involves the novel protein YhbJ in Escherichia coli.* Mol Microbiol, 2007. **65**(6): p. 1518-33.
127. Urban, J.H., et al., *A conserved small RNA promotes discoordinate expression of the glmUS operon mRNA to activate GlmS synthesis.* J Mol Biol, 2007. **373**(3): p. 521-8.
128. Urban, J.H. and J. Vogel, *Two seemingly homologous noncoding RNAs act hierarchically to activate glmS mRNA translation.* PLoS Biol, 2008. **6**(3): p. e64.
129. Majdalani, N., et al., *DsrA RNA regulates translation of RpoS message by an anti-antisense mechanism, independent of its action as an antisilencer of transcription.* Proc Natl Acad Sci U S A, 1998. **95**(21): p. 12462-7.
130. Wassarman, K.M., *6S RNA: a regulator of transcription.* Mol Microbiol, 2007. **65**(6): p. 1425-31.
131. Wassarman, K.M. and G. Storz, *6S RNA regulates E. coli RNA polymerase activity.* Cell, 2000. **101**(6): p. 613-23.
132. Trotochaud, A.E. and K.M. Wassarman, *A highly conserved 6S RNA structure is required for regulation of transcription.* Nat Struct Mol Biol, 2005. **12**(4): p. 313-9.
133. Paul, B.J., et al., *DksA: a critical component of the transcription initiation machinery that potentiates the regulation of rRNA promoters by ppGpp and the initiating NTP.* Cell, 2004. **118**(3): p. 311-22.
134. Primm, T.P., et al., *The stringent response of Mycobacterium tuberculosis is required for long-term survival.* J Bacteriol, 2000. **182**(17): p. 4889-98.
135. Stallings, C.L., et al., *CarD is an essential regulator of rRNA transcription required for Mycobacterium tuberculosis persistence.* Cell, 2009. **138**(1): p. 146-59.
136. Cavanagh, A.T., J.M. Sperger, and K.M. Wassarman, *Regulation of 6S RNA by pRNA synthesis is required for efficient recovery from stationary phase in E. coli and B. subtilis.* Nucleic Acids Res, 2012. **40**(5): p. 2234-46.

137. Trotochaud, A.E. and K.M. Wassarman, *6S RNA function enhances long-term cell survival.* J Bacteriol, 2004. **186**(15): p. 4978-85.
138. Wassarman, K.M. and R.M. Saecker, *Synthesis-mediated release of a small RNA inhibitor of RNA polymerase.* Science, 2006. **314**(5805): p. 1601-3.
139. Vanderpool, C.K. and S. Gottesman, *Involvement of a novel transcriptional activator and small RNA in post-transcriptional regulation of the glucose phosphoenolpyruvate phosphotransferase system.* Mol Microbiol, 2004. **54**(4): p. 1076-89.
140. Wadler, C.S. and C.K. Vanderpool, *A dual function for a bacterial small RNA: SgrS performs base pairing-dependent regulation and encodes a functional polypeptide.* Proc Natl Acad Sci U S A, 2007. **104**(51): p. 20454-9.
141. Nahvi, A., et al., *Genetic control by a metabolite binding mRNA.* Chem Biol, 2002. **9**(9): p. 1043.
142. Warner, D.F., et al., *A riboswitch regulates expression of the coenzyme B12-independent methionine synthase in Mycobacterium tuberculosis: implications for differential methionine synthase function in strains H37Rv and CDC1551.* J Bacteriol, 2007. **189**(9): p. 3655-9.
143. Walters, S.B., et al., *The Mycobacterium tuberculosis PhoPR two-component system regulates genes essential for virulence and complex lipid biosynthesis.* Mol Microbiol, 2006. **60**(2): p. 312-30.
144. Gripenland, J., et al., *RNAs: regulators of bacterial virulence.* Nat Rev Microbiol, 2010. **8**(12): p. 857-66.
145. Vitreschak, A.G., et al., *Comparative genomic analysis of T-box regulatory systems in bacteria.* RNA, 2008. **14**(4): p. 717-35.
146. Nelson, J.W., et al., *Riboswitches in eubacteria sense the second messenger c-di-AMP.* Nat Chem Biol, 2013. **9**(12): p. 834-9.
147. Masse, E. and S. Gottesman, *A small RNA regulates the expression of genes involved in iron metabolism in Escherichia coli.* Proc Natl Acad Sci U S A, 2002. **99**(7): p. 4620-5.
148. Masse, E., C.K. Vanderpool, and S. Gottesman, *Effect of RyhB small RNA on global iron use in Escherichia coli.* J Bacteriol, 2005. **187**(20): p. 6962-71.
149. Sledjeski, D.D., A. Gupta, and S. Gottesman, *The small RNA, DsrA, is essential for the low temperature expression of RpoS during exponential growth in Escherichia coli.* EMBO J, 1996. **15**(15): p. 3993-4000.
150. Padalon-Brauch, G., et al., *Small RNAs encoded within genetic islands of Salmonella typhimurium show host-induced expression and role in virulence.* Nucleic Acids Res, 2008. **36**(6): p. 1913-27.
151. Romby, P., F. Vandenesch, and E.G. Wagner, *The role of RNAs in the regulation of virulence-gene expression.* Curr Opin Microbiol, 2006. **9**(2): p. 229-36.
152. Papenfort, K., et al., *SigmaE-dependent small RNAs of Salmonella respond to membrane stress by accelerating global omp mRNA decay.* Mol Microbiol, 2006. **62**(6): p. 1674-88.
153. Arnvig, K.B. and D.B. Young, *Identification of small RNAs in Mycobacterium tuberculosis.* Mol Microbiol, 2009. **73**(3): p. 397-408.
154. Arnvig, K. and D. Young, *Non-coding RNA and its potential role in Mycobacterium tuberculosis pathogenesis.* RNA Biol, 2012. **9**(4): p. 427-36.
155. Houghton, J., et al., *A Small RNA Encoded in the Rv2660c Locus of Mycobacterium tuberculosis Is Induced during Starvation and Infection.* Plos One, 2013. **8**(12).

156. Solans, L., et al., *The PhoP-dependent ncRNA Mcr7 modulates the TAT secretion system in Mycobacterium tuberculosis.* PLoS Pathog, 2014. **10**(5): p. e1004183.
157. Waddell, S.J. and P.D. Butcher, *Microarray analysis of whole genome expression of intracellular Mycobacterium tuberculosis.* Curr Mol Med, 2007. **7**(3): p. 287-96.
158. Waddell, S.J., P.D. Butcher, and N.G. Stoker, *RNA profiling in host-pathogen interactions.* Curr Opin Microbiol, 2007. **10**(3): p. 297-302.
159. Li, A.H., et al., *Contrasting transcriptional responses of a virulent and an attenuated strain of Mycobacterium tuberculosis infecting macrophages.* PLoS One. **5**(6): p. e11066.
160. Lin, P.L., et al., *Quantitative comparison of active and latent tuberculosis in the cynomolgus macaque model.* Infect Immun, 2009. **77**(10): p. 4631-42.
161. Garton, N.J., et al., *Cytological and transcript analyses reveal fat and lazy persister-like bacilli in tuberculous sputum.* PLoS Med, 2008. **5**(4): p. e75.
162. Rachman, H., et al., *Unique transcriptome signature of Mycobacterium tuberculosis in pulmonary tuberculosis.* Infect Immun, 2006. **74**(2): p. 1233-42.
163. Kery, M.B., et al., *TargetRNA2: identifying targets of small regulatory RNAs in bacteria.* Nucleic Acids Res, 2014. **42**(Web Server issue): p. W124-9.
164. Tjaden, B., *TargetRNA: a tool for predicting targets of small RNA action in bacteria.* Nucleic Acids Res, 2008. **36**(Web Server issue): p. W109-13.
165. Wilderman, P.J., et al., *Identification of tandem duplicate regulatory small RNAs in Pseudomonas aeruginosa involved in iron homeostasis.* Proc Natl Acad Sci U S A, 2004. **101**(26): p. 9792-7.
166. Schnappinger, D., G.K. Schoolnik, and S. Ehrt, *Expression profiling of host pathogen interactions: how Mycobacterium tuberculosis and the macrophage adapt to one another.* Microbes Infect, 2006. **8**(4): p. 1132-40.
167. Smollett, K.L., L.F. Dawson, and E.O. Davis, *SigG does not control gene expression in response to DNA damage in Mycobacterium tuberculosis H37Rv.* J Bacteriol. **193**(4): p. 1007-11.
168. Wang, Z., M. Gerstein, and M. Snyder, *RNA-Seq: a revolutionary tool for transcriptomics.* Nat Rev Genet, 2009. **10**(1): p. 57-63.
169. Kendall, S.L., et al., *What do microarrays really tell us about M. tuberculosis?* Trends Microbiol, 2004. **12**(12): p. 537-44.
170. Pelly, S., W.R. Bishai, and G. Lamichhane, *A screen for non-coding RNA in Mycobacterium tuberculosis reveals a cAMP-responsive RNA that is expressed during infection.* Gene, 2012. **500**(1): p. 85-92.
171. Lamichhane, G., K.B. Arnvig, and K.A. McDonough, *Definition and annotation of (myco)bacterial non-coding RNA.* Tuberculosis (Edinb), 2013. **93**(1): p. 26-9.
172. Cole, S.T., et al., *Deciphering the biology of Mycobacterium tuberculosis from the complete genome sequence.* Nature, 1998. **393**(6685): p. 537-44.
173. Comas, I., et al., *Human T cell epitopes of Mycobacterium tuberculosis are evolutionarily hyperconserved.* Nat Genet, 2010. **42**(6): p. 498-503.
174. Hinds, J., et al., *Enhanced gene replacement in mycobacteria.* Microbiology, 1999. **145 (Pt 3)**: p. 519-27.
175. Hartkoorn, R.C., et al., *Genome-wide definition of the SigF regulon in Mycobacterium tuberculosis.* J Bacteriol, 2012. **194**(8): p. 2001-9.
176. Chen, P., et al., *Construction and characterization of a Mycobacterium tuberculosis mutant lacking the alternate sigma factor gene, sigF.* Infect Immun, 2000. **68**(10): p. 5575-80.

177. Geiman, D.E., et al., *Attenuation of late-stage disease in mice infected by the Mycobacterium tuberculosis mutant lacking the SigF alternate sigma factor and identification of SigF-dependent genes by microarray analysis.* Infect Immun, 2004. **72**(3): p. 1733-45.
178. Karls, R.K., et al., *Examination of Mycobacterium tuberculosis sigma factor mutants using low-dose aerosol infection of guinea pigs suggests a role for SigC in pathogenesis.* Microbiology, 2006. **152**(Pt 6): p. 1591-600.
179. Sturgill-Koszycki, S., et al., *Lack of acidification in Mycobacterium phagosomes produced by exclusion of the vesicular proton-ATPase.* Science, 1994. **263**(5147): p. 678-81.
180. Russell, D.G., *Mycobacterium tuberculosis: here today, and here tomorrow.* Nat Rev Mol Cell Biol, 2001. **2**(8): p. 569-77.
181. Schnappinger, D., et al., *Transcriptional Adaptation of Mycobacterium tuberculosis within Macrophages: Insights into the Phagosomal Environment.* J Exp Med, 2003. **198**(5): p. 693-704.
182. Deana, A. and J.G. Belasco, *Lost in translation: the influence of ribosomes on bacterial mRNA decay.* Genes Dev, 2005. **19**(21): p. 2526-33.
183. Parish, T. and N.G. Stoker, *Use of a flexible cassette method to generate a double unmarked Mycobacterium tuberculosis tlyA plcABC mutant by gene replacement.* Microbiology, 2000. **146 (Pt 8)**: p. 1969-75.
184. Abomoelak, B., et al., *Characterization of a novel heat shock protein (Hsp22.5) involved in the pathogenesis of Mycobacterium tuberculosis.* J Bacteriol, 2011. **193**(14): p. 3497-505.
185. Stewart, G.R., et al., *Dissection of the heat-shock response in Mycobacterium tuberculosis using mutants and microarrays.* Microbiology, 2002. **148**(Pt 10): p. 3129-38.
186. Archuleta, R.J., P. Yvonne Hoppes, and T.P. Primm, *Mycobacterium avium enters a state of metabolic dormancy in response to starvation.* Tuberculosis (Edinb), 2005. **85**(3): p. 147-58.
187. Betts, J.C., et al., *Evaluation of a nutrient starvation model of Mycobacterium tuberculosis persistence by gene and protein expression profiling.* Mol Microbiol, 2002. **43**(3): p. 717-31.
188. Murphy, D.J. and J.R. Brown, *Identification of gene targets against dormant phase Mycobacterium tuberculosis infections.* BMC Infect Dis, 2007. **7**: p. 84.
189. DeMaio, J., et al., *A stationary-phase stress-response sigma factor from Mycobacterium tuberculosis.* Proc Natl Acad Sci U S A, 1996. **93**(7): p. 2790-4.
190. Homuth, G., A. Mogk, and W. Schumann, *Post-transcriptional regulation of the Bacillus subtilis dnaK operon.* Mol Microbiol, 1999. **32**(6): p. 1183-97.
191. Jager, S., A. Jager, and G. Klug, *CIRCE is not involved in heat-dependent transcription of groESL but in stabilization of the mRNA 5'-end in Rhodobacter capsulatus.* Nucleic Acids Res, 2004. **32**(1): p. 386-96.
192. Babitzke, P. and T. Romeo, *CsrB sRNA family: sequestration of RNA-binding regulatory proteins.* Curr Opin Microbiol, 2007. **10**(2): p. 156-63.
193. Nyka, W., *Studies on the effect of starvation on mycobacteria.* Infect Immun, 1974. **9**(5): p. 843-50.
194. Smeulders, M.J., et al., *Adaptation of Mycobacterium smegmatis to stationary phase.* J Bacteriol, 1999. **181**(1): p. 270-83.
195. Sun, R., et al., *Mycobacterium tuberculosis ECF sigma factor sigC is required for lethality in mice and for the conditional expression of a defined gene set.* Mol Microbiol, 2004. **52**(1): p. 25-38.

196. Galagan, J.E., et al., *The Mycobacterium tuberculosis regulatory network and hypoxia.* Nature, 2013. **499**(7457): p. 178-83.
197. Campbell, E.A., et al., *Structural mechanism for rifampicin inhibition of bacterial rna polymerase.* Cell, 2001. **104**(6): p. 901-12.
198. Rustad, T.R., et al., *Global analysis of mRNA stability in Mycobacterium tuberculosis.* Nucleic Acids Res, 2013. **41**(1): p. 509-17.
199. Storz, G., S. Altuvia, and K.M. Wassarman, *An abundance of RNA regulators.* Annu Rev Biochem, 2005. **74**: p. 199-217.
200. Maciag, A., et al., *Global analysis of the Mycobacterium tuberculosis Zur (FurB) regulon.* J Bacteriol, 2007. **189**(3): p. 730-40.
201. Gold, B., et al., *The Mycobacterium tuberculosis IdeR is a dual functional regulator that controls transcription of genes involved in iron acquisition, iron storage and survival in macrophages.* Mol Microbiol, 2001. **42**(3): p. 851-65.
202. Prakash, P., et al., *Computational prediction and experimental verification of novel IdeR binding sites in the upstream sequences of Mycobacterium tuberculosis open reading frames.* Bioinformatics, 2005. **21**(10): p. 2161-6.
203. Solioz, M. and C. Vulpe, *CPx-type ATPases: a class of P-type ATPases that pump heavy metals.* Trends Biochem Sci, 1996. **21**(7): p. 237-41.
204. Robinson, N.J., S.K. Whitehall, and J.S. Cavet, *Microbial metallothioneins.* Adv Microb Physiol, 2001. **44**: p. 183-213.
205. Rodriguez, G.M., et al., *ideR, An essential gene in mycobacterium tuberculosis: role of IdeR in iron-dependent gene expression, iron metabolism, and oxidative stress response.* Infect Immun, 2002. **70**(7): p. 3371-81.
206. Pohl, E., R.K. Holmes, and W.G. Hol, *Crystal structure of the iron-dependent regulator (IdeR) from Mycobacterium tuberculosis shows both metal binding sites fully occupied.* J Mol Biol, 1999. **285**(3): p. 1145-56.
207. De Voss, J.J., et al., *Iron acquisition and metabolism by mycobacteria.* J Bacteriol, 1999. **181**(15): p. 4443-51.
208. Wong, D.K., et al., *Identification of fur, aconitase, and other proteins expressed by Mycobacterium tuberculosis under conditions of low and high concentrations of iron by combined two-dimensional gel electrophoresis and mass spectrometry.* Infect Immun, 1999. **67**(1): p. 327-36.
209. De Voss, J.J., et al., *The salicylate-derived mycobactin siderophores of Mycobacterium tuberculosis are essential for growth in macrophages.* Proc Natl Acad Sci U S A, 2000. **97**(3): p. 1252-7.
210. Manabe, Y.C., et al., *Attenuation of virulence in Mycobacterium tuberculosis expressing a constitutively active iron repressor.* Proc Natl Acad Sci U S A, 1999. **96**(22): p. 12844-8.
211. Rybniker, J., et al., *Anticytolytic screen identifies inhibitors of mycobacterial virulence protein secretion.* Cell Host Microbe, 2014. **16**(4): p. 538-48.
212. Mosmann, T.R. and S. Sad, *The expanding universe of T-cell subsets: Th1, Th2 and more.* Immunol Today, 1996. **17**(3): p. 138-46.
213. Coenye, T. and P. Vandamme, *Intragenomic heterogeneity between multiple 16S ribosomal RNA operons in sequenced bacterial genomes.* FEMS Microbiol Lett, 2003. **228**(1): p. 45-9.
214. Panek, J., et al., *The suboptimal structures find the optimal RNAs: homology search for bacterial non-coding RNAs using suboptimal RNA structures.* Nucleic Acids Res, 2011. **39**(8): p. 3418-26.
215. Hnilicova, J., et al., *Ms1, a novel sRNA interacting with the RNA polymerase core in mycobacteria.* Nucleic Acids Res, 2014. **42**(18): p. 11763-76.

216. Upton, A.M. and J.D. McKinney, *Role of the methylcitrate cycle in propionate metabolism and detoxification in Mycobacterium smegmatis.* Microbiology, 2007. **153**(Pt 12): p. 3973-82.
217. Rainwater, D.L. and P.E. Kolattukudy, *Fatty acid biosynthesis in Mycobacterium tuberculosis var. bovis Bacillus Calmette-Guerin. Purification and characterization of a novel fatty acid synthase, mycocerosic acid synthase, which elongates n-fatty acyl-CoA with methylmalonyl-CoA.* J Biol Chem, 1985. **260**(1): p. 616-23.
218. Azad, A.K., et al., *Targeted replacement of the mycocerosic acid synthase gene in Mycobacterium bovis BCG produces a mutant that lacks mycosides.* Proc Natl Acad Sci U S A, 1996. **93**(10): p. 4787-92.
219. Camacho, L.R., et al., *Identification of a virulence gene cluster of Mycobacterium tuberculosis by signature-tagged transposon mutagenesis.* Mol Microbiol, 1999. **34**(2): p. 257-67.
220. Cox, J.S., et al., *Complex lipid determines tissue-specific replication of Mycobacterium tuberculosis in mice.* Nature, 1999. **402**(6757): p. 79-83.
221. Rousseau, C., et al., *Production of phthiocerol dimycocerosates protects Mycobacterium tuberculosis from the cidal activity of reactive nitrogen intermediates produced by macrophages and modulates the early immune response to infection.* Cell Microbiol, 2004. **6**(3): p. 277-87.
222. Yu, J., et al., *Both phthiocerol dimycocerosates and phenolic glycolipids are required for virulence of Mycobacterium marinum.* Infect Immun, 2012. **80**(4): p. 1381-9.
223. Kirksey, M.A., et al., *Spontaneous phthiocerol dimycocerosate-deficient variants of Mycobacterium tuberculosis are susceptible to gamma interferon-mediated immunity.* Infect Immun, 2011. **79**(7): p. 2829-38.
224. Makarova, K.S., A.A. Mironov, and M.S. Gelfand, *Conservation of the binding site for the arginine repressor in all bacterial lineages.* Genome Biol, 2001. **2**(4): p. RESEARCH0013.
225. Bretl, D.J., et al., *MprA and DosR coregulate a Mycobacterium tuberculosis virulence operon encoding Rv1813c and Rv1812c.* Infect Immun, 2012. **80**(9): p. 3018-33.
226. Milano, A., et al., *Azole resistance in Mycobacterium tuberculosis is mediated by the MmpS5-MmpL5 efflux system.* Tuberculosis (Edinb), 2009. **89**(1): p. 84-90.
227. Turapov, O., et al., *Antimicrobial treatment improves mycobacterial survival in nonpermissive growth conditions.* Antimicrob Agents Chemother, 2014. **58**(5): p. 2798-806.
228. Trauner, A., et al., *The dormancy regulator DosR controls ribosome stability in hypoxic mycobacteria.* J Biol Chem, 2012. **287**(28): p. 24053-63.
229. Cunningham, A.F. and C.L. Spreadbury, *Mycobacterial stationary phase induced by low oxygen tension: cell wall thickening and localization of the 16-kilodalton alpha-crystallin homolog.* J Bacteriol, 1998. **180**(4): p. 801-8.
230. McAdam, R.A., et al., *Characterization of a Mycobacterium tuberculosis H37Rv transposon library reveals insertions in 351 ORFs and mutants with altered virulence.* Microbiology, 2002. **148**(Pt 10): p. 2975-86.
231. D'Souza, C.A., et al., *Cyclic AMP-dependent protein kinase controls virulence of the fungal pathogen Cryptococcus neoformans.* Mol Cell Biol, 2001. **21**(9): p. 3179-91.

232. Shi, L., et al., *Carbon flux rerouting during Mycobacterium tuberculosis growth arrest.* Mol Microbiol, 2010. **78**(5): p. 1199-215.
233. Nazarova, E.V., et al., *Role of lipid components in formation and reactivation of Mycobacterium smegmatis "nonculturable" cells.* Biochemistry (Mosc), 2011. **76**(6): p. 636-44.
234. Kaur, D., et al., *Chapter 2: Biogenesis of the cell wall and other glycoconjugates of Mycobacterium tuberculosis.* Adv Appl Microbiol, 2009. **69**: p. 23-78.
235. Daffe, M. and P. Draper, *The envelope layers of mycobacteria with reference to their pathogenicity.* Adv Microb Physiol, 1998. **39**: p. 131-203.
236. Barry, C.E., 3rd, et al., *Mycolic acids: structure, biosynthesis and physiological functions.* Prog Lipid Res, 1998. **37**(2-3): p. 143-79.
237. Domenech, P. and M.B. Reed, *Rapid and spontaneous loss of phthiocerol dimycocerosate (PDIM) from Mycobacterium tuberculosis grown in vitro: implications for virulence studies.* Microbiology, 2009. **155**(Pt 11): p. 3532-43.
238. Movahedzadeh, F., M.J. Colston, and E.O. Davis, *Determination of DNA sequences required for regulated Mycobacterium tuberculosis RecA expression in response to DNA-damaging agents suggests that two modes of regulation exist.* J Bacteriol, 1997. **179**(11): p. 3509-18.
239. Smollett, K.L., et al., *Global analysis of the regulon of the transcriptional repressor LexA, a key component of SOS response in Mycobacterium tuberculosis.* J Biol Chem, 2012. **287**(26): p. 22004-14.
240. Rand, L., et al., *The majority of inducible DNA repair genes in Mycobacterium tuberculosis are induced independently of RecA.* Mol Microbiol, 2003. **50**(3): p. 1031-42.
241. Wade, J.T., et al., *Genomic analysis of LexA binding reveals the permissive nature of the Escherichia coli genome and identifies unconventional target sites.* Genes Dev, 2005. **19**(21): p. 2619-30.
242. He, H., et al., *MprAB is a stress-responsive two-component system that directly regulates expression of sigma factors SigB and SigE in Mycobacterium tuberculosis.* J Bacteriol, 2006. **188**(6): p. 2134-43.
243. Rustad, T.R., et al., *The enduring hypoxic response of Mycobacterium tuberculosis.* PLoS One, 2008. **3**(1): p. e1502.
244. Voskuil, M.I., K.C. Visconti, and G.K. Schoolnik, *Mycobacterium tuberculosis gene expression during adaptation to stationary phase and low-oxygen dormancy.* Tuberculosis (Edinb), 2004. **84**(3-4): p. 218-27.
245. Aagaard, C., et al., *A multistage tuberculosis vaccine that confers efficient protection before and after exposure.* Nat Med. **17**(2): p. 189-94.
246. Cortes, T., et al., *Genome-wide mapping of transcriptional start sites defines an extensive leaderless transcriptome in Mycobacterium tuberculosis.* Cell Rep, 2013. **5**(4): p. 1121-31.
247. Camus, J.C., et al., *Re-annotation of the genome sequence of Mycobacterium tuberculosis H37Rv.* Microbiology, 2002. **148**(Pt 10): p. 2967-73.
248. Picotti, P. and R. Aebersold, *Selected reaction monitoring-based proteomics: workflows, potential, pitfalls and future directions.* Nat Methods, 2012. **9**(6): p. 555-66.
249. Picotti, P., et al., *Full dynamic range proteome analysis of S. cerevisiae by targeted proteomics.* Cell, 2009. **138**(4): p. 795-806.
250. Schubert, O.T., et al., *The Mtb proteome library: a resource of assays to quantify the complete proteome of Mycobacterium tuberculosis.* Cell Host Microbe, 2013. **13**(5): p. 602-12.

251. Kelley, L.A. and M.J. Sternberg, *Protein structure prediction on the Web: a case study using the Phyre server.* Nat Protoc, 2009. **4**(3): p. 363-71.
252. Uplekar, S., et al., *High-resolution transcriptome and genome-wide dynamics of RNA polymerase and NusA in Mycobacterium tuberculosis.* Nucleic Acids Res, 2013. **41**(2): p. 961-77.
253. Albrethsen, J., et al., *Proteomic profiling of Mycobacterium tuberculosis identifies nutrient-starvation-responsive toxin-antitoxin systems.* Mol Cell Proteomics, 2013. **12**(5): p. 1180-91.
254. Kelkar, D.S., et al., *Proteogenomic analysis of Mycobacterium tuberculosis by high resolution mass spectrometry.* Mol Cell Proteomics, 2011. **10**(12): p. M111 011627.
255. Los, M., et al., *Effective inhibition of lytic development of bacteriophages lambda, P1 and T4 by starvation of their host, Escherichia coli.* BMC Biotechnol, 2007. **7**: p. 13.
256. Williams, M.D., J.A. Fuchs, and M.C. Flickinger, *Null mutation in the stringent starvation protein of Escherichia coli disrupts lytic development of bacteriophage P1.* Gene, 1991. **109**(1): p. 21-30.
257. Slominska, M., P. Neubauer, and G. Wegrzyn, *Regulation of bacteriophage lambda development by guanosine 5'-diphosphate-3'-diphosphate.* Virology, 1999. **262**(2): p. 431-41.
258. Govender, L., et al., *Higher human CD4 T cell response to novel Mycobacterium tuberculosis latency associated antigens Rv2660 and Rv2659 in latent infection compared with tuberculosis disease.* Vaccine, 2010. **29**(1): p. 51-7.
259. Tameris, M.D., et al., *Safety and efficacy of MVA85A, a new tuberculosis vaccine, in infants previously vaccinated with BCG: a randomised, placebo-controlled phase 2b trial.* Lancet, 2013. **381**(9871): p. 1021-8.
260. Tameris, M., et al., *Lessons learnt from the first efficacy trial of a new infant tuberculosis vaccine since BCG.* Tuberculosis (Edinb), 2013. **93**(2): p. 143-9.
261. Sittka, A., et al., *The RNA chaperone Hfq is essential for the virulence of Salmonella typhimurium.* Mol Microbiol, 2007. **63**(1): p. 193-217.
262. Ansong, C., et al., *Global systems-level analysis of Hfq and SmpB deletion mutants in Salmonella: implications for virulence and global protein translation.* PLoS One, 2009. **4**(3): p. e4809.
263. Sittka, A., et al., *Deep sequencing of Salmonella RNA associated with heterologous Hfq proteins in vivo reveals small RNAs as a major target class and identifies RNA processing phenotypes.* RNA Biol, 2009. **6**(3): p. 266-75.
264. Papenfort, K., et al., *Systematic deletion of Salmonella small RNA genes identifies CyaR, a conserved CRP-dependent riboregulator of OmpX synthesis.* Mol Microbiol, 2008. **68**(4): p. 890-906.
265. Toledo-Arana, A., F. Repoila, and P. Cossart, *Small noncoding RNAs controlling pathogenesis.* Curr Opin Microbiol, 2007. **10**(2): p. 182-8.
266. Chabelskaya, S., O. Gaillot, and B. Felden, *A Staphylococcus aureus small RNA is required for bacterial virulence and regulates the expression of an immune-evasion molecule.* PLoS Pathog, 2010. **6**(6): p. e1000927.
267. Schulte, L.N., et al., *Analysis of the host microRNA response to Salmonella uncovers the control of major cytokines by the let-7 family.* EMBO J, 2011. **30**(10): p. 1977-89.
268. Westermann, A.J., S.A. Gorski, and J. Vogel, *Dual RNA-seq of pathogen and host.* Nat Rev Microbiol, 2012. **10**(9): p. 618-30.

269. Sebastiani, G., et al., *Host immune response to Salmonella enterica serovar Typhimurium infection in mice derived from wild strains.* Infect Immun, 2002. **70**(4): p. 1997-2009.
270. Lunse, C.E., A. Schuller, and G. Mayer, *The promise of riboswitches as potential antibacterial drug targets.* Int J Med Microbiol, 2014. **304**(1): p. 79-92.
271. Ster, C., et al., *Experimental treatment of Staphylococcus aureus bovine intramammary infection using a guanine riboswitch ligand analog.* J Dairy Sci, 2013. **96**(2): p. 1000-8.

Appendix I – Media and buffer composition

L-Broth/Agar
10 g Tryptone
5 g Yeast Extract
10 g NaCl
15 g Agar (if required; Difco, Becton Dickinson)
dH_2O to 1 litre
Autoclave at 121 ºC for 15 minutes

Mycobacteria 7H9 Broth
2.35 g Mycobacteria 7H9 Broth Base (Sigma-Aldrich)
4 ml Glycerol
2.5 ml 20% $Tween^{80}$
dH_2O to 900 ml
Autoclave at 121 ºC for 15 minutes
Add 100 ml ADC Supplement (Becton Dickinson)

Mycobacteria 7H11 Agar
21 g Mycobacteria 7H11 Agar Powder (Sigma-Aldrich)
5 ml Glycerol
dH_2O to 900 ml
Autoclave at 121 ºC for 15 minutes
Add 100 ml OADC Supplement (Becton Dickinson)

Sautons Medium
0.5 g KH_2PO_4
+/- 0.5 g $MgSO_4$ where required
4.0 g L-asparagine
60 ml glycerol
0.05 g Ferric ammonium sulphate
2.0 g Citric acid
0.1 ml 1 % $ZnSO4.7H_2O$ dH_2O to 1 litre
Adjust to pH 7.0
Filter sterilized (0.22 µM)

SSC Buffer (20x)
175.2 g NaCl
88.2 g Tris: Sodium Citrate
dH_2O to 1 litre
Adjust to pH 7.0-7.2

TBE Buffer (10X)
121.1 g Tris Base
61.83 g Boric acid
18.6 g EDTA
dH_2O to 1 litre
Adjust to pH 8.0

TE Buffer
1.211 g Tris Base
0.372 g EDTA
dH_2O to 1 litre
Adjust to pH 8.3

PBS
8 g NaCl
0.2 g KCl
1.44 g Na_2HPO_4
0.25 g KH_2PO_4
dH_2O to 1 litre
Adjust to pH 7.5

TBS (5X)
12.1 g Tris
146.2 g NaCl
750 ml dH_2O
Adjust to pH 7.5 and make up to 1 litre.

TTBS (5X)
200 ml 5X TBS
800 ml dH_2O
1 ml $Tween^{20}$
Adjust to pH 7.5 and make up to 1 litre.

Semi-dry transfer buffer
2.9g Glycine
5.8 g Tris Base
1.85 ml 20% SDS
750 ml dH_2O
Check pH is 8.3
200 ml Methanol and make up to 1 litre.

Appendix II – Oligonucleotides used in this study

Primers used for cloning deletion constructs

Primer Name	Sequence (5'-3')	Description
2823_3'F	CGGAATTCAGTGACCGTTTGGCC	ncRv13661 targeting plasmid
2823_3'R	CGACTAGTCCCGCCAGTTGCTTC	ncRv13661 targeting plasmid
2823_5'F	GTAGATATCGCAATGGAAAGCAC	ncRv13661 targeting plasmid
2823_5'R	GCCGAATTCTGCGAAAGTTACGA	ncRv13661 targeting plasmid
G2KOnewFHind	CGCGGCCGCCGACTCACCAATGGG	ncRv11690 targeting plasmid
G2KOnewRNot	CAAGCTTGTCAACGCCTGCTCCAGTTGC	ncRv11690 targeting plasmid
G2SDMF	GGATGATGACCCGTTGTCTCTAGACCCTACC GCCCAGCG	ncRv11690 targeting plasmid
G2SDMR	CGCTGGGCGGTAGGGTCTAGAGACAACGGG TCATCATCC	ncRv11690 targeting plasmid
F6RevXbaI	GGTCTAGACGAGTGATCGGG	ncRv10243 targeting plasmid
F6ForXbaI	GGTCTAGATGGGCTTGCCC	ncRv10243 targeting plasmid
F6RevSDM	GGGGCAAGCCCAAAAAGATCTAGACCGAGT GATCGGGTACCC	ncRv10243 targeting plasmid
F6ForSDM	GGGTACCCGATCACTCGGTCTAGATCTTTTT GGGCTTGCCCC	ncRv10243 targeting plasmid

Primers used for cloning complementing constructs

Primer Name	Sequence (5'-3')	Description
2823compF	GGGGATCCGCGCCCTAGCCGCC	ncRv13661 complementing plasmid
2823compR	GGGAAGCTTTGTCGATTGCCGAGTCGTTG	ncRv13661 complementing plasmid
F6compF	GAAAAGCTTGCCGCTGTTGACCAG	ncRv10243 complementing plasmid
F6compR	CGGATCCCTGCGCGGGCTGA	ncRv10243 complementing plasmid
G2compF	CGGAAGCTTAACCCGCCAAAGATAAGTCA	ncRv11690 complementing plasmid
G2compR	CGA TCT AGA ACG TCC TCG ACG TCC TCG GGT	ncRv11690 complementing plasmid

Primers used for PCR screening of SCO and DCO colonies

Primer Name	Description	Sequence (5'-3')
F6pair2F	ncRv10243 deletion screening	CCGGCGGCCAAGGTGTG
F6pair2R	ncRv10243 deletion screening	ACGGCGTCAAGCGGTTCATTAC
F6pair3F	ncRv10243 deletion screening	GTGGGCGGTGCGGTGCTCAAACA
F6pair3R	ncRv10243 deletion screening	GGGCCTGCGTGCGCTCTACCTCTA
G2pair2F	ncRv11690 deletion screening	GCAGCTCGCGGCACCACCAAACAC
G2pair2R	ncRv11690 deletion screening	GCGCGGCCCGGGAAACCTCTG
G2pair3F	ncRv11690 deletion screening	AGCGCAGGTCGTGGCCAATGTAGG
G2pair3R	ncRv11690 deletion screening	ACGGCACCAAGTTCGGCAAATCAA
2823pair2F	ncRv13661 deletion screening	CGCCGCGCCGTGCTGAAGTC
2823pair2R	ncRv13661 deletion screening	GCTGCGCCCGGAGGTATTGGTGT
2823pair3F	ncRv13661 deletion screening	CCACCGCGACCCCCGATGACC
2823pair3R	ncRv13661 deletion screening	CGACCCGCTGGCTCCGCTAATGG

Oligonucleotides used for probe creation for northern blotting

Riboprobe Name	Sequence (5'-3')
2823nrt	gcacccacgcggagtcatagccacgataacggcagaaCCTGTCTC
G2nrt	atcgatgcatccccaccccatccctcgagataagCCTGTCTC
F6nrt	cggatagccccgtgttgttgtctgaCCTGTCTC
2048nrtLONG	gacctgcggtttcatccacaaaatctgggctgcgtgaactaaatgtCCTGTCTC
2660nrtLONG	aacctttcggtggttgcaccgagtcagttcacatttagttcacgcagcCCTGTCTC

Primers used for qRT-PCR in ncRv10243 investigation

Primer Name	Sequence (5-3')
16sTqmF	TCCCGGGCCTTGTACACA
16sTqmR	CCACTGGCTTCGGGTGTTA
F6TqmF	GGATAGCCCCGTGTTGTTG
F6TqmR	GGGATTGCCCCGCATT
Rv0693TqmF	CGATCCCGGCGAGTTG
Rv0693TqmR	TGCGTTCCAGTTCGTCGAT
Rv0694TqmF	GGAGGCTGCCGAAATCG
Rv0694TqmF	CGACCGTGATTCCCTTTTCA
Rv1130TqmF	TGAAGTGATCGTGGACGAACTG
Rv1130TqmR	CTGTTCAACGGGTTCCACTACA
Rv0169TqmF	CGGGCTGGGCGATAAGTT
Rv0169TqmR	GCGAATTGAGGTCATCCAGAA
Rv0440TqmF	CGTCGTCCTGGAAAAGAAGTG
Rv0440TqmR	GGTCTTCTTGGCTACCTCTTTGAC
Rv3418cTqmF	CGTTGCGGAGGGTGACA
Rv3418cTqmR	TCCTCGCCGTTGTACTTGATC
Rv0990cTqmF	GGCCGCGCACGATCT
Rv0990cTqmR	CGTTTTTCCAGCCTGACATCA
Rv0991cTqmF	TTCAAAGGCACCGGCTTCTA
Rv0991cTqmR	TGGTCTGGCTCTTGGACTTCTT

Primers used for qRT-PCR in ncRv11690 investigation

Primer Name	Sequence (5’- 3’)
G2TqmF	CTTCAGCGGGGGGCTTAT
G2TqmR	ATCTTATCTCGAGGGATGGGG
DesA3TqmF	GGCGCTGCGGTTCATG
DesA3TqmR	CAGGTCCGGATAGAGGTGATG
Rv1535TqmF	GACGCGCAGCCTTTCG
Rv1535TqmR	CCACAACGCGGCGTAGAG
Rv3841TqmF	TGCAATGATGCTCGTGCAA
Rv3841TqmR	TCTACGCCGGGAATTTCG
Rv0791cTqmF	ACATCCAGGGCACCATCTTC
Rv0761cTqmR	CCGGCCTTATACATCGACAAC
Rv0846cTqmF	CGACTGAGCCAGGCCACTA
Rv0846cTqmR	GCCGTCCGTCCAATCG
Rv0634BTqmF	CACCGTAACTACATCACCAAAAAGA
Rv0634BTqmR	CGCAATTCGGGCAGAACT
Rv2582TqmF	CCGATTAGCCTGTGCTTTCG
Rv2582TqmR	CGTTCGAGTTTGCGTTTGG
Rv3116TqmF	GCCCGCCGAGTTCGA
Rv3116TqmR	TCGCCTTTGGGTATCAAGATG
Rv2338cTqmF	TGTCGCAACCTTGGATTGATT
Rv2338cTqmR	GCGATTGCAACGCGACTAT
Rv0891cTqmF	GATGTTGGCCGATGTGAGTTC
Rv0891cTqmR	CGTCTAATCCCTGGTTGGCTAT

Primers used for qRT-PCR in ncRv13661 exponential phase investigation

Primer Name	Sequence (5’-3’)
2823TqmF	GGCGCCCAGCATGGT
2823TqmR	CATCTGCTGTTCGCAATTACG
Rv1130TqmF	TGAAGTGATCGTGGACGAACTG
Rv1130TqmR	CTGTTCAACGGGTTCCACTACA
Rv1131TqmF	CGGGATCTTGCCCAACCT
Rv1131TqmR	GAAGCTGGCGATGTCGAATC
Rv2931TqmF	CTGCGAGTGCCTGAGAAAGAG
Rv2931TqmR	GAATCGCCATTGCCATAAGG
Rv1813cTqmF	CGCCAACGGTTCGATGTC
Rv1813cTqmR	CAATCGCCCCGTAATGGATA
Rv2948cTqmF	GCATAGGTTTGCCGTTGTTGA
Rv2948cTqmR	CGCCACGCACCAATTTC
Rv1935cTqmF	CGGCACTGCTGATCAAGGA
Rv1935cTqmR	AGCTGGTGGATCTTGAAGCAA
Rv2598TqmF	CTACCACCTCCAATCCCATACC
Rv2598TqmR	CGCGTGCAGCGTTCAC
Rv0676cTqmF	CGCCCATGCGTTTTACG
Rv0676cTqmR	CCCCCAAAAGTCCTGCAA
Rv0678TqmF	TGATCCAATTTGGGTTCATTGA
Rv0678TqmR	GCCCGGATGCGTTCAC
Rv2428TqmF	TGCTAACCATTGGCGATCAA
Rv2428TqmR	ACAGGTCACCGCCGATGA
Rv2934TqmF	AAGGCGCGTCCTTGCAT
Rv2934TqmR	CGAATAGTGTCAGCGTTGTTGAG
Rv1592TqmF	TGACCCAAATGGAGCTGTTG
Rv1592TqmR	GGTACTGATACCGCCCATCCT

Primers used for qRT-PCR in ncRv13661 stationary phase investigation

Primer Name	Sequence (5’-3’)
Rv0270TqmF	TCGACCAGCTGGAGAAAACC
Rv0270TqmR	CCGGATACGAACACGATCTTC
Rv0721TqmF	GTCGCTGGGCAGTGACAAC
Rv0721TqmR	GACGTCCTCTATCGGCAAACC
Rv0867cTqmF	CCTTGCCACCGATTTGGA
Rv0867cTqmR	TTCTTCGTATAGGCGATGTTCGA
Rv1252cTqmF	GCCCGATACCTATGGGTTCA
Rv1252cTqmR	CGTCAATGCCACCGTGTCT
Rv2140cTqmF	GCGGTGAAGGTCGAAAAGC
Rv2140cTqmR	CGTGCTGGAACAGGTTGAATC
Rv2692TqmF	CCGCAACGAGTGGCTGTT
Rv2692TqmR	TGACGGCCTCTTCGATCAG
Rv2725cTqmF	GGCTGTGCAGGTTAAGGTTATTG
Rv2725cTqmR	GCATGCTGGGCAAAGATGT
Rv2884TqmF	GCTCACCGAATTCAAACTCATG
Rv2884TqmR	GCCGAGTCCGGGTGAAC
Rv2342TqmF	CGTGGCCAGGTCGATGAT
Rv2342TqmR	CAGGGTCACAAACCCAGCAT

Primers used for qRT-PCR in ncRv13661 propionate growth investigation

Primer Name	Sequence (5’-3’)
Rv1217cTqmF	TGGGTGCGGTCGGAATC
Rv1217cTqmR	GCCGAATCACCGTGAGGAT
Rv1218cTqmF	AAGCGCTGTGCGAAAAGG
Rv1218cTqmR	CGTCTAGTGAACCGCTTTCGA
Rv1219cTqmF	ATGGCCGAGATCGAATCCT
Rv1219cTqmR	CGCCGGATTGCATGCT

Primers used for qRT-PCR in ncRv12659 investigation

Primer Name	Sequence (5-3’)
16sTqmF	TCCCGGGCCTTGTACACA
16sTqmR	CCACTGGCTTCGGGTGTTA
5’q12659F	CACCGGCCCACTAGTGAAAC
5’q12659R	GGATGAAACCGCAGGTCAA
3’q12659F	TGACCTGCGGTTTCATCCA
3'q12659R	TGCACCGAGTCAGTTCACATTTA
2658cTqmF	CGAAGCTTCACGAGCTGAGA
2658cTqmR	GCGCCTCTGCTATTGATGGA
2659cTqmF	GGCTGAAGCAGCGTGGAAT
2659cTqmR	TTGTCCAGCAGTTTGCGATAGT
Rv3229cTqmF	GGCGCTGCGGTTCATG
Rv3229cTqmR	CAGGTCCGGATAGAGGTGATG

Appendix III

SNP analysis from High throughput sequencing of gDNA extracted from *M. tb* strains

SNP	type	coding_type	codon_change	aminoacid_change	gene	gene_name	H37Rv_allele *	derived_allele *	H37Rv	ΔncRv11690B	ΔncRv10243	ΔncRv13661
293606	intergenic	-	-	-	-	-	G	T	G	G	T	G
293607	intergenic	-	-	-	-	-	A	C	A	A	C	A
337959	coding	nonsynonymous	aTc/aGc	I372S	Rv0279c	PE_PGRS4	A	C	C	C	C	A
1212228	coding	synonymous	ggA/ggC	G223	Rv1087	PE_PGRS21	A	C	A	A	A	C
1313338	intergenic	-	-	-	-	-	A	G	A	A	A	G
1313339	intergenic	-	-	-	-	-	A	C	A	A	A	C
1780588	coding	synonymous	cgC/cgG	R130	Rv1575	Rv1575	C	G	G	G	G	C
1916491	coding	synonymous	gcG/gcA	A181	Rv1691	Rv1691	G	A	G	A	G	G
2864730	coding	nonsynonymous	Cgg/Tgg	R102W	Rv2541	Rv2541	C	T	C	C	T	C
3054724	coding	nonsynonymous	Agc/Ggc	S271G	Rv2741	PE_PGRS47	A	G	G	G	G	A
3278306	coding	synonymous	ttC/ttT	F1470	Rv2940c	mas	G	A	G	G	G	A
3278390	coding	synonymous	gtT/gtC	V1442	Rv2940c	mas	A	G	A	A	A	G
3278391	coding	nonsynonymous	gTt/gGt	V1442G	Rv2940c	mas	A	C	A	A	A	C
3550149	intergenic	-	-	-	-	-	G	A	G	G	G	A
4101048	intergenic	-	-	-	-	-	G	A	G	G	G	A
4101049	intergenic	-	-	-	-	-	T	G	T	T	T	G
4178146	intergenic	-	-	-	-	-	C	T	C	C	T	C
17												

	JHD2	JHD3	JHD4	JHD5
SNPs number:	3	1	7	12

* bases are relative to the forward strand, but the codon_change column is strand correct

Appendix IV – Microarray results for ΔncRv11690

ID	Corrected p-value	p-value	Fold change	regulation
MtH37Rv-0097 (1I1)	0.04241779	5.99E-04	2.97	down
MtH37Rv-0098 (1J1)	0.04769973	9.11E-04	2.24	down
MtH37Rv-0128 (8J2)	0.04241779	6.56E-04	2.27	down
MtH37Rv-0310c (2I18)	0.04241779	2.90E-04	2.05	down
MtH37Rv-0348 (2I22)	0.04241779	5.34E-04	2.21	down
MtH37Rv-0465c (1B21)	0.04241779	5.51E-04	2.05	down
MtH37Rv-0467 (9O14)	0.04567742	7.71E-04	2.36	down
MtH37Rv-0565c (9M17)	0.049999036	0.001881779	2.12	down
MtH37Rv-0634B (11F14)	0.04241779	2.64E-04	2.79	down
MtH37Rv-0644c (9O22)	0.04769973	0.001017182	2.17	down
MtH37Rv-0760c (3N19)	0.04241779	3.97E-04	2.07	down
MtH37Rv-0761c (3O19)	0.04769973	0.00104955	2.66	down
MtH37Rv-0846c (4K3)	0.04769973	0.001120128	2.73	down
MtH37Rv-0854 (4I4)	0.04121322	8.95E-05	2.07	down
MtH37Rv-0888 (4O6)	0.048158832	0.001643126	2.23	down
MtH37Rv-0891c (4I7)	0.04075228	1.43E-05	2.48	down
MtH37Rv-0925c (4I10)	0.04121322	8.96E-05	2.17	down
MtH37Rv-1008 (5E5)	0.04241779	3.51E-04	2.07	down
MtH37Rv-1078 (5F11)	0.04241779	6.45E-04	2.29	down
MtH37Rv-1374c (5N1)	0.04769973	0.00120875	2.04	down
MtH37Rv-1490 (5O11)	0.04769973	0.001425657	2.11	down
MtH37Rv-1498c (5N12)	0.04241779	3.01E-04	2.41	down
MtH37Rv-1515c (5C14)	0.04769973	0.001143594	2.54	down
MtH37Rv-1535 (10A22)	0.04769973	0.001074942	3.95	down
MtH37Rv-1724c (7J21)	0.04964896	0.001846333	2.34	down
MtH37Rv-1749c (7K23)	0.04769973	0.001240551	2.03	down
MtH37Rv-1754c (7O23)	0.04241779	3.32E-04	2.53	down
MtH37Rv-1860 (7F8)	0.04241779	3.33E-04	2.50	down
MtH37Rv-1885c (7C11)	0.04241779	4.51E-04	2.55	down
MtH37Rv-1980c (6O6)	0.04241779	6.31E-04	2.30	down
MtH37Rv-2000 (6L14)	0.04241779	5.45E-04	2.59	down
MtH37Rv-2001 (6M14)	0.04241779	4.91E-04	2.43	down
MtH37Rv-2140c (6I19)	0.04121322	1.57E-04	2.08	down
MtH37Rv-2185c (6N23)	0.04241779	5.42E-04	2.16	down
MtH37Rv-2281 (5K21)	0.048893973	0.001685406	2.16	down
MtH37Rv-2288 (8O13)	0.04769973	9.55E-04	2.63	down
MtH37Rv-2289 (5P21)	0.041673273	1.76E-04	2.63	down
MtH37Rv-2299c (5P22)	0.045126397	7.14E-04	2.97	down
MtH37Rv-2332 (6A2)	0.04241779	2.67E-04	2.1	down
MtH37Rv-2338c (6G2)	0.04769973	8.80E-04	2.00	down
MtH37Rv-2429 (6D10)	0.04964896	0.001792336	2.59	down
MtH37Rv-2520c (8P21)	0.04567742	7.60E-04	2.73	down
MtH37Rv-2529 (6E19)	0.04769973	0.001481529	2.10	down
MtH37Rv-2560 (6C22)	0.04121322	1.46E-04	2.42	down
MtH37Rv-2563 (8M23)	0.04121322	9.75E-05	2.18	down
MtH37Rv-2582 (6E24)	0.04121322	4.36E-05	2.94	down
MtH37Rv-2699c (10F4)	0.04769973	9.20E-04	3.53	down

ID	Corrected p-value	p-value	Fold change	regulation
MtH37Rv-2876 (10B11)	0.04964896	0.001754237	2.23	down
MtH37Rv-3033 (3C16)	0.04241779	2.30E-04	2.42	down
MtH37Rv-3116 (3G23)	0.04241779	4.08E-04	2.11	down
MtH37Rv-3168 (3I4)	0.04121322	1.59E-04	2.19	down
MtH37Rv-3169 (3J4)	0.04769973	0.001102102	2.16	down
MtH37Rv-3198A (11M5)	0.04121322	5.51E-05	2.31	down
MtH37Rv-3229c (3P9)	0.04769973	0.001477411	6.70	up
MtH37Rv-3390 (4A12)	0.04241779	6.25E-04	2.07	down
MtH37Rv-3472 (4E19)	0.04612943	7.95E-04	2.06	down
MtH37Rv-3528c (4A24)	0.04567742	7.48E-04	3.48	down
MtH37Rv-3750c (11B6)	0.04769973	8.88E-04	2.24	down
MtH37Rv-3789 (3A12)	0.04241779	3.59E-04	2.07	down
MtH37Rv-3790 (3B12)	0.04121322	1.22E-04	2.53	down
MtH37Rv-3822 (8A3)	0.04769973	0.001499619	2.08	down
MtH37Rv-3831 (8E3)	0.04241779	2.42E-04	2.09	down
MtH37Rv-3841 (8G4)	0.04769973	0.001290105	2.94	up
MtH37Rv-3891c (11A11)	0.04769973	0.001150007	2.14	down
MtH37Rv-3914 (11G11)	0.04769973	0.001338082	2.04	down

Appendix V – Microarray results for over expression of ncRv13661 during growth on propionate

Gene	Fold change	Average p value	Regulation in Over Expression
MT0196	3.0587957	0.00980657	Down
MT1182	3.0006094	0.023238488	Down
MT2011	3.0349927	0.006924124	Down
MT3762	35.238476	0.006237192	Up
Rv0057	2.86091175	0.015669447	Down
Rv0059	2.61027485	0.01868597	Down
Rv0060	3.0894288	0.026269772	Down
Rv0094c	2.957336	0.030012533	Down
Rv0095c	2.8233376	0.014221886	Down
Rv0118c	2.74658885	0.0136694	Up
Rv0181c	3.1077776	0.025533231	Down
Rv0182c	3.0271215	0.029473556	Down
Rv0186	3.7745452	0.01055969	Down
Rv0251c	2.5038342	0.009377076	Down
Rv0336	2.9063153	0.020244885	Down
Rv0412c	2.8750796	0.009912577	Down
Rv0631c	5.8720517	0.048923384	Up
Rv0677c	2.6815865	0.013024882	Up
Rv0678	2.5164318	0.026071586	Up
Rv0867c	3.7430665	0.015942314	Up
Rv1128c	3.4049668	0.024536425	Down
Rv1148c	3.805765	0.010034436	Down
Rv1216c	2.617082	0.006774418	Up
Rv1217c	3.3887401	0.030274616	Up
Rv1218c	2.7499008	0.013520777	Up
Rv1219c	2.705120033	0.019153395	Up
Rv1221	5.0242654	0.00856264	Down
Rv1223	3.7582123	0.024196637	Down
Rv1277	3.3219272	0.024417192	Down
Rv1278	2.8379604	0.015888278	Down
Rv1406	2.554684	0.02209204	Down
Rv1588c	2.84607185	0.017964559	Down
Rv1638	2.7975264	0.013553251	Down
Rv1724c	2.5253325	0.042626966	Down
Rv1765c	2.858969	0.021133548	Down
Rv1833c	3.83359035	0.006236968	Down
Rv1945	3.4613276	0.039719146	Down
Rv1948c	2.6439235	0.029949432	Down
Rv1961	3.91197285	0.007089806	Down
Rv1992c	3.2435637	0.028226381	Down
Rv1993c	2.8233626	0.014726047	Down
Rv1994c	2.76717055	0.019774498	Down
Rv2011c	2.7260609	0.009694663	Down
Rv2015c	2.6771557	0.009516206	Down
Rv2023A	2.9150717	0.048923384	Down
Rv2024c	2.563521	0.019562772	Down
Rv2107	21.123097	0.015234817	Down
Rv2108	6.4326725	0.016876131	Down
Rv2693c	3.85578315	0.007963537	Down

Gene	Fold change	Average p value	Regulation in Over Expression
Rv2710	2.8844397	0.013936628	Down
Rv2717c	3.7130489	0.023848809	Down
Rv2719c	2.864418833	0.013706735	Down
Rv2734	2.8250954	0.017285895	Down
Rv2742c	3.17499335	0.017598349	Down
Rv2934	2.5031354	0.048960336	Down
Rv2974c	2.9324815	0.010789794	Down
Rv3017c	4.145676	0.003636259	Down
Rv3191c	4.200498	0.01055969	Down
Rv3201c	2.8019693	0.016812492	Down
Rv3223c	2.6593902	0.017057654	Down
Rv3252c	2.6010687	0.027826516	Down
Rv3269	2.8918612	0.00440765	Down
Rv3270	2.7440443	0.017680854	Down
Rv3370c	2.63619445	0.020636477	Down
Rv3463	2.8282888	0.008852384	Down
Rv3466	2.5057275	0.00440765	Down
Rv3585	2.5827568	0.012668396	Down
Rv3639c	3.3419392	0.03373858	Down
Rv3640c	4.40455655	0.024131601	Down
Rv3641c	5.045832667	0.029639102	Down
Rv3644c	2.7123706	0.008372897	Down
Rv3776	3.0363762	0.01542011	Down
Rv3839	3.7717898	0.049165383	Down
TBFG_11172	4.214123	0.02545547	Down
TBMG_04080	3.3390186	0.042626966	Down
TBMG_04100	3.1477306	0.00980657	Down
TBMG_04100	2.8947976	0.009516206	Down

Appendix VI - *In vivo* testing of ΔncRv13661 (DCO 3.21)

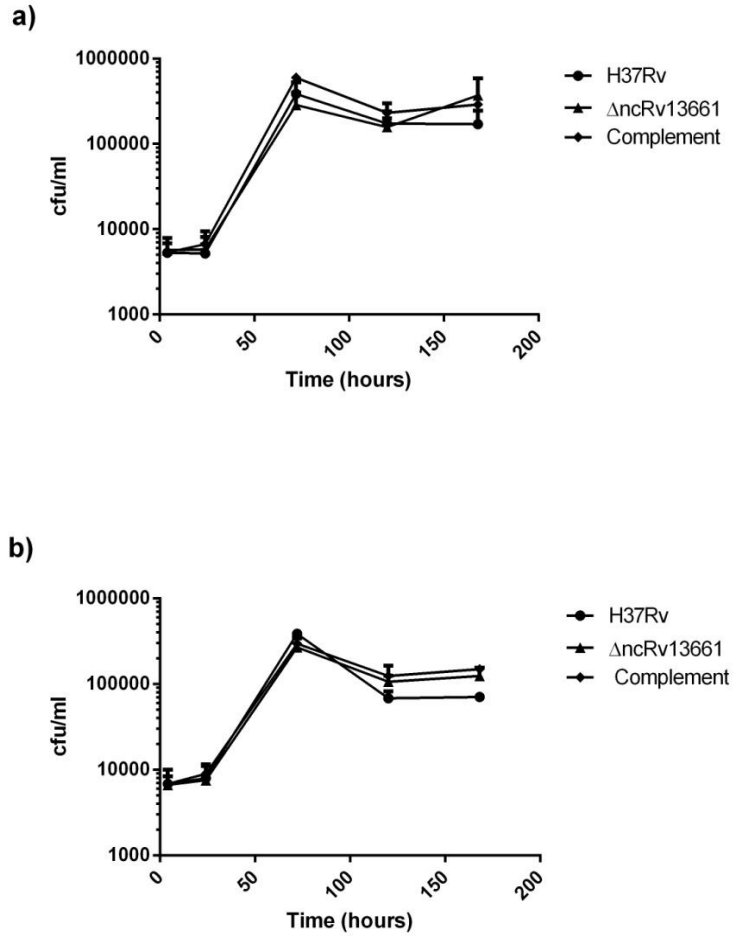

Figure S1 Survival of the ΔncRv13661 in a macrophage model of infection

Survival of Wildtype *M. tb* H37Rv, ΔncRv13661, and complementing strain within naive a) and IFN-γ activated BMDM b) over a time course of infection. Significance was tested with One-way ANOVA $p>0.05$. Data is the mean and standard deviation of triplicate infections.

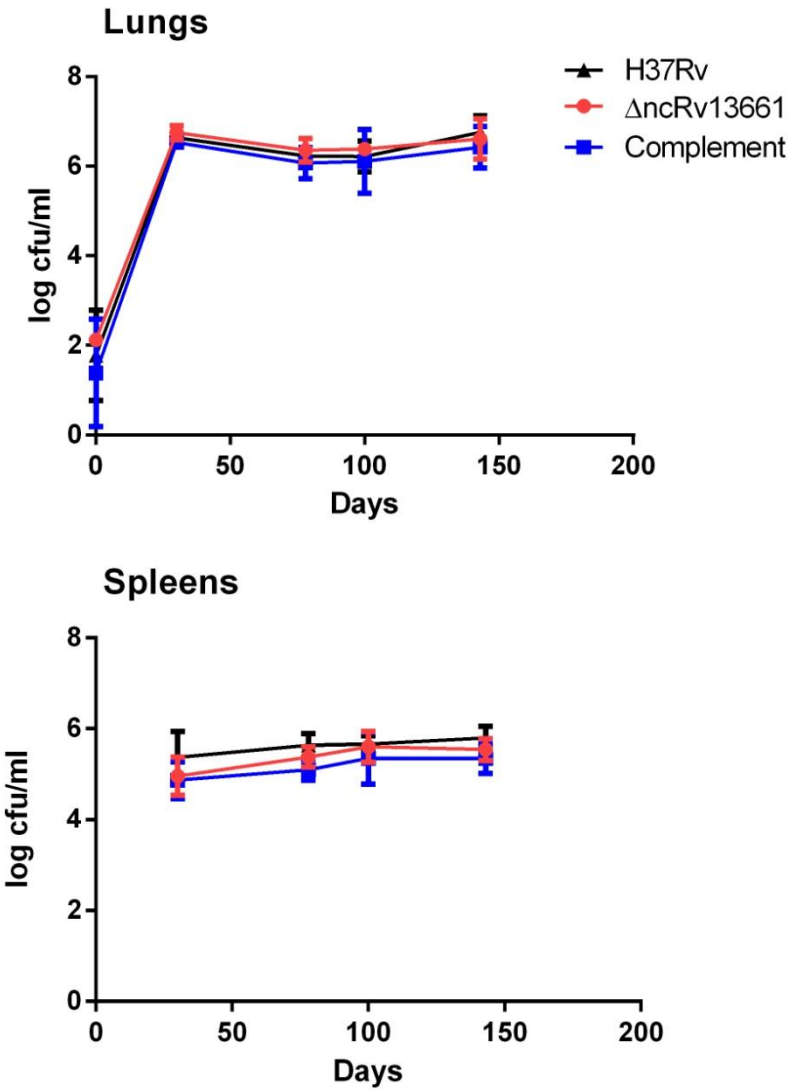

Figure S2 Survival of ΔncRv13661 from aerosol infected mice.

Survival of wildtype *M. tb* H37Rv, ΔncRv13661, and complement within the lungs and spleens of Balb/C mice. The data represents the averages and standard deviations from 5 mice per time point. Significance was tested with Two-way ANOVA.